UNIVERSITY OF CALIFORNIA, SAN DIEGO

Amplified Detection of Protease Activity using Porous Silicon Nanostructures

A dissertation submitted in partial satisfaction of the

requirements for the degree Doctor of Philosophy

in

Chemistry

by

Manuel Orosco

Committee in charge:

Professor Michael J. Sailor, Chair
Professor Farooq Azam
Professor Jennifer Cha
Professor Kimberly Prather
Professor Akif Tezcan

2009

The dissertation of Manuel Orosco is approved, and it is acceptable in quality and form for publication on microfilm and electronically:

_____

_____

_____

_____

_____

Chair

University of California, San Diego

2009

DEDICATION

I dedicate my thesis work to my dad, Richard Sanchez.

TABLE OF CONTENTS

LIST OF FIGURES

LIST OF TABLES

ACKNOWLEDGMENTS

First, I would like to acknowledge all of my family for their love and support throughout the years: Kathy, Lil Ruben, Liz, Albert, Joey, and Anita. My mother, Maria, love you ma and I hope I made you proud.

Much of my thesis work was possible by continuous support and discussion from the Sailor Group: Emily, Lauren, Becky, Sara, Anne, Jason, Yang Yang, Jamie, JiHo, Ester, Joel, Chia-Chen, Liz, Michelle, Shawn, Luo, Jen, Jenny, Matt, Maggie, Kim, Travis, Brain, Gordon (I know there's more but thanks to all the other group members). .

Claudia, of course, was a major help in much of my thesis work and me getting adjusted to the lab. I'm happy you are enjoying life in Germany and I wish you success in the future.

Prof Michael Sailor, thanks for taking me into your lab and more importantly, enabling me to become a better scientist. I'm glad you accepted me even though I initially was a Biochemist. It was a wonderful experience to be a part of new and innovative science and being able to share that knowledge half way around the world!

To Prof. Farooq Azam, thank you for all your help and being willing to collaborate with the Sailor Group. It was an eye opening experience (especially for me being able to go down to SIO) and I learned a lot about marine chemistry and what goes on in our oceans. Special thanks to Francesca and Steve for working on the biosensor projects and helping the project come to fruition.

Finally, I would like to thank all my friends I made throughout my career at UCSD. Thank you for helping maintain my sanity and making San Diego enjoyable.

Chapters two, three, four, and five are, in part, reprints of the following publications:

Orosco, M.M., Pacholski, C., Sailor, M.J., Real-time monitoring of enzyme activity in a mesoporous silicon double layer. ***Nat. Nanotech.*** 2009, in press.

Gu, L., Orosco, M.M., Sailor, M.J., Detection of protease activity by FRET using porous silicon as an energy acceptor. ***Phys. Stat. Sol. A***, 2009, in press.

Orosco, M.M., Pacholski, C., Miskelly, G., Sailor, M.J., Protein-coated porous-silicon photonic crystals for amplified optical detection of protease activity. ***Adv. Mater.*** 2006, 18, 1393-1396

VITA

June 2004	B.S., Biochemistry emphasis in Biology, University of California , Riverside
June 2006	M.S., Chemistry., University of California, San Diego
June 2009	Ph.D., Chemistry, University of California, San Diego

PUBLICATIONS

Orosco, M.M., Pacholski, C., Sailor, M.J., Real-time monitoring of enzyme activity in a mesoporous silicon double layer. ***Nat. Nanotech.*** 2009, in press.

Gu, L., Orosco, M.M., Sailor, M.J., Detection of protease activity by FRET using porous silicon as an energy acceptor. ***Phys. Stat. Sol. A***, 2009, in press.

Orosco, M.M., Pacholski, C., Miskelly, G., Sailor, M.J., Protein-coated porous-silicon photonic crystals for amplified optical detection of protease activity. ***Adv. Mater.*** 2006, 18, 1393-1396

ABSTRACT OF THE DISSERTATION

Amplified Detection of Protease Activity using Porous Silicon Nanostructures

by

Manuel Orosco

Doctor of Philosophy in Chemistry

University of California, San Diego, 2009

Professor Michael J. Sailor, Chair

This dissertation will focus on harnessing the optical properties of porous silicon to sense protease activity. Electrochemical etching of polished silicon wafers produces porous silicon with unique optical properties such as Fabry-Perot fringes or a dielectric mirror reflecting specific wavelengths. Porous silicon

optical transducers are coupled to a biochemical reaction (protease activity) and optically measured in a label-free manner.

The first chapter is an introductory chapter discussing the current methods of detecting protease activity. Also discussed is the use of porous silicon for label-free sensing.

The second chapter discusses the use of thin protein layers that are spin coated on the surface of a porous silicon film and excluded from the porous matrix based on size. When active proteases are introduced to the protein layer, small peptide fragments are generated, causing a change in refractive index from low to high. This can be used as a tool to monitor protease activity and amplify the signal to the naked eye.

To extend on the second chapter, a double layered porous silicon film with the first layer have large pores and the second layer etched below having small pores was used for sensing protease activity. Proteases are adsorbed into the first layer and introduction of whole protein substrate produces small peptide fragments that can enter the second layer (changing the effective optical thickness).

The fourth chapter describes a method of using luminescent transducers coupled to protein films. An “on-off” sensor using protein coated luminescent porous silicon was used to detect a decrease in the intensity of luminescence due to degradation of the protein film. An “off-on” sensor involved a fluorescent dye housed in the porous film and capped with a protein coating. The release of

the dye is caused by the action of a protease causing an increase in fluorescent intensity from the dye.

1 Introduction to Detection of Protease Activity

1.1 Introduction

Proteases have gained much interest in the past 15 years because of their vital role in regulation of gene transcription[1, 2], cell metastasis[3] , and virulence factors[4]. Proteases were initially thought of as nonspecific degradative enzymes that were only associated with protein catabolism. Proteolysis is now being recognized as a key player in biological processing in all living organisms. This process achieves precise cellular control through specific cleavage of a peptide bond. Activation of substrates through hydrolysis affords activation of cellular pathways. For many years, scientists used colorimetric methods to study the cleavage of peptide bonds and the kinetics involved. The scientific community was limited by the sensitivity of the Folin-Ciocalteu regent until the use of fluorescent dyes conjugated to synthetic substrates. The inherent sensitivity of fluorescent dye substrates allowed for quantification of protease activity at small protease concentrations. In general, there are two main methods used for quantifying protease activity: Spectrophotometry and Fluorometry. A new approach for quantification uses nano-porous silicon films to monitor mass changes of the substrate due to peptide bond cleavage. Much of the thesis work presented here uses changes in refractive index of porous silicon films to monitor substrate cleavage. This chapter describes various assays for protease activity as well as details the method used in each assay.

1.2 Spectrophotometry

UV-visible spectroscopy is the study of interactions between photons and matter in the UV-visible region[5].A spectrometer works by measuring the intensity of light passing through a sample (I), and compares it to the intensity of light before it passes through the sample (I_o). This ratio (I/I_o) is the amount of energy that is transmitted (%T). The absorbance (A) is the –log (%T). Molecules absorb photons from a light source and this allows an electronic transition of an electron from an orbital in the ground state to an unoccupied orbital. Highest Occupied Molecular Orbital (HOMO) and Lowest Unoccupied Molecular Orbital (LUMO) are two important orbitals for absorption and fluorescence spectroscopy. HOMO and LUMO are the ground states of molecules and they require the least amount of energy in order to excite an electron (HOMO) to an anti-bonding orbital (LUMO). Various transitions involving π bond, σ bond, and non- bonding orbitals can also take place at different energy requirements. Some absorption transitions are not allowed because they require a conversion of spin. Singlet-triplet and triplet-singlet are not allowed but an excited singlet state (S_1) can undergo intersystem crossing to an excited triplet state (T_1). Forbidden transitions can also be caused by the symmetry of a molecule. Radiative and non-radiative transitions between electronic states are represented in Figure 1.1. These processes are further discussed in Section 1.3.

In the case of protease activity, spectrophotoscopic methods rely on the

differences in molar absorptivity between substrates and products. Proteins contain aromatic amino acids that can undergo electronic transitions. This is a useful means of quantifying the amount of protein in a sample. Beer's law correlates the molar absorptivity with the concentration of the sample. Crude extracts and the enzymes themselves absorb in the UV range and quantification of the products becomes difficult. It is thus desirable to have products absorb in the visible region. Chromogenic chemicals allow protein substrates to be assayed colormetrically by enhancing the absorption in the visible range. These substrates minimize the signal due to impurities and employ similar work-up techniques as regular protein substrates. Section 1.4 explains the different types of protease assay that use spectrophotometry methods.

1.3 Fluorescence Spectroscopy

In fluorescence spectroscopy, the species are first excited, by absorbing a photon of light, from its ground electronic state (S_0) to one of the various vibrational states in the excited electronic state. Collisions with other molecules cause the excited molecule to lose vibrational energy until it reaches the lowest vibrational state of the excited electronic state (S_1)[5]. A photon is emitted at a lower energy as the excited molecule radiatively transitions from S_1 to S_0. Although photon absorption is just as fast as photon emission, the excited molecules stay in the S_1 state for a few pico to nano seconds before emitting a photon or undergo de-excitation processes such as intersystem crossing or internal conversion. The photon emission is measured by a fluorometer and

usually expressed as wavelength. It is often the case that vibrational levels are similar in ground and excited states and the fluorescence spectrum mirror the absorption spectrum. The gap between the first absorption maximum and the fluorescence maximum is the Stoke shift. Depending on how large the Stoke shift is, distinguishing between excitation and emission can become difficult. Intersystem crossing allows excited states (S_1) to non-radiatively transition to an energetic vibrational level of a triplet state (T_n). Vibrational relaxation of the T_n state brings it to the lowest vibrational state (T_1). This crossing is forbidden if the states have different spin multiplicities. T_1 can radiatively emit a photon to a S_0 but this rate is slower than S_1 relaxation because of spin conversion. This type of emission is called phosphorescence. Typically, T_1 excited state undergoes de-excitation non-radiatively by intersystem crossing (delayed fluorescence) and vibrational relaxation in S_0.

Often times the excited states of molecules can interact with each other and cause the transfer of energy. Forster energy transfer (sometime referred to as fluorescence resonance energy transfer or FRET) has a donor in an excited state (S_1) and emits the energy radiatively. This emission excites an acceptor from a ground state S_0 to S_1. Energy transfer of this type works through coulombic interactions of dipoles of molecules and do not require molecules to be within a close distance (Forster radius). The dipole of the excited state induces a dipole on a neighbor molecule and causes the energy transfer. Forster transfer could be used to harvest the excited states from non-efficient emitters to efficient-emitters. Most quencher systems use the Forster energy transfer

process by measuring the efficiency in the energy transfer between two proximal fluorophores (donor and acceptor). In a good quencher system, there must be good spectral over lap between the donors fluorescence with the acceptors absorbance. Commercial protease activity assays tend to use this system because of its inherent sensitivity. Dexter energy transfer allows an excited donor to transfer the energy to an acceptor in the ground state. In order for this to happen, the energy levels of the donor and acceptor should be about the same and there must be some intermolecular overlap. This type of energy transfer can harvest the triple energy of a donor and give it to an acceptor that is an efficient emitter. Figure 1.2 explains these two processes. Section 1.4.4 and 1.7 describe different protease assay that use fluorescence.

1.4 Protease Assays with Natural Substrates

Proteases are enzymes that activate protein/peptide substrate through specific hydrolysis of a peptide bond[6]. The scissile site has recognition elements that the protease recognizes for activation. Natural substrates are less likely to perturb the activity of the protease because of this reason. Although the work-up procedures are time consuming, the enzyme kinetics and peptide cleavage reflect the true kinetic values as opposed to synthetic substrates. Various assays with natural substrates will be described in the next subsections.

1.4.1 Protein Substrates

This general method uses natural protein substrates to be assayed. Typically, the substrate must be suitable for the protease of interest (e.g. collagen substrate for collagenase). Inexpensive, easily purified casein and haemoglobin are protein substrates used in most protocols for quantification of protease activity. The protein substrates are incubated with the protease and peptides fragments are generated. These fragments are soluble in trichloroacetic acid (TCA) and whole protein substrates precipitate out. The solution is spun down and the absorbance of the supernatant is measured at 280nm (absorbance of tyrosine, phenylalanine, and tryptophan residues). Although the substrates are inexpensive, there are relatively long workup times, sensitivity is limited by solubility of peptides generated, and sensitive UV spectrophotometers are needed. Also, large peptide fragments might be insoluble in TCA and whole protein could be soluble in TCA. This could make it difficult to detect protease activity.

1.4.2 Chromogenic Substrates

An alternative to measuring the absorbance at 280nm is to modify whole protein substrates with chromogenic chemicals. Proteins can be modified with azo dyes and still allow the whole protein substrate to have scissile sites for peptide bond cleavage[7]. These chemicals are good candidates because of their π-delocalization of electrons that allows measurements in the visible range. Because the measurements are taken at 440nm, protein contaminants found in enzyme extracts do not affect the measurement. These substrates tend to

precipitate in TCA and provide a more accurate measure of protease activity. Extensive workup protocols are still required and modification of the whole protein substrates is need. These modifications could potentially affect the rate of cleavage.

The Folin-Ciocalteu reagent used in Lowry assays has been a standard means of quantification of protease activity[8]. It works by measuring the amount of the substance being tested needed to inhibit the oxidation of the reagent. Copper (II) enhances color formation by chelation with the peptide backbone, thus facilitating the transfer of electrons to the chromogens. These complexes react with Folin-Ciocalteu reagent that is a mixture of phosphotungstic acid and phosphomolybdic acid in phenol and this reagent is used for the colorimetric analysis of phenolic and polyphenol antioxidants. The product becomes reduced to molybdenum/tungsten blue and can be detected by absorbance at 750 nm. The main drawback to using Folin-Ciocalteu reagent is that it will react with any reducing substance in the sample. The reagent therefore measures the total reducing capacity of a sample, not just the level of phenolic compounds. This becomes an issue for samples contaminated with some nitrogen-containing compounds such as hydroxylamine and guanidine and other reducing reagents.

1.4.3 Colorimetric Assays

The previous hurtles of precipitating proteins for measurements was solved by using Coomassie dyes[9]. These dyes bind to whole protein substrates though charge interactions with amino acids. It is assumed that small peptide

fragments do not bind to the dye because there are less amino acids that can interaction with the dye. The generation of peptide fragments causes a decrease in the dye absorbance at 595nm. This dye exists in the different ionic states with different absorption maximums: anion form (blue), neutral form (green), and cation form (red). Protein tends to exclusively bind to the anionic form and this causes a blue shift in the absorbance spectrum. This assay simplified the work-up protocol and could be used with low cost colorimeters. The major drawbacks to this system are that large/small peptides cannot be detected because the dye will not bind to the peptides. A majority of proteases cleave just single peptide bonds for the activation of substrates. An example of this is the polypeptide amyloid precursor protein that, upon single cleavage, makes amyloid beta found in the brain plaques of Alzheimer's disease patients[10].The detector and the range of concentration the substrates are assayed limit sensitivity of this system.

1.4.4 Fluorescent Protein Substrates

Most of the systems described prior lack sensitivity needed for protease assays. A fluorescent molecule can afford sensitivity just by excitation with single photons from light. Fluorescent dyes such as fluorescein isothiocyanate (FITC) is a good label for proteins because it is highly fluorescent and reacts with free amino groups to yield a fluorescent protein derivative[11]. Modification of the protein still allows the substrate to be soluble in most cases. This substrate is incubated with the protease of interest, precipitated with TCA, and the supernatant is assayed with a fluorometer. Although this assay affords sensitivity,

supernatant volumes need to be carefully measured in order to minimize the amount of background fluorescence. Protein modification with these dyes can affect the rate of peptide cleavage by inhibiting certain scissile recognition sites. Light scattering from the sample and quenching effects are also concerns in these assays. These fluorescent dyes suffer from small stokes shifts, pH sensitive, and photo bleaching of these dyes are inherent. The pH problems and the high background were solved with a new class of dyes (BOPIDY)[12]. These dyes have less ionizable groups so they are less affected by pH changes. Quenching of the dye by the whole protein substrates allows for a low fluorescence background. They also have narrow emission bandwidths and high quantum yields. One major drawback is that quenching of the dye does not occur with large/small peptides and this makes it impossible to detect protease activity with a high background**.**

1.5 Protease Assays with Synthetic Substrates

Many commercial protease substrates are synthetic because the manufacturing these substrates is relatively simple and scissile recognition sites can be modified for each specific protease. Easy attachment of highly fluorescent dyes to synthetic substrates makes them desirable for assay and readout. Different synthetic substrates assays will be described in Sections 1.6 and 1.7.

1.6 Spectrophotometric Assays

1.6.1 4-nitroaniline

4-nitroaniline is conjugated to an amino acid to mimic a peptide bond[13].

When the peptide bond is cleaved, the 4-nitroaniline is released and the absorbance at 400nm increases. Real-time measurements can be taken by measuring the increase in absorbance at 400nm. 2-napthylamine works in a similar fashion as 4-nitroaniline but absorbs at 340nm[14]. Some concerns with the use of these substrates are that they are carcinogenic and they are insoluble in most aqueous solutions. The indicator can block recognition elements of the substrate and this could affect rate of proteolysis. Many nitroanilide substrates will hydrolyze spontaneously in basic solutions, give false positives, and create high background.

1.6.2 Amide and Ester Containing Substrates

Amino/endopeptidase substrates are usually amino acid amides, esters of amino acids, and N-blocked amino acids. The hydrolysis of amide substrates can be measured at 230nm as a decrease in absorbance. Large amounts of protein substrate and enzyme are needed and this could cause high background. Ways around this is to uses chemicals that react with free amines. Ninhydrin is a chemical used to detect ammonia or primary/secondary amines in solution[15]. When the protein substrate is cleaved, amides are released and react with the ninhydrin. A reading is taken at 570nm and a standard curve with $_{L}$-Leu is used to determine the activity of the enzyme. Carboxypeptidase requires a free carboxyl group for the cleavage of peptide bonds from the C-terminal end of the peptide. These enzymes can also catalyze the cleavage of an ester bond. N-dansylated peptides allow the COOH groups to be free for catalysis and the

fluorescence measurements are taken after the cleavage[16]. These substrates suffer from false positives because the crude extracts might have esterase and endopeptidases to facilitate the bond cleavage.

1.7 Fluorescence Assays

1.7.1 Fluorescent Dyes

A typical synthetic fluorescent substrate has a fluorescent molecule flanking the peptide substrate with a quencher on the opposite end of the scissile site. Cleavage of the peptide bond releases the fluorescent dye into the solution and the fluorescence is measured. Conventional peptidase substrate consists of a doubly blocked aminoacyl residue in which the acyl group is amine-bonded to a group that yields a chromophore upon hydrolysis. Benzoyl, acetyl and succinyl group are attached to the a-amino group of the peptide and they act as quencher molecules. a-COOH groups are modified with a fluorescent substrate such as 7-amin-4-methylcoumarin[17]. Other commercial dyes such as Cy3, Texas Red, and Alexa488 give very bright fluorescence and are used in most synthetic substrate protease activity assays. The drawbacks to using these substrates are that they are pH sensitive, have narrow absorption bandwidths coupled to broad emission spectra, some undergo photo/chemical degradation, and have small Stokes shifts. Sometimes donor and acceptor have emission spectral overlap that can complicate data analysis. Furthermore, direct acceptor excitation could occur if the absorbance of the donor is similar to the acceptor.

1.7.2 Quantum Dots

Quantum dots (Q dots) are semiconductors that can be tuned to emit at various wavelengths. Unlike fluorescent molecules, Q dots have broad absorbance bands that allow them to be excited over a large range[18]. This is because semiconductors have bands of energy levels instead of distinct energy levels. The ground state for semiconductors is the valance band (similar to HOMO) and the excited ground state is the conduction band (similar to LUMO). The emission of the Q dots is based on tuning the size. Increasing the size of the Q dot lower the amount of quantum confinement and this increase the band gap (the energy difference between the valance and conduction bands). This will blue shift the emission spectrum. The spectrum can be red shifted by decreasing the size of the Q dots. The ability to tune the wavelength of emission could be useful for FRET based systems where the donor and acceptor emissions could overlap and complicate the data analysis. Some concerns with Q dots are that synthesis is complicated, molecules are larger than conventional dye, and they are toxic to cells.

1.7.3 HPLC of Fluorescent Substrates

High performance liquid chromatography (HPLC) is a type of column chromatography that is used to separate, identify, and quantify compounds[19]. It is based on the interaction between the stationary phase and the mobile phase. The amount of time the sample interacts with stationary phase is the retention time. This time can be plotted versus the fluorescence of the product. 4-

nitroanilide substrates are coupled to HPLC to get product separation and high sensitivity. Several disadvantages to using HPLC: costly instrumentation for analysis of products, long turn-around times, only single samples can be measured at a time, and contamination of the column can yield low signal to noise ratios.

1.8 Other Methods of Detecting Protease Activity

Some interesting methods for detecting protease activity are starting to gain interest by scientist in this field. SDS-PolyAcrylamide Gel Electrophoresis (SDS-PAGE) has been a powerful tool for separation of proteins based on their electrophoretic mobility[20]. After staining, the products will size separate into bands on the gel. The products can then be extracted out of the bands and be assayed further. This tool is useful if the size of the substrate is known. This can be coupled to Matrix Assisted Laser Desorption Ionization Mass Spectrometry (MALDI-MS) to get a specific mass for the product[21]. MALDI-MS uses an organic matrix to harness the energy from the laser to ionize the sample. De-sorption of the ionized sample is collect and measured by a mass detector. The read-out gives mass signatures that correlate with a specific mass. This method allows for the analysis of multiple samples with good reproducibility between samples.

A new fluorescent assay involves recombinant means to generate polypeptides to Green Fluorescent Protein (GFP)[22]. The scissile site is N-terminal to the GFP label and is expressed as a vector that contains histidine residues. The expression of this modified gene yields a fluorescent substrate with a

specific cleavage site of interest. This substrate is incubated with the protease and metal beads are added to chelate the histidine residues. Un-reacted substrate and chelated product are discarded and the supernatant's fluorescence is measured. Multiple samples can be analysis and the assay is very robust.

1.9 Optical Transducers

Optical transducers measure thickness and/or refractive index changes at a liquid-solid interface of an analyte absorption layer in a label-free fashion. A molecular recognition element (i.e. antibodies, oligonucleotides, sugars) is usually coupled to the sensor surface through adsorption or chemical attachment. Upon binding of target analyte to the recognition element, buffer becomes displaced and the local index at that interface change to a higher index. The differences in index of each analyte can be measured by this optical transducer. This method can be useful for label-free sensing coupled to specificity through specific molecular probes. This thesis work employs porous silicon to exploit this method for detecting protease activity.

1.10 Sensing using Porous Silicon

All of the assays previously described use the interactions between photons from light and matter. A relatively new method for studying protease activity uses reflected light from materials. In particular, porous Si causes interference of reflected light at normal incidence angle to the surface. This reflection is governed by Bragg's Law and the light interacting with porous Si.

This interaction could be used as a transduction element for sensing. This section describes the basic optical properties of porous silicon and how the material is made. Subsequent sub-sections will explain how to harness these properties for sensing.

1.10.1 Introduction to Porous Silicon

Porous Si was first discovered by Bell Laboratories as a failed attempt to electrolytically shape and polish Si[23]. Instead, they created intricate mesoporous variation of silicon. The discovery of photoluminescence from porous Si popularized the research in this field because of its potential use in electronic displays[24]. This discovery lead to a variety of applications ranging from semiconductor processing techniques, microelectronic devices technologies, and chemical and biological sensing. The ease of fabricating control pore size and shapes makes porous Si an attractive material for further development of devices and studies with this material.

Depending on the dopant used in Si wafers, electrochemical etching of Si involves an appropriate electrolyte and possibly light to initiate etching. Anodization of highly doped p-type Si etches pores at nucleated surfaces in the z-direction of the silicon crystal lattice<100>. Polarization of the Si atoms at the surface with an electrical current causes these atoms to be attacked by fluoride ions in an electrolytic solution. This leads to the formation of SiF_6 and H_2 gas evolution. The Si atoms are replaced with reactive silicon hydride and this allows for further chemical attachments through conventional covalent chemistries.

Herein, electrochemical etching was performed using 48% aqueous HF and ethanol solution (3:1 HF/Ethanol). Although there is no specific mechanism universally agreed upon, a general one is proposed in Figure 1.3 and represented by the equation below (eq 1.1):

$$Si + 2h^{+} + 6HF(aq) \rightarrow SiF_6^{2-}(aq) + H_2(g) + 4H^{+}(aq) \qquad \text{Eq. (1.1)}$$

When porous Si is etched it leaves silicon hydride on the surface and these hydrides are very reactive to environmental oxidation by oxygen and water. Making the surface less reactive could be easily achieved through covalent attachments of functional chemicals[25] or oxidation at high temperatures[26, 27]. These treatments terminate the surface and cause the porous material to be more resistant to environmental oxidation. Stability of the material is key to making the transducing element robust for sensing applications. Control over the physical and chemical features of porous Si allows this material to be used in a variety of applications.

1.10.2 Optical Properties of Porous Silicon

There are two types of porous silicon structures used in this thesis work. Each structure exhibits different optical properties that could be used as transducing elements for sensing. The reflectivity spectrum can be electrochemically tuned with either a constant current pulse or a sinusoidal modulation of the current. When porous Si films are illuminated at normal angle

incidence to the surface, an interference pattern is reflected and can be seen with a charge couple device spectrometer. Using a constant current creates an interference pattern known as Fabry-Perot interference[28] (Figure 1.4). This interference is governed by constructive and destructive interference of light interacting with the porous Si/cSi and porous Si /air interfaces. Variation of the current through sinusoidal modulation creates an interference pattern that resonates a single reflection in the visible spectrum (Figure1.5). This type of structure resembles a rugated structure that acts as a dielectric mirror. The reflection of the peak can be easily tuned through prepared etching conditions. Changes in the Fabry-Perot interference pattern can be used as a transducing element for analytes infusing/diffusing out of the porous material. Fabry-Perot interference is governed by the following equation[29]:

$$m\lambda=2nL \qquad \text{Eq. (1.2)}$$

For normal incidence, m is the spectral order of the fringe at wavelength λ. The refractive index, n, is a composite of the material (e.g. porous Si and air) and L is the thickness of the film. The path length of the light traveled in and out of the film is represented by the constant 2. The transducing element in this thesis work is represented as the effective optical thickness (2nL). If an analyte enters porous Si matrix, the refractive index of the composite changes and this causes a spectral shift to either higher or lower wavelengths depending on the refractive index of the analyte. 2nL is measured by making a Fast-Fourier transform (FFT) on the reflected spectrum. The FFT gives a single peak that represents 2nL and the position of the peak is monitored by changes in either n and/or L. A porous Si

rugated film can directly measure the amount of analyte infusing/diffusing though changes in refractive index of the composite. Further processing of the reflected spectrum is not need because the sinusoidal etch makes the Fourier transform already built into the nanostructure.

1.10.3 Chemical and Biological Sensing using Porous Silicon

The two porous silicon nanostructures described above have been used in a number of applications for chemical and biological sensing. In terms of chemical sensing, a variety of chemical vapors can be sensed in a nondestructive, label-free fashion. Early works with these types of sensors used changes in refractive index of porous silicon composite with the replacement of air with chemical vapor[30, 31]. The surface chemistries dictated the sensor response and showed the importance of surface chemistry with the analyte of interest.

Proof of concept papers detailing the use of porous Si as interferometers provided a convenient methodology for biological sensing[32, 33]. Tailoring the surface with functional chemicals paved the way for highly specific and sensitive biosensors[34]. Pacholski's work used double-layered porous Si structures for size exclusion of large biomolecules[26]. Through prepared conditions, the size of the pores can selectively exclude molecules based on size. These structures also provide reference channels for suppression of background noise and changes in matrix composition. Coupling antibodies to these surfaces adds extra specificity

needed for sensing in complex matrices[35]. The thesis work presented here trails much of the previous work done with biological sensing and the optical properties of porous Si will be exploited for use in detecting protease activity.

1.11 Summary

Spectrophotometry and fluorometry are two important tools used for the analysis and quantification of protease activity. A different approach to quantifying protease activity uses visible spectroscopy of reflected light from porous Si. Much of the drawbacks in the previous assays were alleviated with the use of porous Si interferometers. Harvesting the optical properties of porous Si can provide a label-free, specific detection of proteases and relative substrates. This thesis work will outline the various porous Si interferometers used for the detection of protease activity.

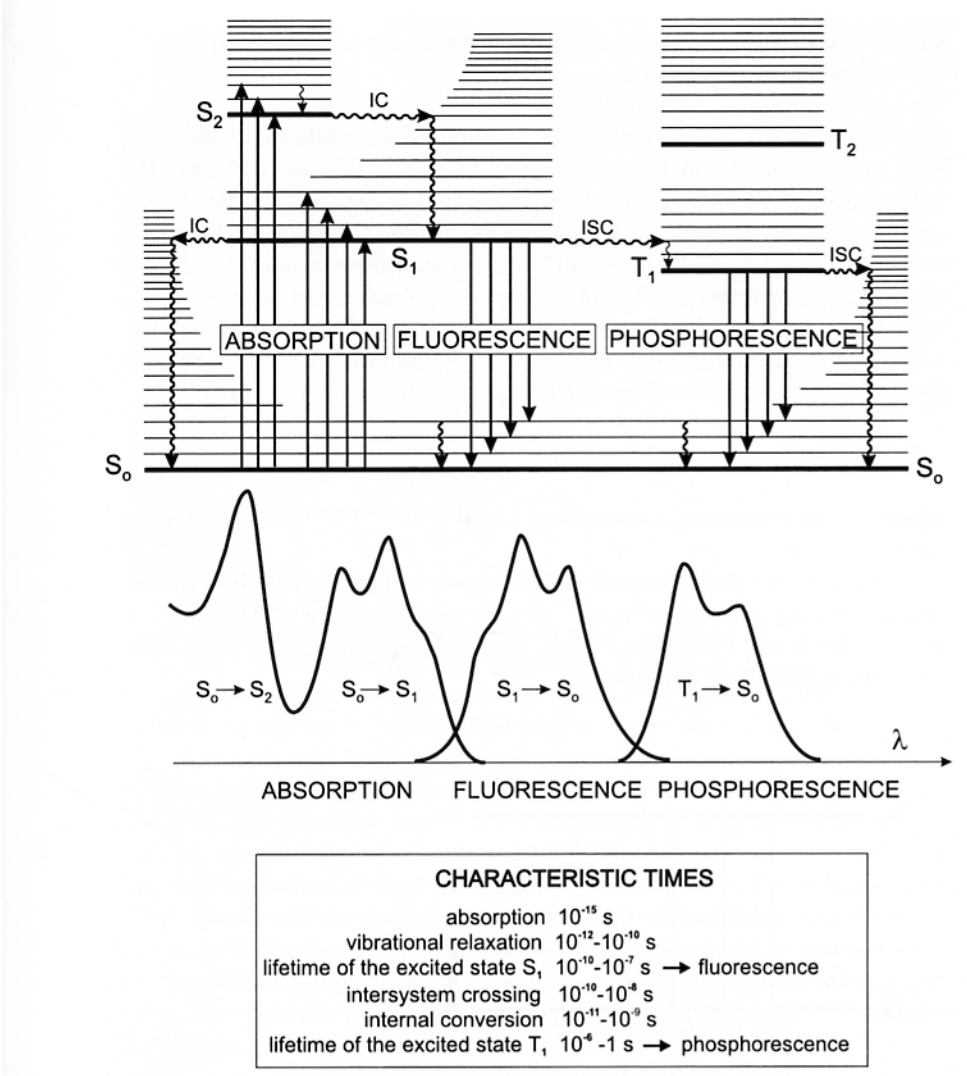

Figure 1.1Radiative and non-radiative transitions between electronic states. Image from Valeur, B. Molecular Fluoresecnce: Principles and Applications (Wiley-VCH, 2002).

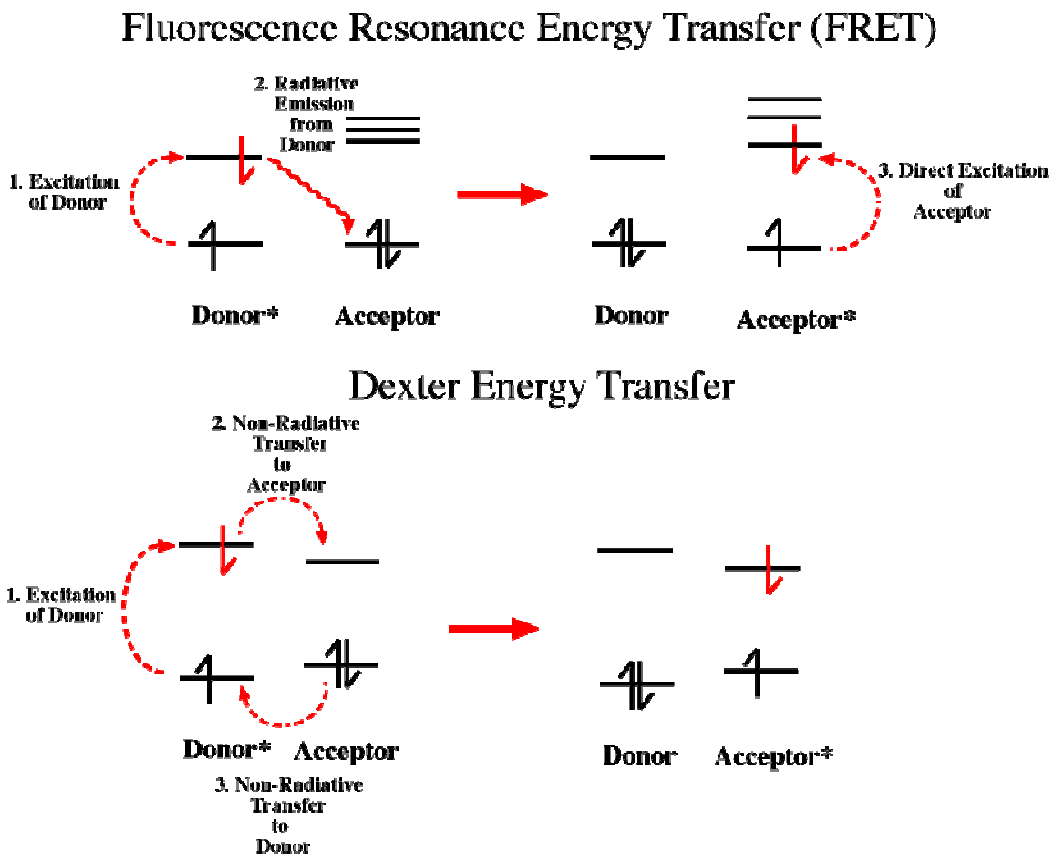

Figure 1.2 Different types of energy transfer. Fluorescence resonance energy transfer (FRET) use direct acceptor excitation with a donor's emission. Dexter energy transfer non-radiatively transfers an excited donor's energy to an acceptor. The acceptor in turn non-radiatively transfers an electron to the ground state of the donor.

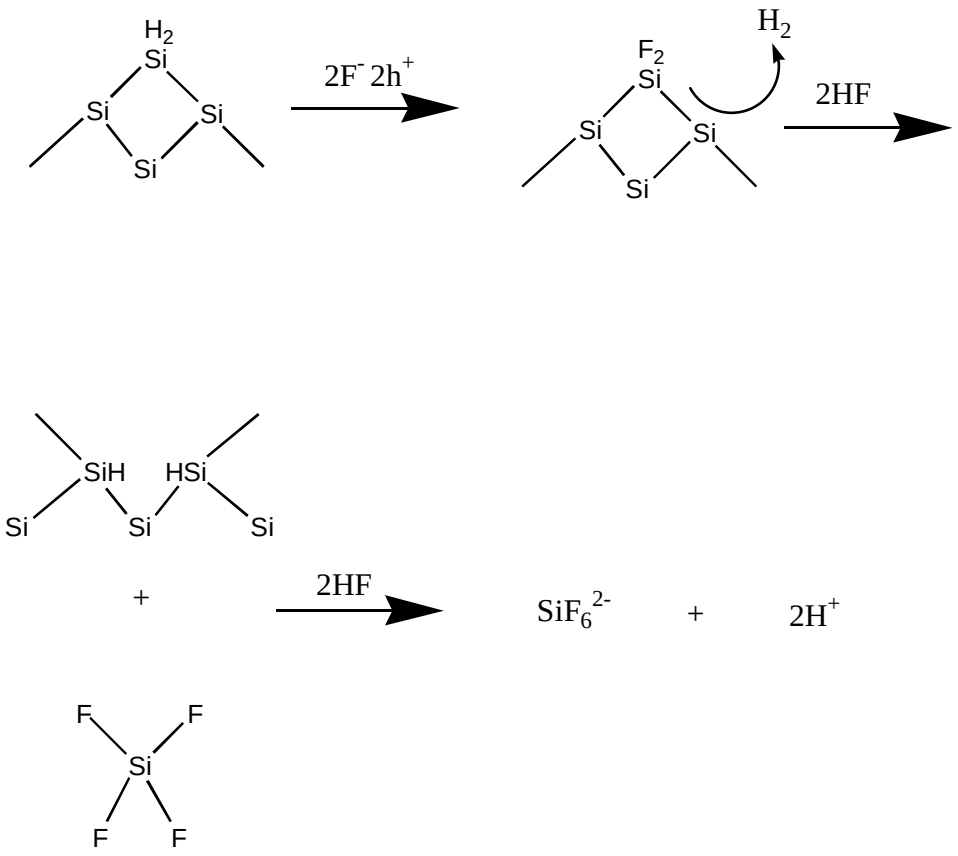

Figure 1.3 Mechanism of porous silicon formation.

a b

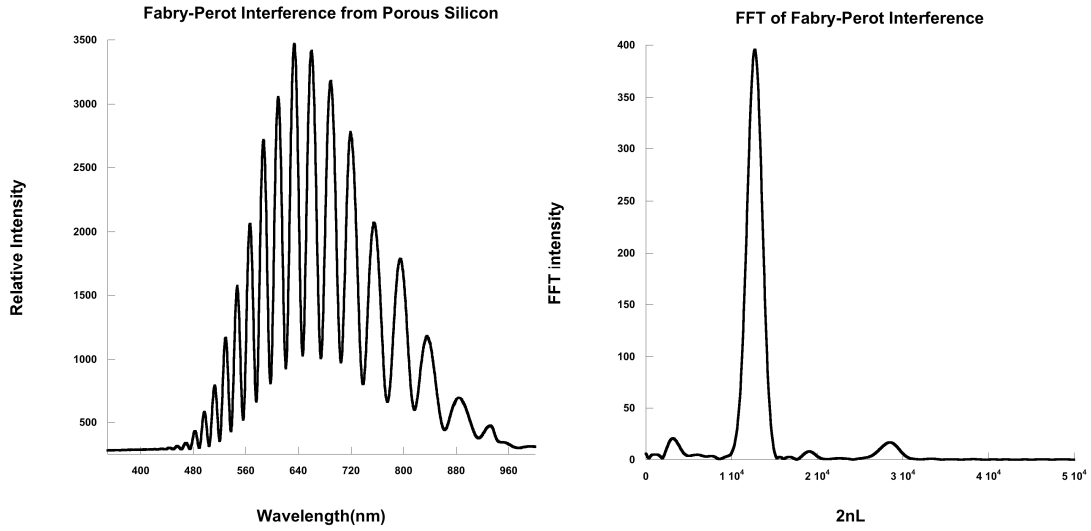

Figure 1.4 Fabry-Perot interference from porous Si. a. Reflection from single layered porous Si. b. A Fast Fourier Transform(FFT) is applied to the reflected spectrum to give a peak that corresponds to the effective optical thickness(2nL) of the porous Si film.

a b

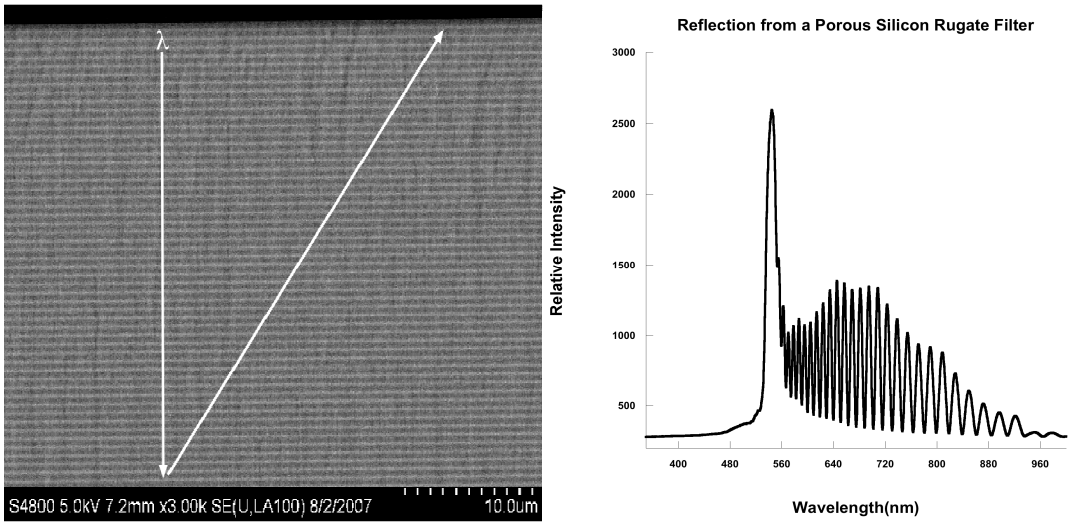

Figure 1.5 Rugate filter made from porous Si. a. Scanning electron microscope image of porous Si photonic crystals. This image was taken at 90^0 angle to obtain a cross-sectional view. Bands of high and low density of silicon represent the high and low current applied during the etch. b. Reflection from the porous Si/cSi interface produces a single wavelength band with some Fabry-Perot interference.

2 Porous Silicon Photonic Crystals for Detection of Protease Activity

2.1 Abstract

There is a need for rapid and fieldable assays that can detect protease activity in samples because of their important roles in intra and intercellular processes. Porous silicon is a promising material because it has been used in a number of applications such as chemical and biological sensing, drug delivery, and encoding technologies. In this work, porous silicon photonic crystals were electrochemically etched from bulk crystalline silicon and further functionalized using electrochemical reduction of CH_3I in acetonitrile. These chemically modified surfaces were characterized by Fourier Transform Infrared spectroscopy (FTIR). These samples were then coated with a hydrophobic maize protein, zein, to form multi-layers of protein on top of the underlying photonic crystal. Pepsin, an aspartic protease, was incubated with the protein coated- porous silicon samples in a 1μL droplet for 1 hour after which the droplet was allowed to air dry. The reflectivity spectra were measured before and after the incubation of protease and the spectra were compared. The presence of an active protease will digest the zein multilayer into smaller peptides that are then allowed to enter the porous silicon film. This causes a measurable change in the refractive index of the porous layer (from air to fragments, n=1 to n=1.42) that red shifts the reflectivity spectra to higher wavelengths. These materials can be easily translated into high-throughput screens for various proteases for a particular substrate and find possible drug candidates for those proteases. A major advance to this method is the use of natural substrates and the ability to measure protease activity in a

label-free fashion. Ideally, this method can be employed by the bench-top biochemist that would be interested in detecting enzyme activity (i.e. protease, DNase, RNase) in samples without the use of expensive analysis equipment and to amplify the enzyme activity to the naked eye.

2.2 Introduction

Conventional fluorescent and colorimetric assays must employ substrates that have been modified from their native forms in order to incorporate the relevant indicator chemistries. For example, a standard method to detect protease activity uses a fluorescent molecule conjugated to casein or bovine serum albumin substrates.[36] Some concerns with the use of fluorescent-conjugated substrates are that the presence of the dye may affect the proteolytic cleavage rate, quantification requires a sensitive fluorimeter, and the reagents are costly. The well-known colorimetric assay using the Folin-Ciocalteu reagent operates on native substrates, but it is less sensitive than fluorescence methods and it requires an extensive workup procedure.[37]. In all cases, relatively large quantities of time and reagents are required (See Section 1.4-1.8 for more methods of detecting protease activity).

The unique optical properties of photonic crystals made from porous Si have been harnessed to generate very sensitive chemical or biochemical detectors.[38-40] Precise control of the current used to etch porous Si provides peaks in the reflectivity spectrum that are much sharper than can be obtained with molecular dyes or quantum dots,[41] and allowing the use of such materials in

high-throughput, multiplexed assays.[42] The present work takes advantage of these features, using color changes induced in a porous silicon photonic crystal as a sensitive probe of protease activity. Amounts of protease as small as a few pmol in a 1 μL aliquot can be detected as a color change that is visible to the unaided eye. By contrast, current colorimetric assays require the use of a spectrophotometer, and require 100-500 μL aliquots to obtain comparable detection limits (7 pmol, or 240 ng for pepsin).

Fabrication of the photonic crystal involves anodic etching of a p-type, boron-doped silicon wafer polished on the (100) face (Figure 2.1).[43] A sinusoidal etch waveform produces a film with an alternating porosity gradient in the <100> direction that acts as a one-dimensional photonic crystal; the film displays a distinct optical diffraction peak in the white light reflectivity spectrum.[41, 44]. The wavelength of the peak is determined by the period of the waveform used in preparation. The porous Si layer is then methylated to impart stability and hydrophobicity using an electrochemical grafting procedure.[45]

A protease sensor is prepared from the porous Si photonic crystal following the procedure of Figure 2.1. A solution of the hydrophobic, naturally occurring protein zein in methanol (10 mg/ml) is spin-coated onto the methylated porous Si film, creating an even protein coating. Zein tends to form multilayered films on silicon surfaces through molecular and electrostatic interactions.[46] In the present case, spectral measurements indicate that a similar layer is produced on the porous Si film; the pores are small enough (ca. 10 nm) that only a small amount of the intact protein (24 kDa, 16 x 4.6 x 1.2 nm^3)[46] infiltrates the porous

Si film (Figure 2.2). The presence of the zein coating is observed as a thin layer that does not obscure the reflectivity spectrum of the underlying photonic crystal.

The wavelength of the spectral peak reflected from the porous Si photonic crystal is dependent on the refractive index of the porous Si matrix. Changes in refractive index (*n*) of the porous Si layer, as solution (*n* = 1.34) or protein fragments (*n* = 1.42) replace air (*n* = 1) in the pores, result in a redshift of the reflectivity peak, producing an observable color change[47] . This color change was used to measure protease activity in 1μL droplets.

2.3 Experimental

2.3.1 Sample Preparation

Preparation of one-dimensional photonic crystals of porous silicon involved anodic etching of degenerate p-type, boron-doped, (100)-oriented silicon wafers (Siltronix, Inc.) with resistivity < 2 mΩ-cm in a 3:1 (v/v), 49% aqueous HF/ethanol (EMD Biosciences) solution. A Teflon etch cell that exposed 1.2 cm^2 of the silicon wafer was employed. The current density was modulated with a sinusoidal waveform ranging between 8.3 - 38 mA/cm^2, with a period of 9s for 60 cycles, generating a multilayered optical structure known as a rugate filter.[48] Methylation of the porous Si film was achieved by passing a cathodic current density of 5.4 mA/cm^2 through the porous Si film immersed in 3.5 ml of an electrolyte solution containing 0.5 M iodomethane (99+%, Alfa Aesar) and 0.2 M anhydrous lithium iodide (99%, Arcos Organics) in anhydrous acetonitrile (Fisher Chemicals) for 2 min.[45] Samples were illuminated with 200 mW/cm^2 of white

(tungsten lamp) light during the methyl grafting procedure. The electrolyte solution was removed and the sample rinsed sequentially with glacial acetic acid, acetonitrile, and ethanol. A 200 μL aliquot solution of 10mg/ml zein (Sigma) in methanol (Fisher Chemicals) was then spin-coated onto the photonic crystal film.

2.3.2 Enzymatic Digestion Procedure

Active pepsin solutions were prepared by adding pepsin A (150 units/mg solid, Sigma) to a prepared 10 mM pH 2.0 buffer containing phosphoric acid (99.9%, Aldrich) sodium phosphate monohydrate (enzyme grade, Fisher chemicals), HCl (EM Science) and deionized water. Heat-inactivated pepsin solution was obtained by heating the above solution to 100 ℃ for 5 min. The pH-inactivated pepsin solution was prepared in pH 10.0 buffer (Fisher chemicals). Pepstatin inhibitor (Sigma) was dissolved in 9:1 methanol: acetic acid (v/v) and mixed with activated pepsin solution. Pronase E (Type XIV, ~4 units/mg solid, powder, Sigma) was added to Dulbecco's phosphate buffered saline solution containing calcium chloride and magnesium chloride (Sigma). Controls included deionized water and Dulbecco's phosphate buffered saline. Aliquots of 1 μL of the pepsin solutions or controls were deposited onto the zein-coated porous Si photonic crystal by microliter syringe. The sample was maintained in a humid chamber at room temperature for one hour, after which the sample was removed to the laboratory air and the solution allowed to evaporate in air for 10-20 min.

before performing the spectroscopic or microscopic measurements. Samples were not rinsed after the drying step.

2.3.3 Data Acquisition and Analysis

Interferometric reflectance spectra were obtained with an Ocean Optics S-2000 CCD spectrometer fitted with a microscope objective lens. The lens was coupled to a bifurcated fiber optic cable such that both illumination and detection of reflected light could be performed on the same spot on the sample, along an axis coincident with the surface normal. A tungsten light source was input to one of the two fiber ends and focused onto the center of the sample surface with a spot diameter of approximately 2 mm^2. Reflectivity data were recorded in the wavelength range 400-1000 nm, with a spectral acquisition time of 100 ms.

Spectral red shifts were determined from Gaussian fits to the spectral peaks. The function used to fit each spectrum is a sum of two Gaussian curves:

$$f(x) = Y_1+A_1*\exp(-((x-offset_1)/width_1)^2)+ Y_2+A_2*\exp(-((x-offset_2)/width_2)^2) \quad (1)$$

where Y_1 is the baseline offset, A_1 is the amplitude, $offset_1$ is the wavelength maximum, and $width_1$ represents the peak width of Gaussian #1. A_2, $offset_2$, and $width_2$ represent the corresponding values for Gaussian #2. A non-linear least-squares fitting routine involving iterative minimization of the sum of the chi-squared values, using the Levenberg-Marquardt algorithm, was applied (IGOR PRO program, Wavemetrics, inc.). The parameter Y_1 was set as a constant in the

fitting routine. Initial input values were obtained from a single Gaussian fit of the "in air" spectral peak (obtained before addition of protease). The quantity ($offset_2$-$offset_1$) is the total red shift upon addition of a given amount of protease.

2.4 Results and Discussion

2.4.1 Porous Silicon Modification and Characterization

Freshly etched porous silicon tends to have issues of stability as it easily corrodes and oxidizes in air and/or aqueous media. Chemical modification of a hydride terminated surface is thus important to impart stability. The chemistry used to functionalize the surface involved reductive electrolysis of alkyl iodide[45] (Figure 2.3). The derivatization step may occur either by direct reaction of the surface silicon radical with an alkyl radical [Figure 2.3, Eq. (3)], or by reduction of the silicon radical to the anion followed by nucleophilic attack on the organo halide [Figure 2.3, Eqs. (4) and (5)]. Solution-based silicon radicals are known to abstract halogen atoms from organo halides, to produce Si˘X and the corresponding organic radical[49].

The FTIR spectrum of a freshly etched porous silicon sample (Figure 2.4) indicates the presence of hydrides with bands assigned to Si-Hx stretching modes at 2137cm^{-1}(νSi-H3), 2114cm^{-1}(νSi-H2), and 2087cm^{-1}(νSi-H). Bands characteristic of Si-H deformations are also apparent at 910cm^{-1}. After derivitazation of the surface, stretching vibrations of the terminal CH_3 group is apparent at 2959cm^{-1} and the formation of Si-C stretching mode at 766cm^{-1}. Although most of the grafting procedure is done in a deoxygenated environment,

there is the presence of vibration band in the region of 1200-1000cm-1 that corresponds to the asymmetric Si-O-Si stretching.

The photonic-crystal sensor needed to contain hydrophobic functional groups in order to more effectively exclude buffer solution from the porous structure. Methyl groups are grafted to the porous Si layer by the electrochemical reduction of CH_3I in acetonitrile as described above. After methyl grafting, the position of the reflectivity peak red-shifts when a drop of buffer solution containing protein digestion fragments is placed on the film (Figure 2.5). Pure buffer solution produces no significant change in color. The peptide and amino acid digestion products enhance the sensor's response by facilitating solution infiltration into the hydrophobic layer.

A secondary purpose of the methylation step is to improve the chemical stability of the porous Si layer. As-prepared porous Si corrodes rapidly in buffer solutions; the methylation step stabilizes the porous Si layer such that no significant degradation of the spectral properties occurs on the timescale of the present experiments[50]. When the zein layer is cast onto the porous Si film, the reflectance peak red-shifts by < 4 nm (Figure 2.2). If the zein protein is first digested with pepsin and the solution then spotted on the porous Si film, the reflectance peak shifts by a larger amount, 34 nm (Figure 2.5). This indicates that the intact zein protein is effectively excluded, whereas the digestion products are better able to infiltrate the porous Si film.

2.4.2 Detection of Protease Activity with Porous Silicon Photonic Crystals

The zein coating, combined with the methylation of the porous Si matrix, effectively prevents infiltration of aqueous solutions and their contents until the protein layer is digested by the action of a protease. In order to perform the protease assay, a 1μL drop of aqueous buffer containing protease is placed on the top surface of the zein layer and the chip is maintained in a controlled-humidity environment at room temperature for 1 hour. The chip is then removed from the chamber and allowed to dry. A visibly detectable color change in the photonic crystal is observed for pepsin quantities as low as 7.2 pmol (240 ng) (Figure 2.6A). The reflectivity spectra obtained upon exposure of the structure to an analyte solution for 1 hour followed by drying allows quantification of protease activity. Reflectivity spectra obtained from zein-coated porous photonic crystals display a single strong peak corresponding to the stop band of the empty (air-filled) photonic crystal (Figure 2.6B)[44]. Etalon fringes due to Fabry–Pérot interference in the porous-Si film are also apparent in the spectra. The action of pepsin on the zein layer results in the appearance of a second peak, red-shifted from the first. This new peak is assigned to regions of the porous-Si photonic crystal that contain protease digestion products.

Introduction of protein fragments produces a red-shift in the photonic peak due to an increase in the total refractive index of the porous film. The Bruggemann effective-medium model predicts that the peak shift will be larger in spectra of samples containing larger quantities of protein fragments[51]. Consistent

with this, samples that have been exposed to higher concentrations of protease show greater spectral shifts. For samples treated with 1 μL aliquots containing > 14 pmol of pepsin, the spectra display two distinct peaks (Figure 2.6B) and the red-shift is clearly visible by eye (Figure 2.6A). For samples exposed to concentrations of pepsin < 14 pmol in 1 μL, the spectral shift can be resolved by applying a double Gaussian fit to the spectral profile, allowing reliable detection of as little as 7.2 pmol of pepsin (Figure. 2.7). For protease quantities in excess of 7.2 pmol, the peak corresponding to the presence of digestion products (at longer wavelength in the reflectivity spectrum) is more intense than the shorter-wavelength peak. As with the correlation of the spectral shift to the protease concentration, the observed increase in peak intensity is consistent with an increase in the quantity of digestion fragments produced by the larger concentration of protease. The amount of protein infiltrated in the porous film can be obtained from a quantitative fit of the shift in the Fabry–Pérot interference fringes observed in the spectrum to the single-layer interference equation and the Bruggeman effective-medium model[26]. Assuming an average refractive index of 1.42 for the protease digestion products, the fractional filling of the film for a sample exposed to 7.2 pmol of pepsin is calculated to be 20 ±6%.

Several control experiments were performed, following the same protocol as that used for the active pepsin assay described above. A 1 μL drop of the pH2 buffer solution placed on the zein methylated film produces no visible color change and a spectral red-shift of < 2 nm (see Figures 2.6A, 2.8). Controls using heat-denatured pepsin, active pepsin in pH10 buffer (where pepsin has minimal

activity[23]), or active pepsin in a solution containing the inhibitor pepstatin[24] produce negligible changes in the observed color and peak positions (see Figure 2.8A, 2.8B). Use of the protease Pronase E produces similar results to those observed with pepsin (Figure 2.9).

2.5 Conclusions

The simple protease-activity assay described here can detect picomole quantities of protease at room temperature. The silicon-chip-based system could be compatible with a high-throughput array configuration important for many biotechnological applications, such as medical diagnostics, quality-control testing, enzyme purification, cell-extract assays, or drug discovery. The main advantage of this system is its ability to operate with natural enzymatic substrates and amplify enzyme activity to the unaided eyed. Although demonstrated with the maize-derived protein zein, in principle a variety of native substrates, including those targeted by DNases and RNases, could be used.

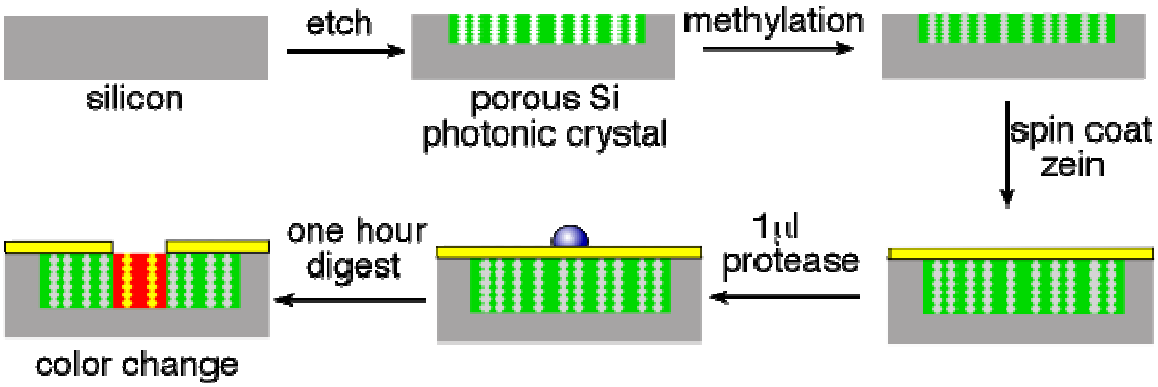

Figure 2.1Enzymatic assay using a protein-coated porous Si photonic crystal. A hydrophobic, one-dimensional photonic crystal is prepared by electrochemical etch of Si, followed by electrochemical grafting of methyl species to the inner pore walls. A thin layer of zein is then added. The assay is carried out by addition of a small drop of solution containing active protease (pepsin or pronase E in the present work), which digests the protein layer. Infiltration of proteolytic cleavage products to the photonic crystal leads to a color change that is readily observable to the unaided eye.

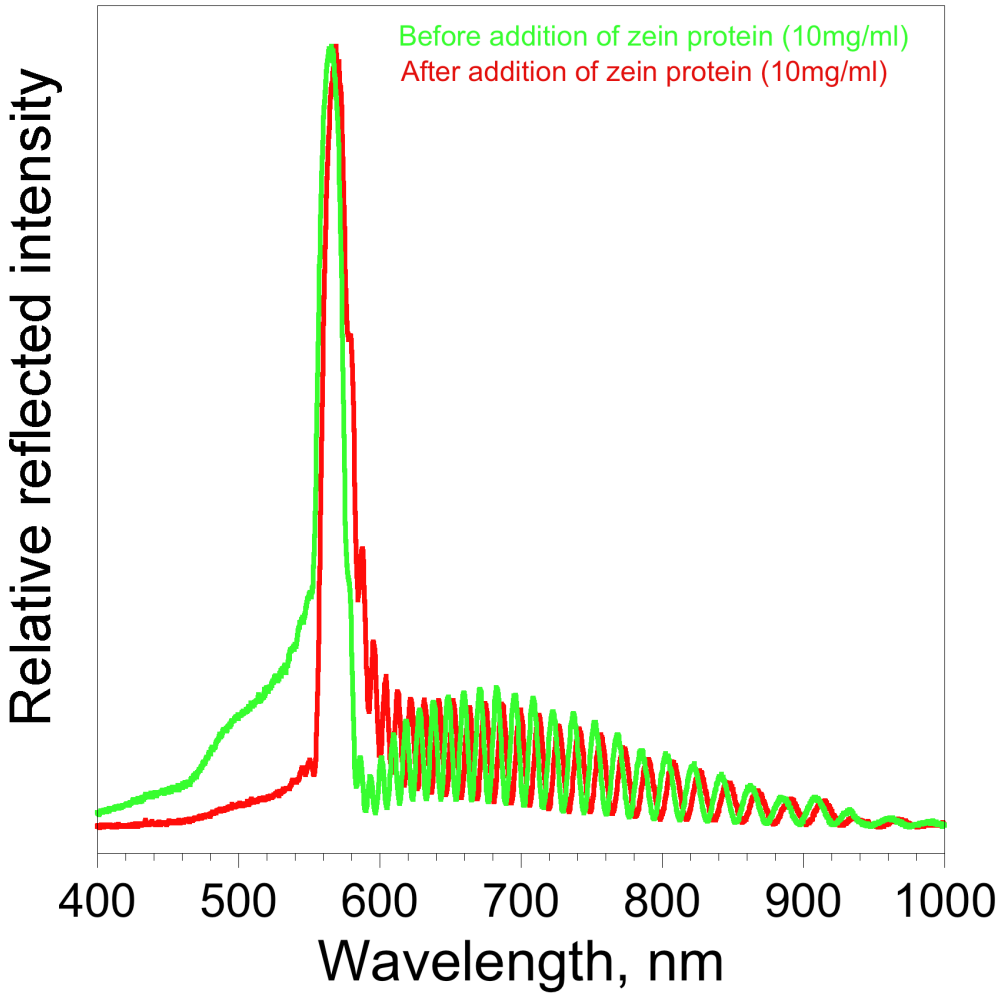

Figure 2.2 Reflectance spectrum of a methylated porousSi crystal film before and after addition of the zein coating. Reflectance spectra were obtained on the same spot on a methylated porous Si film before (green trace) and after (red trace) addition of zein protein. The amount of red shift is less than 4 nm, indicating that the zein protein does not infiltrate the pores appreciably.

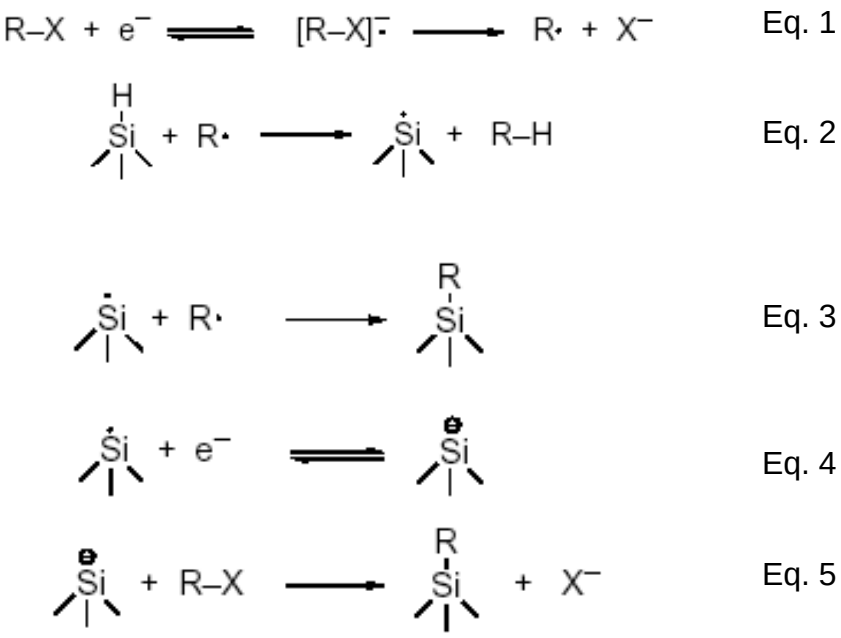

Figure 2.3 Chemical modification of porous silicon

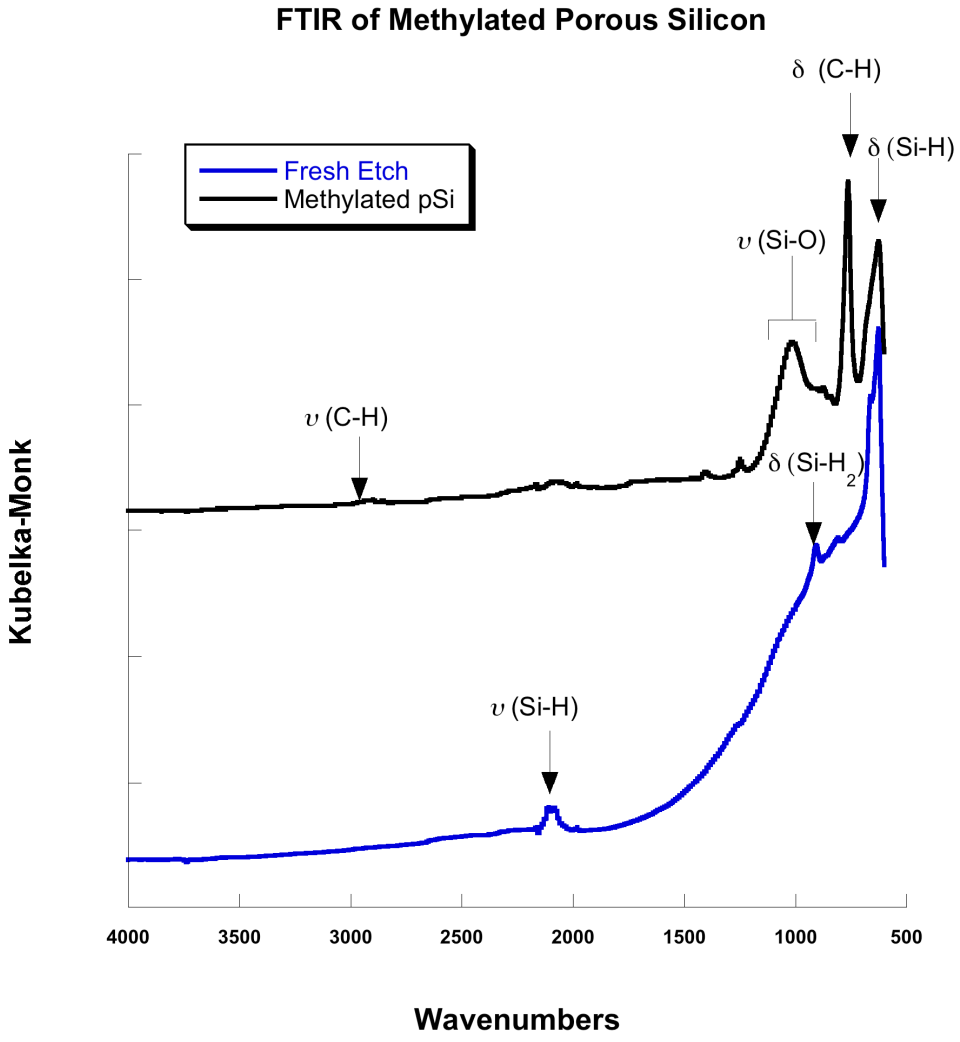

Figure 2.4 FTIR of functionalized porous silicon

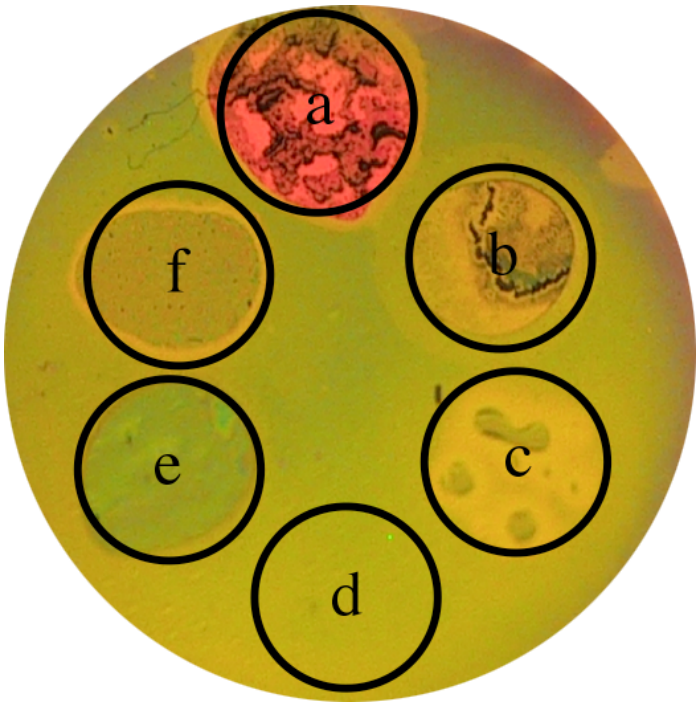

Figure 2.5 Control experiments using methylated porous silicon film without zein coating. (a) Film spotted with a solution of zein fragments, generated by digestion in a pH 2.0 buffer solution containing 1mg/ml zein with 1mg/ml of the protease pepsin (digestion for 1 h at room temperature); (b) Film spotted with pH 7.4 PBS buffer; (c) Film spotted with pH 2.0 buffer; (d) Film spotted with deionized H_2O; (e) Film spotted with pH 10.0 buffer; (f) Film spotted with active protease pepsin (1mg/ml) in pH 2.0 buffer. All spotting experiments used a 1 μL aliquot of solution, and the incubation protocol was the same as described in the text.

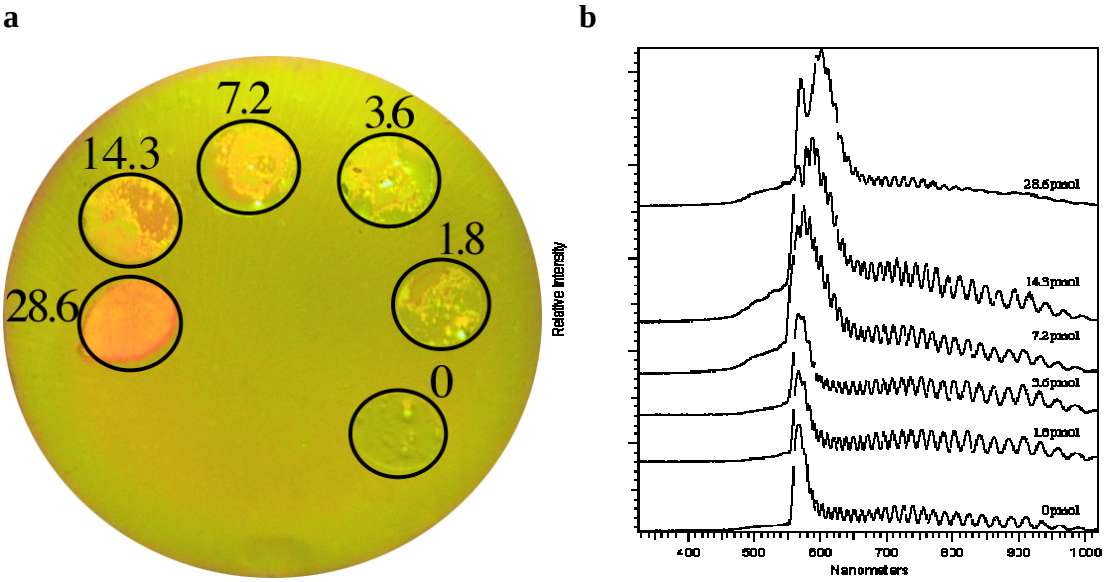

Figure 2.6 Dilution series for active protease pepsin, showing the effect of pepsin concentration on the observed color change in the porous Si photonic crystal. (a).One μl-aliquots of buffer solutions (pH 2.0) containing the indicated amounts (in pmol) of active pepsin were placed on the zein-coated photonic crystal wafer and allowed to react for 1h. A distinct color change of the photonic crystal from green to red is observed for quantities of pepsin as low as 7 pmol. The sample shown is 1.2 cm in diameter.(b).Each spectrum corresponds to a spot in the dilution series indicated in Figure 2.4.a. A peak assigned to regions of the porous Si photonic crystal that have become infiltrated with protease digestion products appears to the low energy side of the original spectral band. The original peak (unfilled with digestion products) is indicated with a vertical dashed line. Amount of enzyme spotted is indicated above each trace. Spectra are offset along the y-axis for clarity.

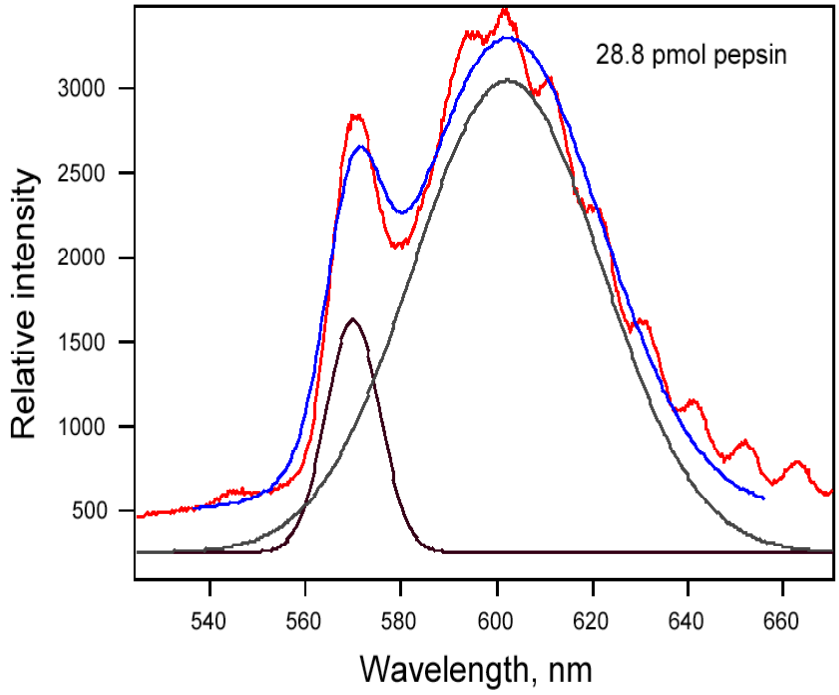

Figure 2.7 Reflectivity spectra and the results of the double Gaussian fits used to determine limits of detection for the method. The red trace is the reflectivity spectrum of the zein-coated porous silicon photonic crystal. The blue trace plots the result of the double Gaussian fit. The two individual Gaussian peaks from the fit are shown as the black traces. Each spectrum was obtained after the drying step discussed in the experimental section. Drying effects, scattering, changes in incident angle of the probing optics, and other experimental variables can cause shifts in the reflectivity spectrum. The presence of two peaks in the spectrum allows compensation for such effects; the peak at short wavelength derives from regions that are not infiltrated by protein fragments, and provides an internal standard in the measurement.

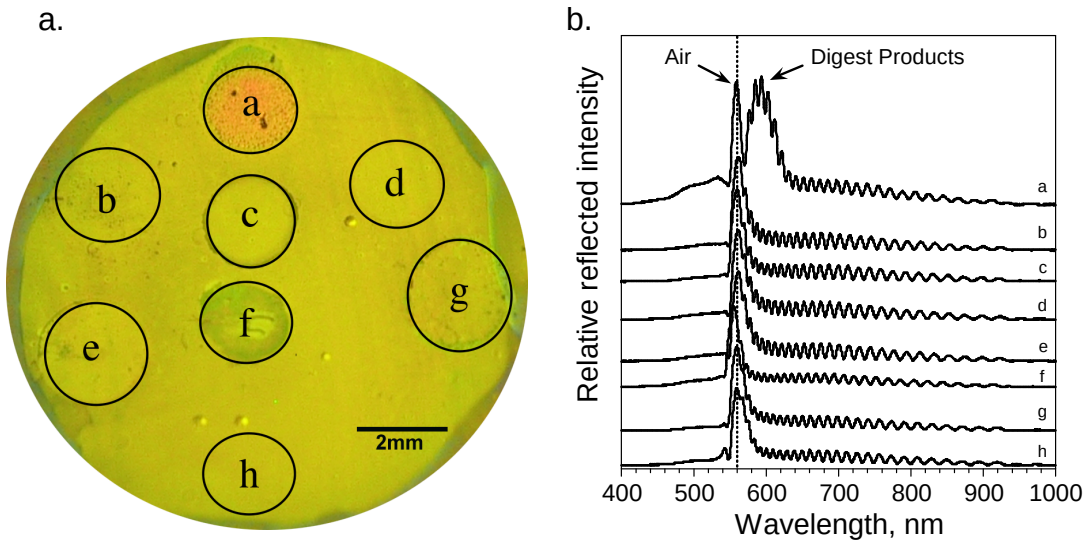

Figure 2.8 Control experiments using methylated porous silicon film with zein coating. (a) Film spotted with a 1 μl solution of active protease pepsin (1mg/ml) in pH 2.0 buffer; (b) Film spotted with pH 2.0 buffer; (c) Film spotted with de-ionized water; (d) Film spotted with pH 7.4 PBS buffer; (e) Film spotted with pH 2.0 buffer solution containing 1mg/ml of pepsin that had been inactivated by treatment with the inhibitor pepstatin (1:1 pepsin:pepstatin); (f) Film spotted with pH 10.0 buffer solution containing 1mg/ml of pepsin (pepsin is inactive at pH 10); (g) Film spotted with pH 2.0 buffer solution containing 1mg/ml of pepsin that had been inactivated by heat treatment. (h) A pristine region of the zein-coated chip that was used to obtain the background spectrum of Figure S4. This region has not been exposed to any of the sample or control solutions. All spotting experiments used a 1 μL aliquot of solution, and the incubation protocol was the same as described in this chapter. B. Reflectance spectra of the methylated porous Si chip from Figure 2.8A, after completion of the reaction and drying of the solutions. Spectra correspond to the lettered regions of Figure 2.8A.Spectra are offset along the y-axis for clarity.

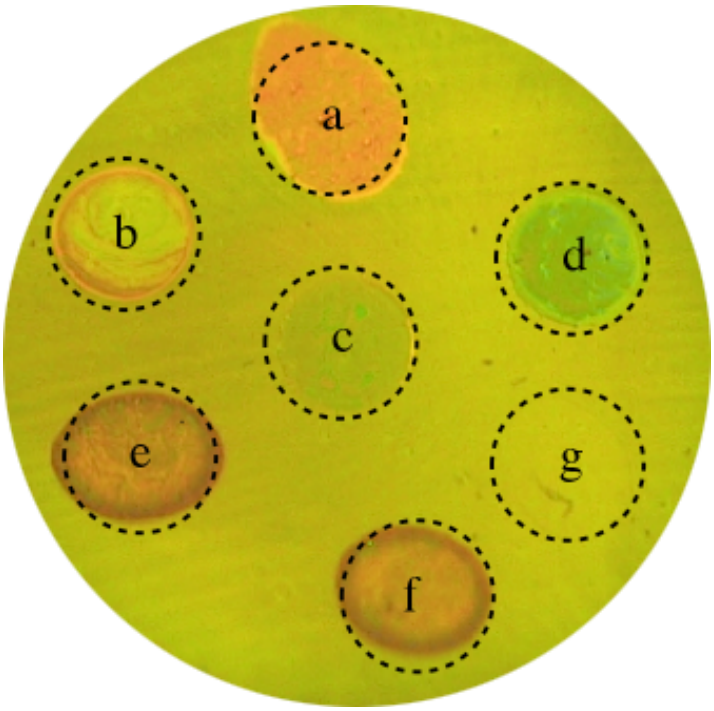

Figure 2.9 Protease activity assay comparing pepsin with pronase E. Assay protocol is the same as described in the text and above, using 1 μl aliquots of solution. (a) pepsin (1mg/ml) in pH 2.0 buffer; (b) pronase E (1mg/ml) in deionized H_2O; (c) pH 2.0 buffer; (d) heat-denatured pronase E in PBS; (e) and (f) represent replicate doses of pronase E (1mg/ml) in PBS; (g) deionized H_2O. Note that the activity of the Pronase E used in these experiments is less than the activity of Pepsin (4 unit/mg solid vs. 150 unit/mg solid, respectively). A unit of pronase E is defined by hydrolysis of casein to produce a color equivalent to 1.0 mmole (181 μg) of tyrosine per min at pH 7.5 at 37 ℃ (color by F olin-Ciocalteu reagent). One unit of pepsin will produce a change in absorbance at 280 nm (ΔA_{280}) of 0.001 per min at pH 2.0 at 37 ℃, measured as th e TCA-soluble products using hemoglobin as substrate. (Final volume = 16 ml. Light path = 1 cm)

Chapter two, in part, is a reprint (with co-author permission) of the material as it appears in the following publication: Orosco, M.M., Pacholski, C., Miskelly, G., Sailor, M.J., Protein-Coated Porous-Silicon Photonic Crystals for Amplified Optical Detection of Protease Activity. ***Adv. Mater.*** 2006, 18, 1393-1396. The author of this dissertation is the primary author of this manuscript.

3 Measuring Protease Activity in a Porous Silicon Double Layer

3.1 Abstract

Proteases in biological systems are often red flags for various disease states such as cancer[1, 3], stroke[1], and neurodegeneracy[10 52]. Means of quantifying protease activity are based on fluoresence resonance energy transfer[18, 36, 53, 54] of engineered peptides or whole protein substrates. Major drawbacks to these substrates are that they require modification to the native substrate in order to incorporate the relevant indicator chemistries. Screening for potential drug candidates using these methods is time consuming and suffer from small Stoke shifts, photochemical degradation, pH sensitivity and they are toxic. This work involves porous silicon made with high and low current densities (creating a double layered nano-reactor) that is able to detect protease activity. The pore length and diameter can be tuned electrochemically to exclude large proteins. Active protease is adsorbed into the first layer and excluded from the second layer. Introduction of substrate to the first layer produces small fragments that infiltrate the pores of the second layer. This produces an observable change in effective optical thickness. Quantitative parameters such as Michaelis-Menten kinetics and enzymatic activity can be extracted from this system. This system can be used for high-throughput or clinical screening of inhibitors with patterned arrays through standard lithography methods.

3.2 Introduction

A common method to quantify protease activity is based on Fluorescence

Resonance Energy Transfer[36, 53] (FRET) measurements using fluorescently tagged protein substrates. A major drawback to this approach is that a chemically modified substrate may not exhibit the same reactivity as the native substrate. While fluorescent labels can provide high sensitivity, the attachment of a probe requires an extra step that increases analysis time and complexity. In addition, fluorescent probes can be subject to photochemical degradation and pH-dependent responses. Porous Si-based interferometers operate by measuring a change in refractive index in a volume of solution contained within the porous nanostructure, and they have been shown to provide a simple, label-free method for detection of proteins that minimizes the quantity of reagents used[38, 55-58]. Recently, the advantage of using more complicated porous Si optical structures to correct for zero-point drift or non-specific binding has been demonstrated[26, 59]. Additionally, recent work has shown how catalytic reactions can be harnessed to improve sensitivity of these nanosensory systems[60, 61].

The two-layer porous Si nanostructure was prepared by electrochemical etching of silicon in an HF-containing electrolyte. The double layer was then thermally oxidized (600 ℃ for 1.5 h, in air) to ge nerate a stable silicon oxide (SiO_2) surface. The size, shape, and population of the pores in a film are determined by the current, allowing one to “dial in” a specific porosity pattern[62]. Thus a double layer containing large pores on top of small pores is prepared by decreasing the applied current density midway through the etch, resulting in the abrupt decrease in pore size shown in the cross-sectional scanning electron microscope (SEM) image of Figure 3.1. The tunability of the pore etching process

provides a convenient means to build such nanostructured matrices that can act as reservoirs[63, 64] or size exclusion membranes[65, 66]. The programmability can also be used to build optical structures with useful sensing properties.

The average diameter of the pores in the present structure is ~100 nm in the top layer and ~6 nm in the bottom. Being smaller than the wavelength of visible light, the features in this nanostructure do not scatter light, and the sample displays well-resolved Fabry-Pérot interference fringes in the optical reflectivity spectrum (Figure 3.2). The reflectivity spectrum displays an interference pattern that arises from a combination of Fabry-Pérot interference from the very flat interfaces bordering the two layers.

It has been shown that the Fourier transform of the reflectivity spectrum yields peaks that correspond to the optical thickness $2n_iL_i$ of each layer or combination of layers, where n_i is the refractive index and L_i the thickness of layer i in the stack[26, 59]. The optical spectrum can be used to sense molecules because it is sensitive to the refractive index of any substance filling the pores. Most biomolecules and proteins have a refractive index of ~1.40, whereas aqueous buffers posses an index close to 1.34. The introduction or removal of a chemical or biochemical species from a porous layer is thus detected as a shift in the value of $2nL$[26, 38, 59, 61, 67]. Differential responses between two stacked layers have been used to correct for zero point drift in the detection of proteins and antibodies[26, 59]. The method is referred to as Reflective Interferometric Fourier Transform Spectroscopy, or RIFTS. For the double-layer structure used in the present work, it is found that the method can also quantify the partitioning of

molecules between the two layers, by measurement of the position of the peaks in the Fourier transform spectrum that correspond to each layer.

The nano-reactor layer is loaded with an enzyme by electrostatic adsorption from an aqueous buffer solution at pH 2.0 (Figure 3.3). Pepsin was chosen as a model protease because it and its reaction kinetics are well-characterized[68, 69]. Pepsin is continually cycled through a flow cell containing the porous Si sample for 90 min, at which point the cell is flushed with pure pH 2.0 buffer to remove excess pepsin not adsorbed to the sample. The adsorption of pepsin into the nano-reactor layer is detected as a ~15 nm increase in the value of 2nL in the Fourier transform spectrum, corresponding to a loading of 200 ng of enzyme in the 5 nanoliter volume probed by the optic (Table 3.1). The surface of oxidized porous Si is negatively charged at pH 2.0[55], leading to a strong attraction between the surface and pepsin, which carries a net positive charge at this pH[70]. Because of this non-specific adsorption, the effective concentration of enzyme in the pores is ~ 2 mM, representing an increase by a factor of 70 relative to the free solution concentration. The relatively large pepsin molecule (35 kDa, 10 x 6 x 20 nm)[71] is excluded from the smaller pores in the second layer of the porous Si double layer.

3.3 Experimental

3.3.1 Sample Preparation

Porous Si samples were prepared by anodic electrochemical etch of highly B-doped (p^{++}-type), (100)-oriented silicon wafers with resistivity of ~ 1 mΩ-cm (Siltronix), in a 3:1 (v/v), 49% aqueous HF/ethanol solution. A Teflon etching cell that exposed 1.2 cm^2 of the silicon wafer was employed. The exposed polished surface was etched at a current density of 707 mA/cm^2 for 10 s followed by a current density of 44 mA/cm^2 for 170 s. Samples were then thermally oxidized at 600 ℃ for 1.5 h. Pepsin (150 units/mg sol id, Sigma Chemicals) was dissolved in a 10 mM pH 2.0 buffer containing phosphoric acid (99.9%, Aldrich Chemicals), sodium phosphate monohydrate (enzyme grade, Fisher chemicals), HCl (EM Science), and de-ionized water. The nano-reactor was loaded with pepsin by cycling 3.5 mL of a pH 2.0 solution 28 μM pepsin through a flow cell fitted with a 1 cm-diameter optical window through which the reflectivity spectrum of the nano-reactor could be monitored.

3.3.2 Enzymatic Digestion Procedure

The α-casein substrate (Sigma-Aldrich Chemicals) was dissolved in pH 2.0 buffer and heated to 37 ℃ until fully dissolved. For each experiment, 3.0 mL of solution of the requisite concentration was cycled through an airtight flow-cell. For the enzyme inhibition studies, pepstatin A inhibitor (Sigma-Aldrich

Chemicals) was dissolved in a minimal amount of 9:1 methanol: acetic acid (v/v) solution. The solution was diluted with pH 2.0 aqueous buffer to the desired concentration. The pepsin-loaded nano-reactor in the flow cell was then incubated with a continuously flowing solution of the inhibitor and the casein substrate.

3.3.3 Data Acquisition and Analysis

Interferometric reflectance spectra were collected by using an Ocean Optics S-2000 CCD spectrometer fitted with a microscope objective lens coupled to a bifurcated fiber optic cable. A tungsten light source was focused onto the center of the porous Si sample surface with a spot size approximately 1.5 mm in diameter. Both the illumination of the surface and the detection of the reflected light were performed along an axis coincident with the surface normal. Reflectivity spectra were recorded in the wavelength range 400-1000 nm, with a spectral acquisition time of 20 ms. Typically 100 spectral scans (2 s total integration time) were averaged for Fourier transform processing. Details of the Fourier transform and spectral data fitting routines are published elsewhere[26].

3.3.4 Enzyme Kinetics

Initial reaction velocity (V_o) was obtained using a linear fit of the Δ2nL vs time plot, obtained from Layer 2 of the structure. Data acquired between 1200 and 1800 s after addition of α-casein were used in the fit (the dead-time in the tubing leading to the cell was ~360 s). The initial rates for each concentration of

substrate were plotted against the concentration of α-casein. A non-linear least-squares fit was used to determine the Michaelis-Menten parameters. It was assumed that the steady-state value of Δ2nL is directly proportional to the steady-state product concentration in the layer. The V_{max} value from the least-squares fit is then converted from units of Δ2nL second^{-1} to μM min^{-1} using the linear relationship of Figure 3.7b For inhibition studies, initial velocity rates were determined by a linear fit of the Δ2nL-time plots at the point of inflection (typically 360 s after addition of substrate). Errors quoted are > 95% CI.

3.4 Results and Discussion

3.4.1 Relationship Between 2nL and Products

Reactions were carried out in the enzyme-loaded nanoreactor by introducing various substrate/inhibitor combinations into the flow stream of the cell. The reactions were monitored in real-time by acquisition of reflectivity spectra from the double-layer; the Fourier transform provides a direct measure of the amount of protein infiltrated in each layer. Figure 3.4 (and Figures 3.5, 3.6) shows the effect of introduction of the protein substrate α-casein into the nanoreactor. The top layer of the nanostructure (Layer 1), containing 100 nm-diameter pores, admits α-casein and the value of the optical thickness, 2nL, initially increases as protein accumulates in this layer. The value of 2nL decreases as pepsin digests the protein and the digestion products escape into solution and into Layer 2 of the reactor. The value of 2nL for this lower layer

increases as the smaller products of enzymatic digestion diffuse into the ~6 nm-diameter pores of the lower nanostructure. Control experiments performed with no pepsin (or with an inhibitor present) verify that intact α-casein does not enter the small pores of Layer 2. The digestion results are similar if the enzyme is loaded from a more complex buffer solution resembling Eagle's medium, that contains a mixture of amino acids, sugars, and vitamins (Figure 3.6). It is important to point out that the temporal behavior of the two layers, in particular the transient of Layer 1, is a characteristic of the action of the enzyme on the substrate. Introduction of small molecules that are not digested by the enzyme produce a signal-time characteristic in both of the layers that are similar to that observed in Layer 2 for the digested substrate.

3.4.2 Michaelis-Menten Enzyme Kinetics

The optical spectra can be used to quantify the kinetics of the enzymatic reaction. Figure 3.7(a) shows Δ2nL vs time traces obtained for several different initial concentrations of α-casein. The response of Layer 2 is monitored; its small pores exclude the intact protein and the protease while admitting the smaller digestion products generated by the action of the protease. The quantity 2nL is proportional to mass[58], and so the increasing value of Δ2nL as a function of time depicted in Figure 3.7 is indicative of the entry of protein fragments into Layer 2. As expected, the initial slope and the final steady-state value of the traces in Figure 3.7(a) increase with increasing concentration of α-casein. A double

reciprocal plot of the steady-state value of Δ(2nL) and [α-casein] is linear (Figure 3.7(b)), consistent with a reaction that is 1st order in substrate.

Analysis of the data involves an assumption that the change in the optical measurement 2nL relates to mass of material entering or leaving the porous layer. The relationship is established by Figure 3.7b. These data are used to convert Δ2nL into concentration of casein by the following:

Δ2nL from the 2nd Layer were converted using the linear fit in the plot 1/Δ2nL vs 1/(casein concentration), Figure 3.7(b):

$$y=mx + b$$

$$y=1.0609e\text{-}7x + 0.0081304$$

The value of x is the inverse of the substrate concentration and can be solved by rearranging the equation:

$$x= m/(y-b);\ y=1/\Delta 2nL \qquad \text{Eq. 3.1}$$

The converted concentration values were then plotted versus time in minutes.

The data are consistent with the known kinetics of the enzyme in free solution. Initial reaction velocity (V_o) is typically characterized as the mass of product formed per unit time during the initial stage of conversion of substrate to product. In the case of the nano-reactor, the mass of products generated is proportional to the value of Δ(2nL) measured in Layer 2. V_o was obtained by a linear fit of the initial phase of the curves depicted in Figure 3.7(a). A non-linear least-squares fit of V_o vs concentration of substrate α-casein (Figure 3.8) was

performed. Higher concentrations of a-casein produce larger changes in the quantity 2nL measured from Layer 2 because a greater mass of substrate is digested per unit time. The reaction velocity (V_o) is taken as the slope of the initial, linear region of the curves shown in Figure 3.7(a) of the main text (first 30 min). The initial reaction velocity (V_o) is then plotted versus the concentration of α-casein substrate. The data are then fit (non-linear least-squares) to the Michaelis-Menten relationship:

$$V = V_{max}[S]/(K_m + [S]) \qquad \text{Eq.3.2}$$

where (V) is the initial velocity, K_m is the Michaelis constant, V_{max} is the maximum velocity, and [S] is the concentration of substrate α-casein. This calculation yields a value of 0.35 μM/min for the maximum reaction velocity (V_{max}) and 18 μM for the Michaelis-Menten constant (K_m). These kinetic parameters are somewhat smaller than the literature values for pepsin (V_{max} = 1.20-2.69 μM/min; K_m = 37-109 μM)[72]. The enzymatic reaction in the nanoreactor is thus apparently slower than in free solution, which may be a result of the restricted dimensions in the porous matrix or adsorption of substrate to the pore walls.

3.4.3 Enzyme Inhibition

Aspartic protease inhibitor pepstatin A was used to perform enzymatic inhibition studies. Pepstatin A is a competitive inhibitor of pepsin. This means

that pepstatin A will compete for substrate as it can freely difuse in and out of the active site. A good competitive inhibitor would signifantly lower the rate of catalysis. In this system, the amount of turn-over to product (Δ2nL) over time should be less. The initial rate of digestion of α-casein was quantified using a series of pepsin-infused nano-reactors that were treated with solutions containing various concentrations of α-casein and a fixed concentration of the inhibitor (1μM). In order to get the rate of inhibition (Ki), a non-linear least-squares fit of V_o vs. α-casein in the presence of 1μM pepstatin A was performed. The reaction velocity (V_o) is taken as the slope of the initial, linear region of the curves at the point of inflection shown in Figure 3.9. The initial reaction (V_o) is then plotted versus the concentration of α-casein substrate. The data are then fitted to a non-linear least-squares fit using the following Michaelis-Menton relationship:

$$V = V_{max\ app}\,[S]/(K_{m\ app} + [S]) \qquad \text{Eq. 3.3}$$

where (V) is the initial velocity, $K_{m\ app}$ is the apparent Michaelis constant, $V_{max\ app}$ is the apparent maximum reaction velocity, and [S] is the concentration of substrate α-casein. The fit yields values of K_m (apparent) of 0.30 mM and V_{max} (apparent) of 0.40 μM/min. In a competitive inhibitor model, the value of V_{max} (apparent) should be equal to V_{max} (= 0.35 μM/min), and K_m (apparent) should be larger than K_m (= 18 μM). Thus the values obtained from the nano-reactor are consistent with a competitive inhibition model.

For pepstatin A inhibition, a competitive inhibition model was used to find the inhibition constant, K_i:

$$K_{m\ app} = K_m(1 + [I]/K_i) \qquad \text{Eq.3.4}$$

Where $K_{m\ app}$ is the Michaelis-Menten constant in the presence of an inhibitor I, K_m is the Michaelis-Menten constant, [I] is the concentration of inhibitor, and K_i is the inhibition constant. The calculation yields a rate of competitive inhibition K_i of 84 nM, somewhat larger than the literature value of 1 nM[73]. The larger value of K_i relative to the literature is attributed to adsorption of the inhibitor in the porous nanostructure, leading to a reduction in the effective concentration of inhibitor available to the enzyme.

To show the extent of inhibition as a function of inhibitor concentration, different concentrations of Pepstatin A was cycled over the nano-reactor and then incubating with a-casein substrate. The Δ2nLwas monitored over time (Figure 3.11). As expected, increasing concentrations of inhibitor cause less Δ2nL over time. Although pre-incubation with inhibitor does inhibit the amount of protease activity, it could not be analyzed with a competitive enzyme model because both substrate and inhibitor have to be incubated together.

3.5 Conclusions

In summary, a self-reporting nano-reactor that is able to capture enzymes, host a catalytic reaction in a mesoporous cavity, isolate and quantify the reaction products, and provide information on the reaction kinetics in a volume of ~5 nanoliters has been demonstrated. This work provides a general method to

quantify kinetics of an immobilized enzymatic reaction. The specific example in this work involved quantification of protease activity, but the approach is applicable to a range of reactions of interest to the high-throughput analytical and synthetic communities, such as DNA amplification, polymerization, enzyme-linked assays, and protein purification.

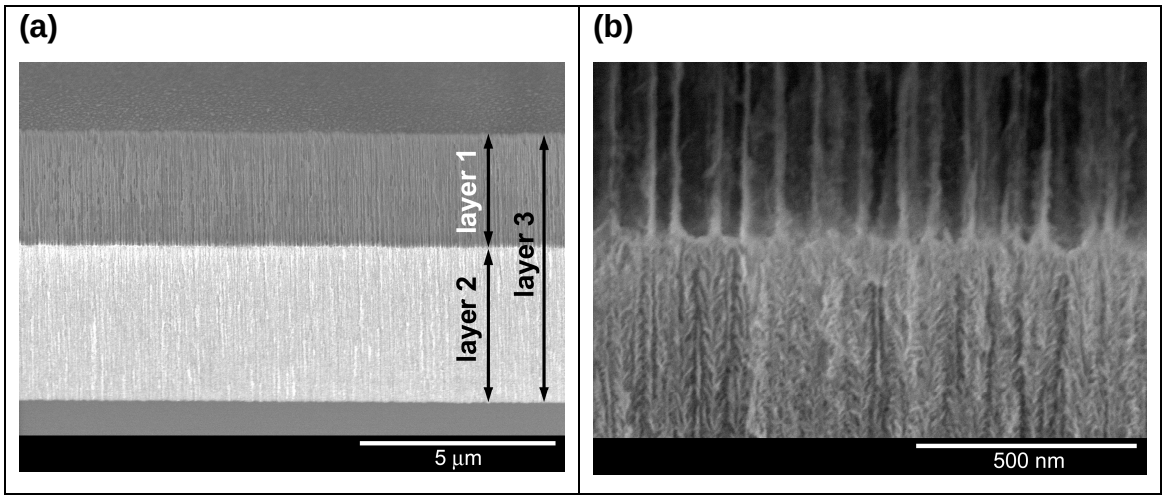

Figure 3.1 Scanning electron micrographs (secondary electron image, 5 kV) of the porous Si double-layer structure used in this study. (a) Image showing both porous layers, the top interface, and the Si substrate. (b) Close-up view of the interface between the two porous layers. The 1st layer contains pore sizes ranging from 80-120 nm and acts as a host layer for the protease pepsin in the present work. The 2nd layer has pores sizes ranging from 2-10 nm. This lower layer excludes the protease and large proteins such as a-casein (25 kDa) but admits the degradation fragments resulting from action of the enzyme on casein. Top layer is 3.2 μm thick, 75% porous; bottom layer is 4.4 μm thick, 37% porous.

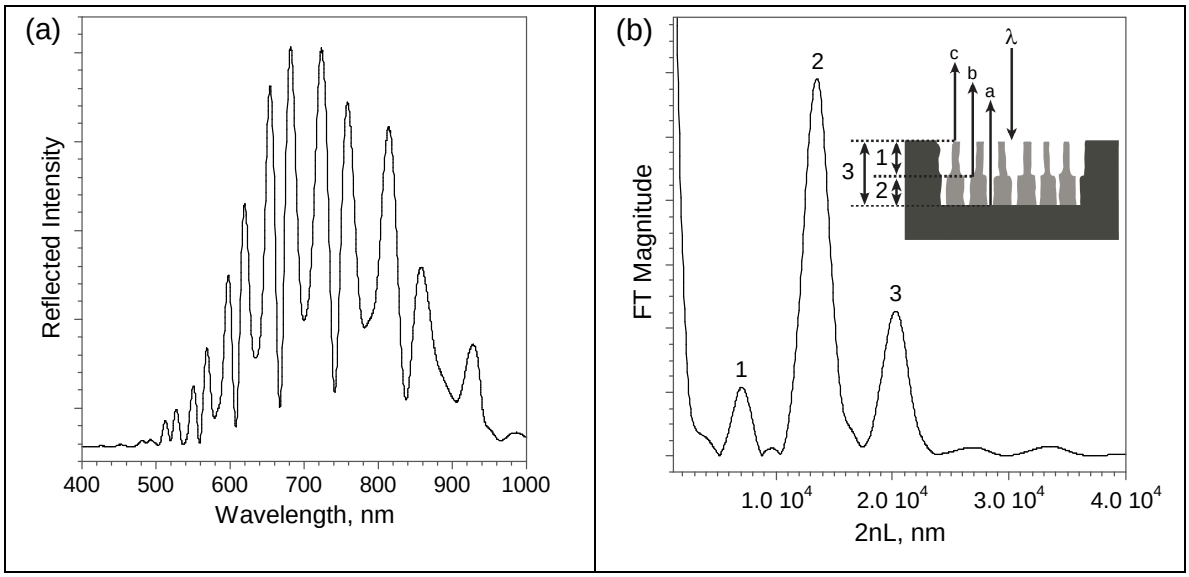

Figure 3.2 Reflectivity spectrum (a) and corresponding Fourier transform (b) of a porous Si double layer film. The peaks in the FT spectrum are assigned to the porous layers indicated in the inset. The three reflected interfering beams are indicated with the letters a, b, and c. Reflectivity trace is measured in air and is not corrected for instrumental spectral response.

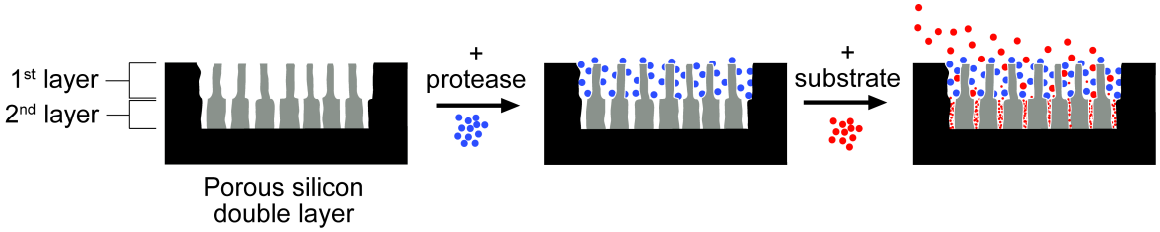

Figure 3.3 Nanoreactor used to process protein and quantify proteolytic activity. Active protease (pepsin) is absorbed into the first layer. The assay is then carried out by addition of substrate (α-casein). The pores of the second layer are too small to admit the protease or its substrate. However, digestion of the substrate by pepsin produces fragments sufficiently small to infiltrate the 2nd layer. The entire structure is probed by optical reflectivity, and the enzymatic reaction can be monitored in real-time.

Table 3.1 Calculation of Mass Loading of Pepsin.. The mass loading of pepsin was determined from the optical reflectivity spectrum by application of the Bruggeman effective medium model. Table S1 contains the assumptions and measurements that went into the calculation. A three-component Bruggeman approximation was applied to model the refractive index of the layer (see: Pickering, C., Beale, M.I.J., Robbins, D.J., Pearson, P.J. & Greef, R. Optical studies of the structure of porous siicon films formed in p-type degenerate and non-degenerate silicon. J. Phys. C *17*, 6535-6552 (1984)), and the resulting % loading of protein is 3%, the mass loading is 192 ng in the volume element in the path of the 0.15 cm-dia optical beam, or a total loading of 13 mg of pepsin in the (1.2 cm^2) chip.

TABLE S1: Parameters used to determine pepsin loading in nanoreactor		
Parameter	Value	Comment
Pepsin molecular weight	34.5 kDa	Fujinaga, M., Chernaia, M. M., Tarasova, N. I., Mosimann, S. C. & James, M. N. Crystal structure of human pepsin and its complex with pepstatin. Protein science : a publication of the Protein Society 4, 960-72 (1995)
Pepsin refractive index	1.43	
Buffer refractive index	1.33	
Porous SiO_2 refractive index	1.90	
Pepsin density	1.42 g/mL	Fischer, H., Polikarpov, I. & Craievich, A.F. Average protein density is a molecular-weight-dependent function. Prot. Sci. 13, 2825-2828 (2004).
Optical probe spot size (dia)	0.15 cm	
1^{st} thickness	3104 nm	
1^{st} porosity	75.5%	
2nL value in buffer, before loading pepsin	9104 nm	
2nL value in buffer, after loading pepsin	9119 nm	

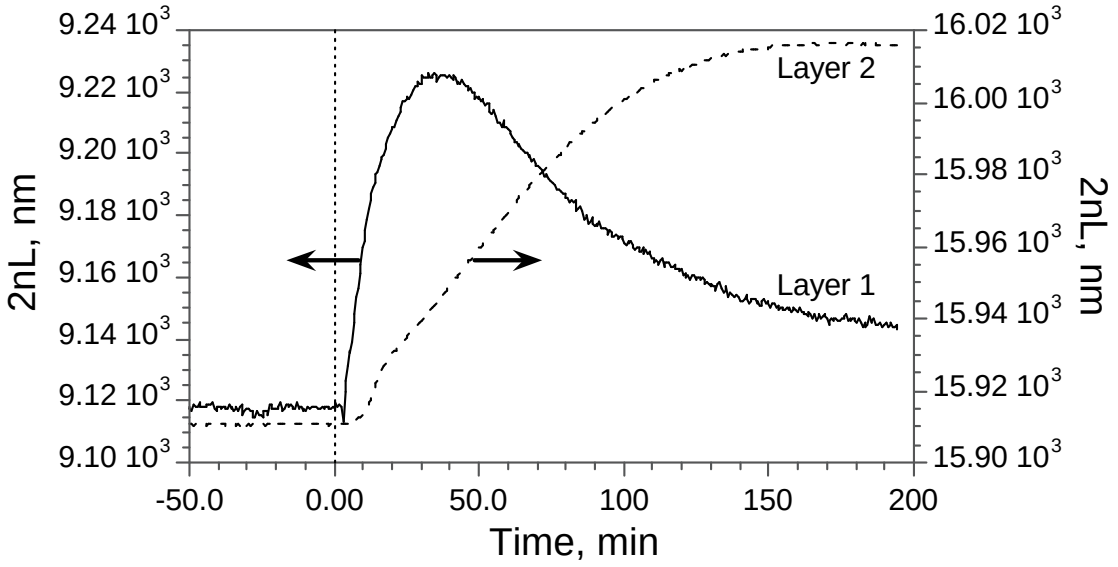

Figure 3.4 Optical response of the two layers in a pepsin-loaded nanoreactor to α-casein. The solid trace ("Layer 1") represents the top layer of the nanostructure containing 100 nm-diameter pores. The dashed trace ("Layer 2") corresponds to the bottom layer, which contains much smaller 6 nm-diameter pores. A solution of the a-casein protein substrate is introduced to the system at time = 0. The value of 2nL for Layer 1 initially increases as intact casein infiltrates the layer, and then it decreases as casein is digested by pepsin. The value of 2nL for Layer 2 increases as the smaller products of enzymatic digestion diffuse into the small pores of the layer.

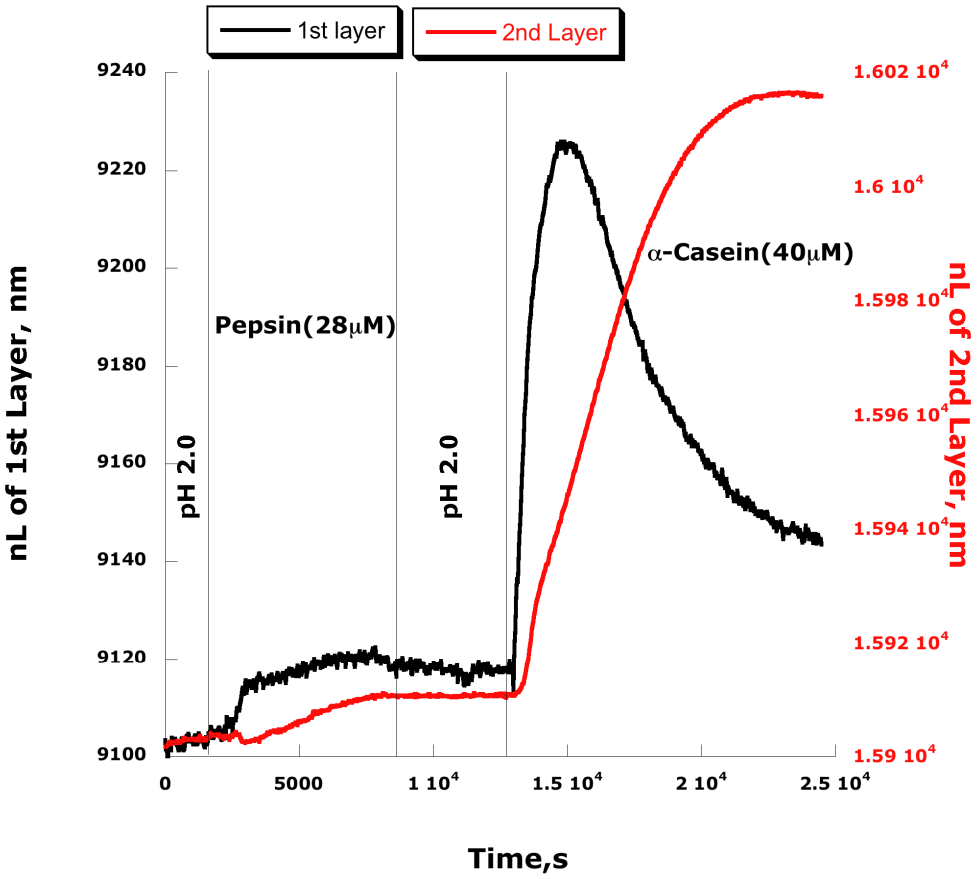

Figure 3.5. Time course of the optical response of both porous Si layers during enzymatic loading and subsequent digestion. In the beginning of the experiment, the porous Si double layer sample is flushed with pH 2.0 buffer. A 28 μM solution of pepsin in pH 2.0 buffer is then introduced, and the optical thickness of Layer 1 is observed to increase, corresponding to ~3 % loading of pepsin (see calculations above). The enzyme is effectively excluded from Layer 2 due to its much smaller pore dimensions. The system is flushed with pH 2.0 buffer and the rest of the experiment proceeds as described in Fig 3 of the main text. The y-axis records the value of nL in the 1st (top, large pore) or the 2nd (bottom, small pore) layers, as indicated. The slight increase in optical thickness of the 2nd layer upon addition of pepsin indicates accumulation of pepsin at the interface between the two layers.

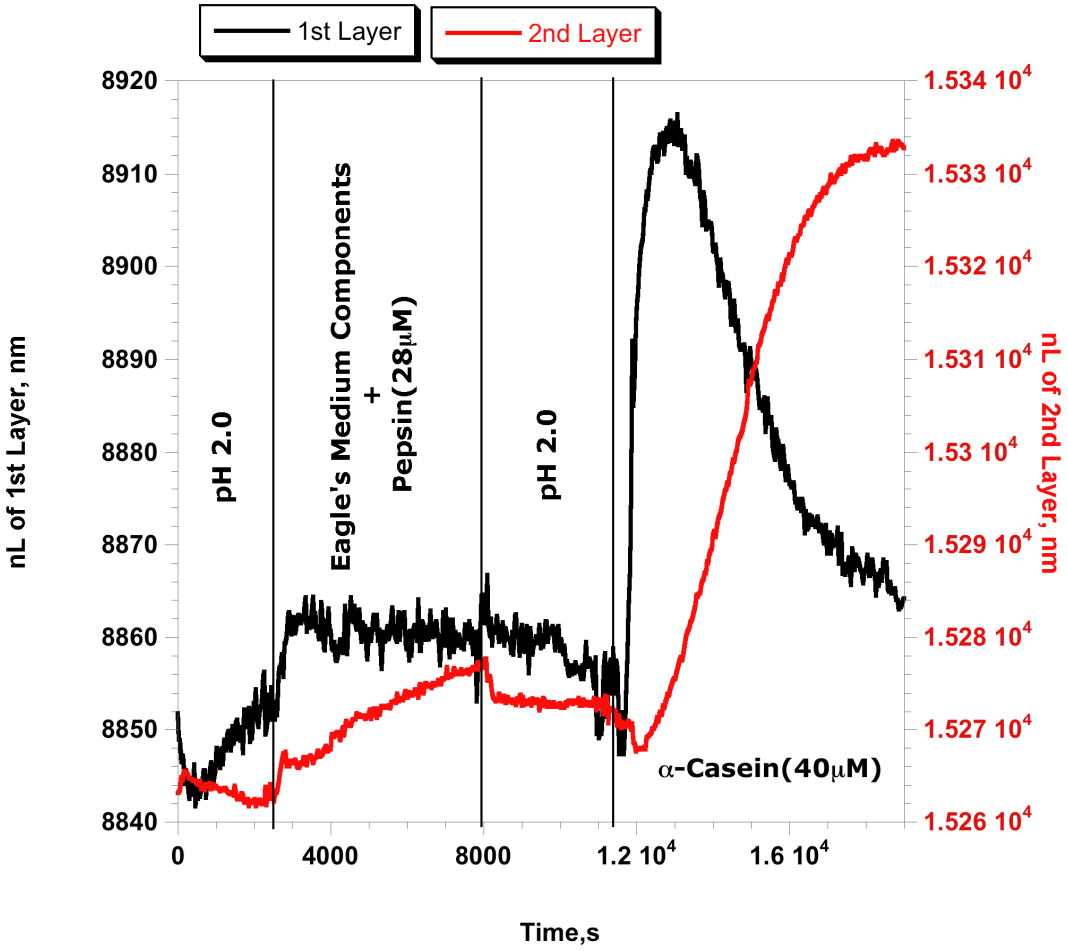

Figure 3.6 Time course of the optical response of both porous Si layers during enzymatic loading and subsequent digestion, enzyme loaded from a complex mixture. Experiment similar to that described in Figure 3.5, but the enzyme is loaded from a complex mixture. An array of amino acids, sugars and vitamins were mixed in a pH 2.0 buffer (closely resembling Eagle's Medium). Pepsin was then spiked into the media and the enzyme loading and substrate digestion experiment similar to that shown in Figure 3.5 was performed. The y-axis records the value of nL in the 1st (top, large pore) or the 2nd (bottom, small pore) layers, as indicated. The slight increase in optical thickness of the 2nd layer upon addition of pepsin indicates accumulation of pepsin at the interface between the two layers.

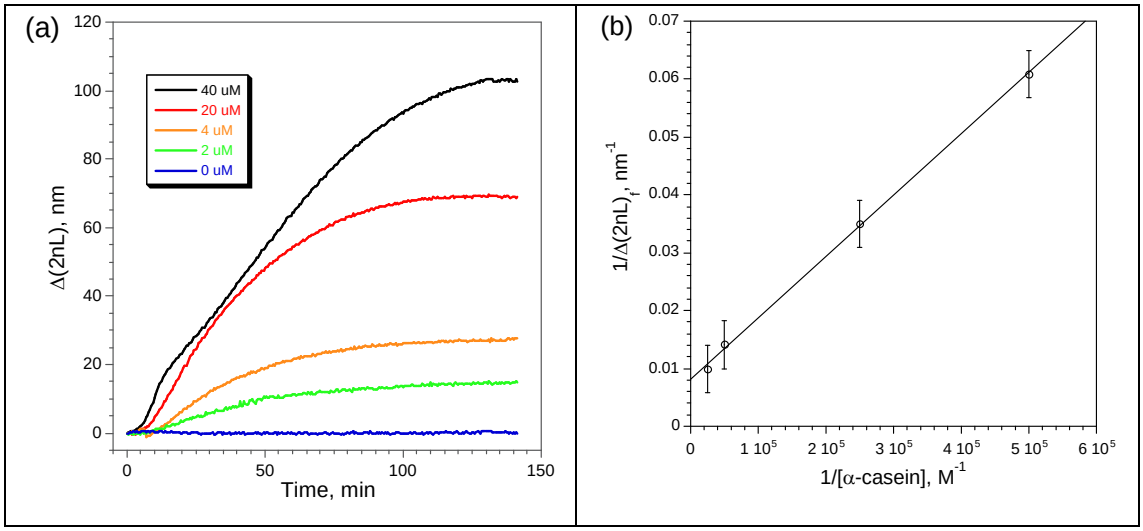

Figure 3.7 Kinetics of digestion of a-casein by pepsin in the nanoreactor as a function of protein concentration. (a) Appearance of digestion products in Layer 2 of the nanoreactor as a function of time, measured as the change in optical thickness of the layer. The action of pepsin generates small peptide fragments from a-casein that enter Layer 2. The quantity Δ2nL represents the change in 2nL relative to its value immediately before introduction of casein, nominally 16,000 nm for this series of experiments. The initial slope of the curves and the steady-state values of Δ(2nL) correlate with the initial concentration of casein used in each experiment. (a) Double reciprocal plot of $\Delta(2nL)_f$ and [α-casein], where $\Delta(2nL)_f$ is the steady-state value of Δ(2nL) measured 140 min after introduction of α-casein. Each data point represents triplicate measurements.

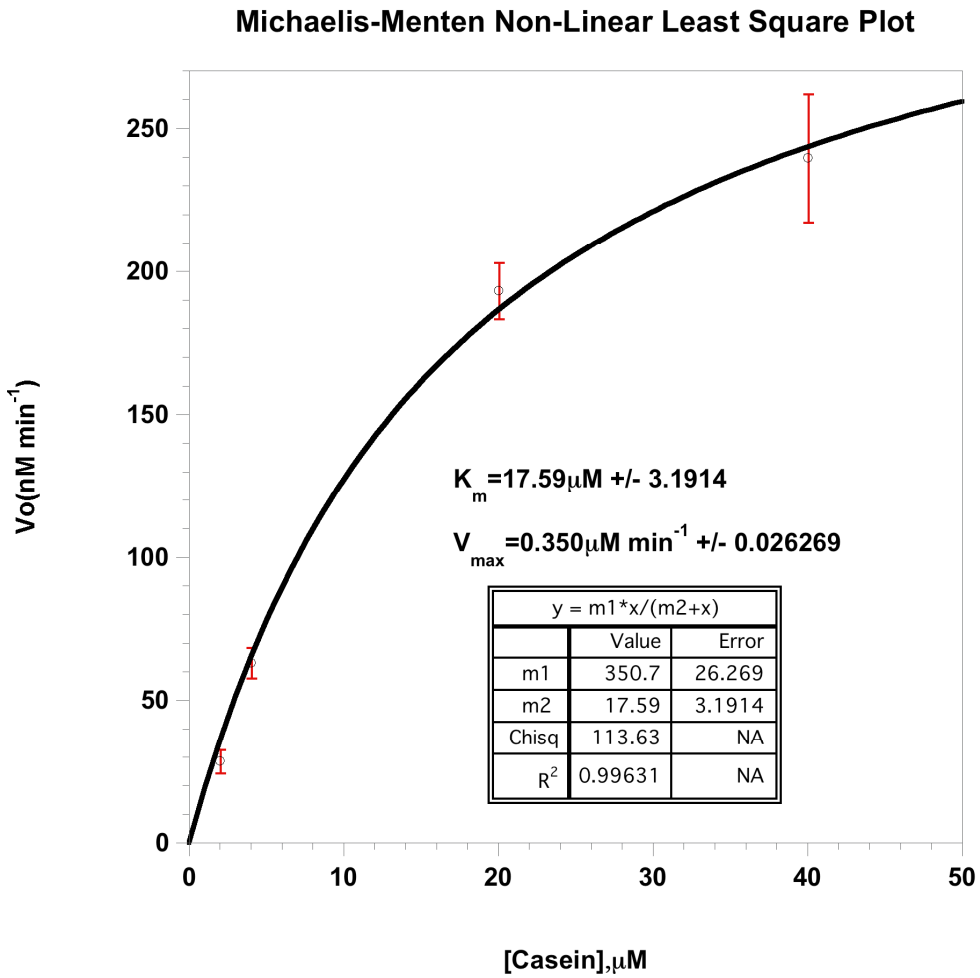

Figure 3.8 Non-linear least-squares fit of nano-reactor data to a Michaelis-Menten Kinetics Model.

.

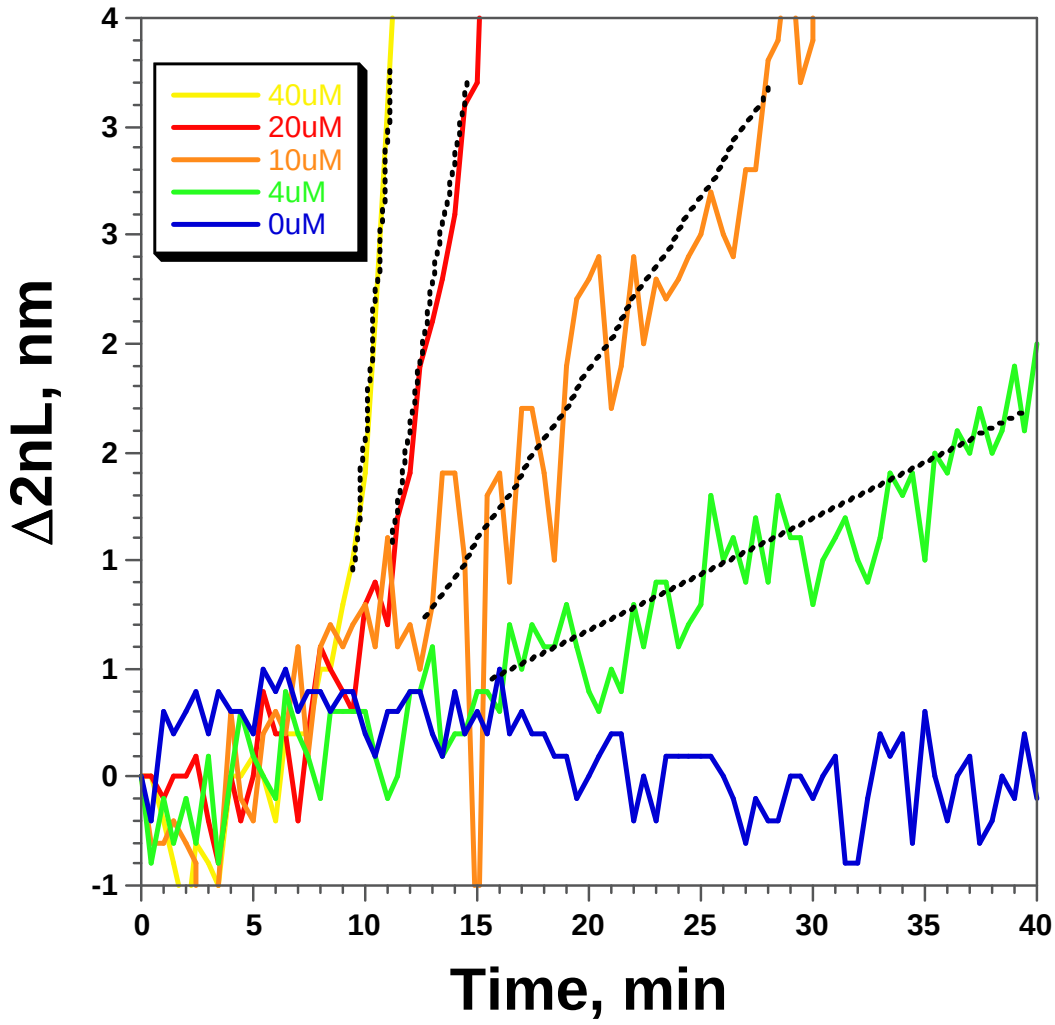

Figure 3.9 Inhibition of the Activity of Pepsin in the Nano-Reactor using Pepstatin A. As in Figure3.7, data are presented in terms of the response of the size exclusion Layer 2 as a function of time. The quantity Δ2nL represents the change in 2nL relative to its value immediately before introduction of the α-casein substrate and inhibitor. The initial slope of each curve is indicated by a dashed lined. Each curve corresponds to a fixed concentration of inhibitor (1 μM) and a different concentration of substrate as indicated in the legend

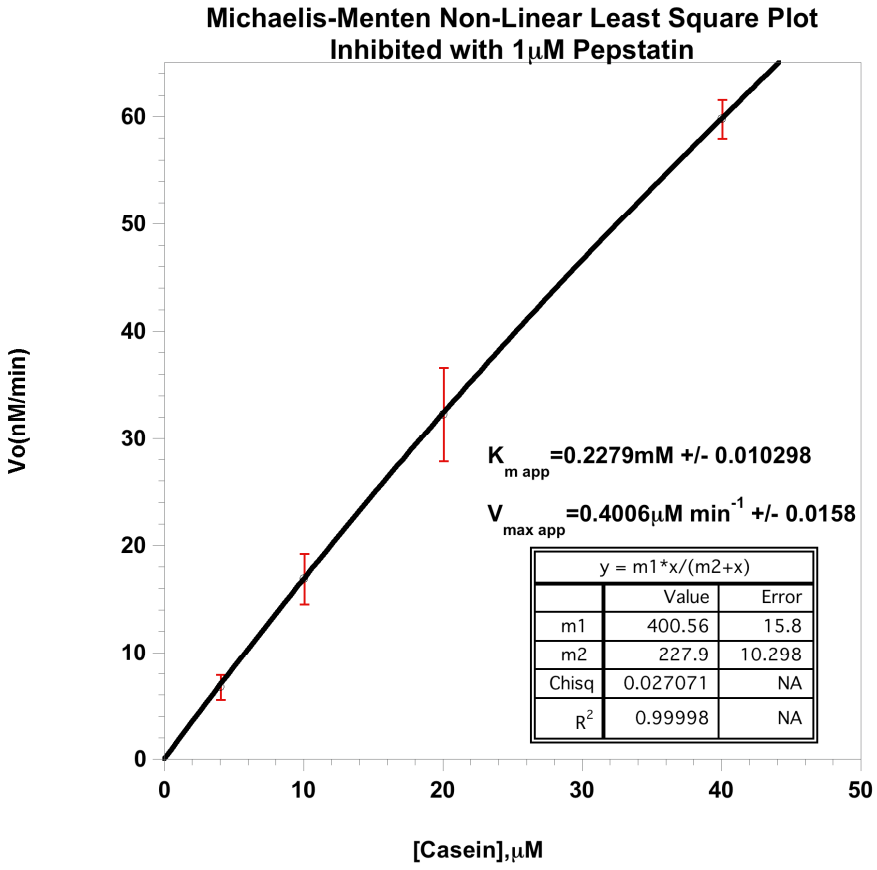

Figure 3.10 Non-linear least-squares fit of reactor data with inhibitor to a Michaelis-Menten Kinetics Model.

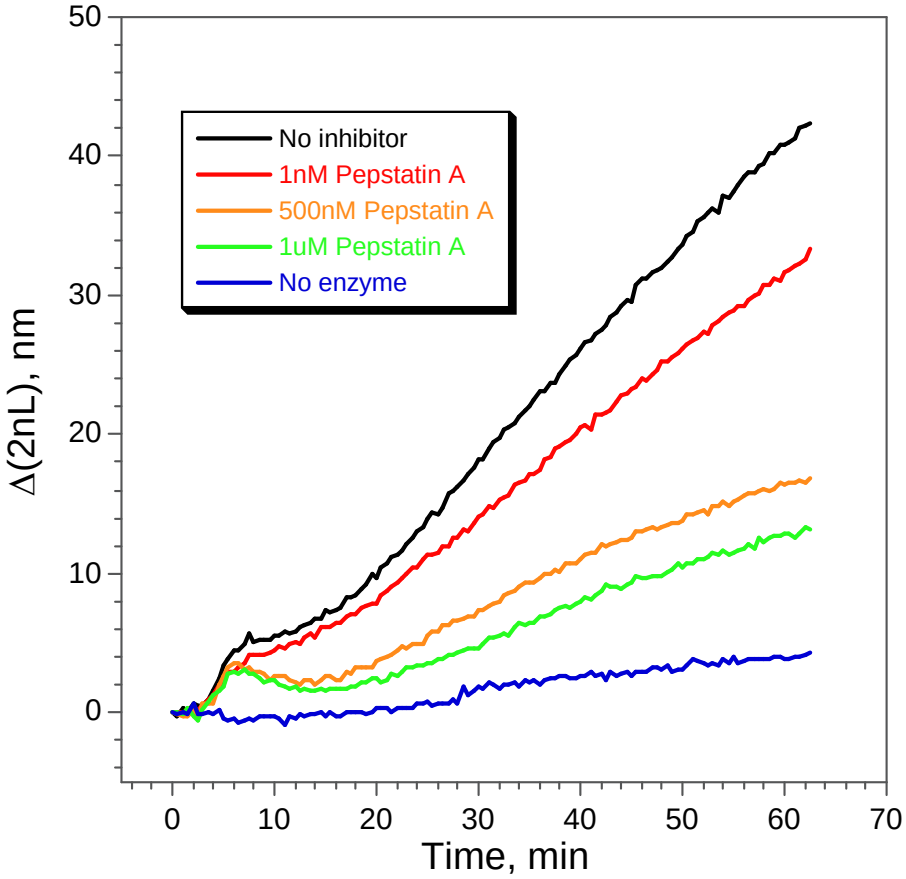

Figure 3.11 Inhibition of the Activity of Pepsin in the Nano-Reactor using Pepstatin A. As in Figure 3.7, data are presented in terms of the response of the size exclusion Layer 2 as a function of time. The quantity Δ2nL represents the change in 2nL relative to its value immediately before introduction of the α-casein substrate and inhibitor, nominally 15,500 nm for this series of experiments. Only the initial slope of each curve is shown. Each curve corresponds to a different concentration of inhibitor with a fixed concentration of substrate (40μM) as indicated in the legend.

Chapter three, in part, is a reprint (with co-author permission) of the material as it appears in the following publication: Orosco, M.M., Pacholski, Sailor, M.J., Real-time monitoring of enzyme activity in a mesoporous silicon double layer. ***Nat. Nanotech.*** 2009, in press. The author of this dissertation is the primary author of this manuscript.

4 Coupling Luminescent Transducers to Protein Coatings for Proteases

4.1 Abstract

Protease activity can be detected by a number of methods described in the earlier chapters. Specifically, Chapter 2 described a method of which thin films of protein are spin coated on a porous silicon surface and assayed for protease activity. Although this method is useful for label free detection of proteases, it lacks in sensitivity (when compared to fluorescent dyes conjugated to synthetic substrates). In this work, protease activity was measured by coupling protein multi-layers to changes in luminescence (either from porous silicon or fluorescent dye). P-type porous silicon was electrochemically prepared to have intrinsic luminescent nanostructures and whole protein substrates were spin coated on top of the surface. Depending on the specific etch conditions, the protein would either line the porous matrix or be excluded from it. One of the p-type methods involves using a luminescent thin porous silicon film coated with protein substrate to detect protease activity. When the protein gets digested, the thin silicon film is susceptible to degradation and the luminescence of that film will decrease. A number of issues arose when using porous silicon as luminescence transducing element and more sensitive approaches were necessary. A fluorescent dye was impregnated into a porous silicon film and is quenched by the porous silicon acceptor. A protein coating is used to trap the dye into the porous matrix and gets released in solution by the action of a protease.

4.2 Introduction

Fluorescence has always been the gold standard for achieving sensitivity on the molecular level and typical protease assays incorporate these fluorescent molecules. A commercial protease assay kit usually involves a fluorescent dye attached to peptide with a quencher flanking the substrate[18]. The action of a protease will cleave specifically at the scissile site allowing the fluorescent dye to fully fluoresce. This general method is good for detection of a small concentration of protease. Some major drawbacks are that the substrates are chemically modified in order to incorporate the fluorescent dye and the natural substrate is not used. Other systems use the natural substrates to incorporate dyes but cross-linking of the protein substrate is required[11].

Porous silicon has been used as a transducing element for protease activity in a label free manner[84]. The sensitivity, however, is limited by changes in index of refraction (n). Most biological assays are done in solution and measuring changes of n can become difficult since buffers are closely matched in index to biomolecules. To overcome the sensitivity issue, protein coatings were added to a luminescent transducing element (from either the porous silicon or dye). Spin coating provides an even coating and allows the protein to forms multi-layers on the surface. This protein substrate can also act as a cap to protect the silicon from degradation and can be used to trap molecules within the pores.

The first method employs luminescence from porous silicon itself (Figure 4.1). The luminescent structures are generated by quantum confinement and

oxide defects at the surface. The porous material at the surface forms a layer of oxide that allows quantum confinement of the silicon nano-clusters within. As the clusters get exposed to more oxidant, the band gap of porous silicon changes and causes a blue shift in the luminescent spectrum. It has been shown previously that protein matrix can be used to protect silica dissolution in seawater[85]. The process of dissolution in this work involves oxidation and corrosion of the porous silicon layer by various buffers. These luminescent structures were spin-coated with naturally occurring zein maize protein to form multilayers on the surface. These samples were then incubated with a model protease, Pronase E, to digest the protein substrate layer. Digestion of the layer will expose the surface to further corrosion and this will cause the luminescence from the porous silicon to blue shift and the intensity will decrease. This general design is based on the “on-off” method in which a fluorphore (porous silicon in this case) that is excited and after exposure to a protease, the luminescence signal decreases in intensity.

The second method involves the fluorescence from a molecular dye coupled to an acceptor (porous silicon). A slightly oxidized porous silicon film is infused with fluorecene and the solvent is allowed to evaporate. The dye becomes trapped within the porous matrix and capped with zein protein via spin coating. When the protein layer is exposed to a protease that is able to cleave the substrate, the dye is released into solution and turning on a strong fluorescence signal. The response is quantified by measuring the restoration of fluorescence of a dye impregnated in the porous silicon matrix—a solid-state

analog of Fluorescence Resonance Energy Transfer (FRET). The dye itself is not coupled directly to the substrate making it a facile, label-free method for detecting proteases in solution. This general design is based on the “off-on” method in which a fluorphore is quenched and after exposure to a protease, the fluorescence signal restores in intensity.

4.3 Experimental

4.3.1 Sample Preparation

Porous silicon samples for dye infused experiments were prepared by an anodic electrochemical etch of boron doped p-type silicon wafers (4-5 W cm resistivity, <100> orientation, Silicon Quest International, Inc.) in a 1:1 (v/v) 48 % aqueous hydrofluoric acid (EMD Chemicals, Inc.) to ethanol solution in the dark. A Teflon etch cell with 1.1 cm^2 of silicon wafer exposed was used. Samples were etched at a constant current density of 18 mA/cm^2 for 5 min. Porous silicon samples were then placed in a tube furnace (Lindberg/Blue M) and heated to 300 ºC for one hour under ambient atmosphere, resulting in a slightly oxidized porous layer. 0.8 μL of an ethanol (99.5 %, PHARMCO-AAPER) solution 0.1 mg/mL in fluorescein (95 %, Sigma-Aldrich) was added to the porous film and the solvent was allowed to dry at room temperature under ambient atmosphere. A 200 μL aliquot of 5 mg/mL zein (Sigma) in methanol (99.9 %, Fisher Chemicals) was then spin-coated (2000 rpm, 30s) onto the porous film to seal the dye into the porous Si matrix. Highly doped p-type luminescent porous silicon was etched at 707mA/cm2 for 10 seconds, rinsed with ethanol, and dried with a stream of

nitrogen. These samples were then oxidized at 450 ^{0}C for 1.5 hours. Sample were then rinsed with 3:1 HF: Ethanol to remove the porous layer, aged in air for 1 day, and spin-coated (2000 rpm, 30s) with 200 μL aliquot of 5 mg/mL zein in methanol.

4.3.2 Enzymatic Digestion Procedure

Pronase E solution was prepared by dissolving Pronase E (Type XIV, ca. 4 units mg^{-1} solid powder, Sigma) in various buffers. Controls included deionized water and heat-denatured Pronase E solution. Heat-denatured Pronase E solution was obtained by heating the above active Pronase E solution to 95 ºC for 25 minutes. Aliquots of 7 μL of the Pronase E solution or controls were deposited onto the zein-coated porous Si film. The sample was maintained in a humid chamber at room temperature for 30 minutes. For “on-off” sensor, the protein coated porous silicon chip was exposed to 100μL of protease.

4.3.3 Fluorescence Measurements

Fluorescence spectra were obtained with a liquid nitrogen-cooled charge-coupled device (Princeton Instruments, LN/CCD-1152) and a dual grating monochromator (Acton, SpectrPro-150) coupled with an optical fiber and focusing lenses. A blue LED with peak emission at 470 nm (Nichia, NSPB500S) was used as the excitation light source. A 480/40 nm bandpass filter and a 510 nm long pass filter were used as the excitation and emission filters, respectively.

4.4 Result and Discussions

4.4.1 Protein Coated Highly Doped P-type Luminescent thin films

The preparation and use of the protease sensor follows the procedure shown in Figure 4.1. The sample must be partially oxidized in order to obtain thin luminescent film. If the sample is fully oxidized, the porous silicon goes from a semiconductor to an insulator and no luminescence will be observed. It is possible to achieve a p-type luminescent porous silicon film by electrochemical etching and activating visible photoluminescence is based on the specific etch conditions and aging of sample. This method of generating p-type luminescent structures is much quicker and the layer is thin enough for faster corrosions times. These samples were then spin-coated with protein biopolymer zein. The coating serves two purposes: to protect the thin film from corrosion by aqueous media and acts as a substrate for proteases. As a consequence of the protein coating, the luminescence intensity decreases by 35%. This could be due to the protein layer acting as a quencher of the porous silicon luminescence. The decrease in luminescence intensity is also seen aqueous solutions partly due to high concentrations of salts that can quench the luminescence and absorption of UV light by the solution. The intensity decreases with various aqueous solutions (Table 4.1). The % quenched ratio is calculated by the final luminescent intensity at 30 minutes over the initial intensity (0 minutes). The amount of aqueous media quenching highly depends on type of solution (ranging from 23-96%)

These zein-coated samples were tested for their ability to quench in the presence of an active protease. If there is protease activity, the zein multi-layer will degrade and the thin film will be exposed to corrosion by aqueous solution. This destruction of the porous silicon nano-structure leads to a faster decrease in luminescence intensity that can be measured over time. Pronase E has a higher % quenched ratio (%88) than solution because the protein layer is degrading and corrosion is taking place at a faster rate (after 30 minutes). This change, however, is not very significant and could not be useful in detecting small quantities of protease.

The main drawback to this method was the changes in luminescence were based on the amount of oxidation a specific solution can have. If the aqueous solution is a higher pH, the rate of dissolution of porous silicon is greater and a rapid decrease in intensity will occur. This could become an issue at lower pHs. Also, the luminescence of the thin film is not exactly uniform and can cause variations in intensity (see Figure 4.2). This method, in part, leads to a new design where the transducing element does not come from the porous silicon itself but rather a fluorescent dye.

4.4.2 Protein Coated, Dye Infused P-type Porous Silicon

The preparation and use of the protease sensor follows the procedure shown in Figure 4.3. A solution of the naturally occurring protein zein in methanol (5 mg/mL) is spin-coated onto of the slightly oxidized porous silicon film loaded with fluorescein to form a thin protein layer and to seal the dye into the porous

nanostructure. Zein tends to form multilayered films on surfaces through molecular and electrostatic interactions[86]. The porous Si film was prepared by electrochemically etching of p-type Si wafer using a low current density (18 mA/cm^2). The porous structure has pores (< 10 nm) that are small enough to exclude most of the intact zein protein (24 kDa, 16 nm x 4.6 nm x 1.2 nm) infiltrates the porous Si film[84, 86].

Initial fluorescence from fluorescein is negligible because of the quenching of the dye by the porous Si matrix. Porous Si has a high quenching efficiency because of its relatively high density of electronic states and the large surface area of the porous structure[87]. It was found that the degree of quenching could be adjusted by changing the distance (thickness of the silicon oxide layer) between the fluorescent dye molecules and the silicon matrix. Figure 4.4 shows the residual intensity of fluorescence from fluorescein incorporated in porous silicon films as a function of the degree of oxidation. To test if the low fluorescence intensity arises from self-quenching of fluorescein, controls were carried out using a fully oxidized porous silica film (Fig. 4.4(d)) and a polished quartz slide (Fig. 4.4(e)). The same fluorescein loading protocol was followed. Significant self-quenching is expected from fluorescein dried on a quartz slide, and as expected, negligible fluorescence is observed from this type of sample. On the other hand, the fully oxidized porous silica sample possesses ~1000x larger surface area, increasing the separation between adsorbed fluorescein molecules and reducing the likelihood of self-quenching. Oxidation converts the porous silicon semiconductor to a porous SiO_2 insulator, significantly reducing

the free carrier concentration and density of free electronic states. The relatively high fluorescence intensity observed on the fully oxidized samples is consistent with emission from isolated, unquenched fluorescein. Thus the fluorescence quenching observed with the freshly etched or slightly oxidized porous silicon samples is attributed to energy transfer between fluorescein and semiconducting silicon.

The surface of freshly etched porous silicon is hydrogen-terminated which makes it hydrophobic. This surface effectively repels aqueous solutions in the absence of a surfactant [9], so a mild oxidation (300 ºC, 1 hour) was employed to generate a very thin oxide layer on the surface. The oxide layer is thin enough that the porous silicon matrix can still quench the fluorescein molecules (Figure 4.4(b)), and it imparts a more hydrophilic nature to the porous matrix[31, 88], allowing the analyte solution to enter the pores and release the trapped fluorescein (Figure 4.5).

There is a possibility that the observed lack of fluorescence from fluorescein loaded in porous silicon arises from a chemical reaction with the reactive hydrides on the porous silicon surface. To eliminate this possibility, films loaded with fluorescein were rinsed with ethanol to extract the free fluorescein. The ethanol solutions display similar fluorescence intensity from either the freshly etched or the oxidized samples. The result of Figure 4.5 also indicates that the fluorescein molecules trapped inside the pores can be leached out of the matrix intact, and that the fluorescein loads into the pores rather than aggregating on the top of the porous films.

Detection of Pronase E activity was performed on the sensors prepared following the procedure used in Figure 4.3. An aliquot of 7 μL of 0.5 mg/mL Pronase E was deposited on the zein-coated porous silicon film. Deionized water and heat-denatured Pronase E solutions were used as controls. The sample was maintained in a humid chamber at room temperature for 30 minutes. The fluorescence of the samples was then measured *in situ*. No significant increase in fluorescence intensity was detected from the water blank (Figure 4.6(a)). Taken with the result of Figure 4.5(b), it can be concluded that the zein layer effectively forms a barrier between an added water drop and fluorescein trapped in the partially oxidized porous silicon film. Addition of active Pronase E results in the appearance of a strong fluorescence signal within 30 min (Figure 4.6(b)), resulting from the action of Pronase E on the zein layer. The heat-denatured Protease E sample displays a smaller increase in fluorescence intensity (Figure 4.6(c)), though it is still much larger than the water blank. One possibility is that there is still residual activity in the denatured protease. The sensor was also tested with different buffers. Some of the buffers also produced an increased fluorescence signal, suggesting that under certain conditions some fluorescein can leach through the intact zein layer.

4.5 Conclusion

This work represents a new method for detection of protease activity using both luminescent structures of porous silicon and fluorescent dye infused in porous silicon. The main advantage of the system is the use of natural substrates

for the assay coupled to changes in luminescence. This system could provide sensitive detection of protease activity without the use of chemical modifications to substrates. Particularly, the “off-on” sensor is most useful because it works on the principle of sensitive detection with fluorescent probes with low background.

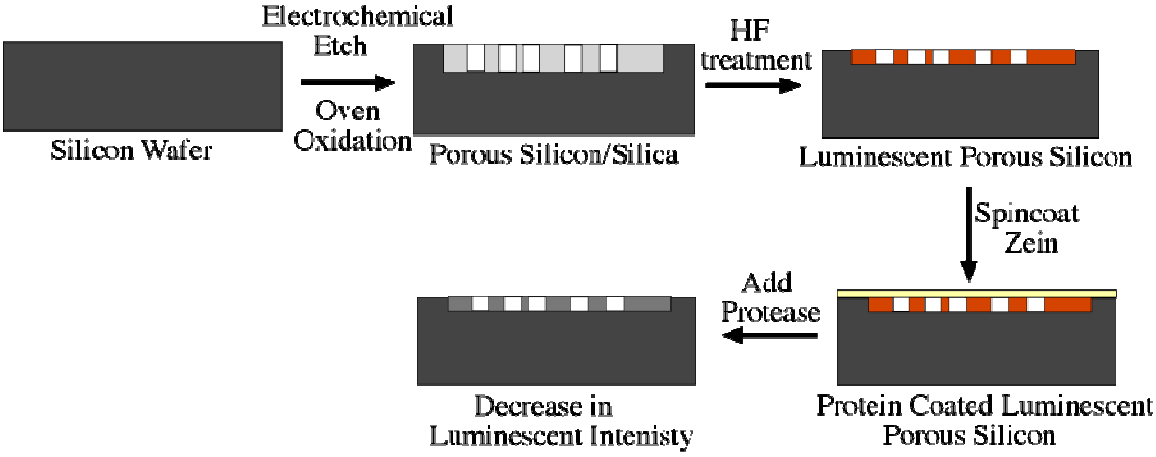

Figure 4.1 Schematic of an "on-off" protease biosensor constructed with large mesopores.

Table 4.1 Quenching effects of different aqueous solutions. The % quenching ratio is calculated as the final intensity after 30 minutes of incubation with solution over initial luminescent intensity. The peak shift is calculated as the peak max position at 0 minute subtracted from the peak max position at 30 minutes.

	pH 2.0 Buffer	pH 4.0 Buffer	Millipore water	PBS	Seawater	pH 10.0 Buffer
% Quenching (Uncoated)	33%	56%	29%	59%	63%	93%
Peak Shift (Uncoated)	+4nm	+2nm	+3nm	-5nm	-14nm	-13nm
% Quenching (Zeincoated)	24%	27%	29%	66%	76%	96%
Peak Shift (Zein coated)	+6nm	0nm	+3nm	-39nm	-11nm	-3nm

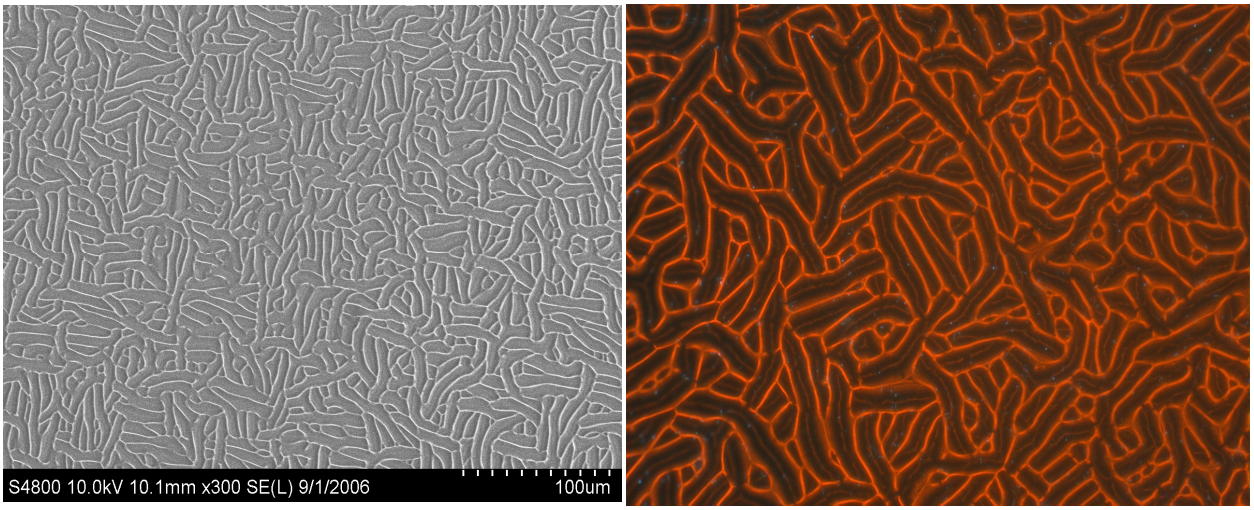

Figure 4.2 Highly doped p-type luminescent porous silicon. (a) An SEM image of the thin film produced after treatment with HF. (b) The same structure excited with a UV source.

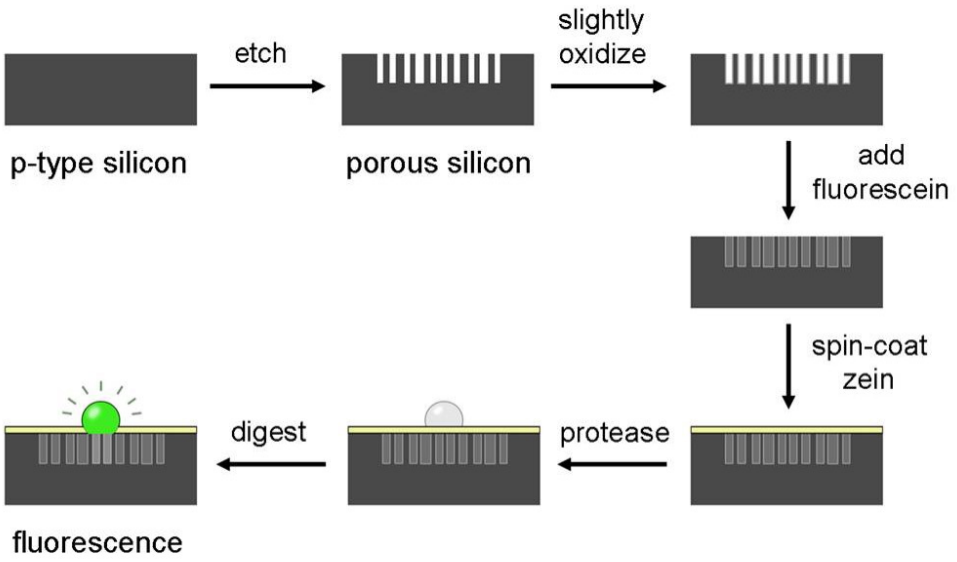

Figure 4.3 Schematic of an "off-on" protease biosensor constructed with small pores.

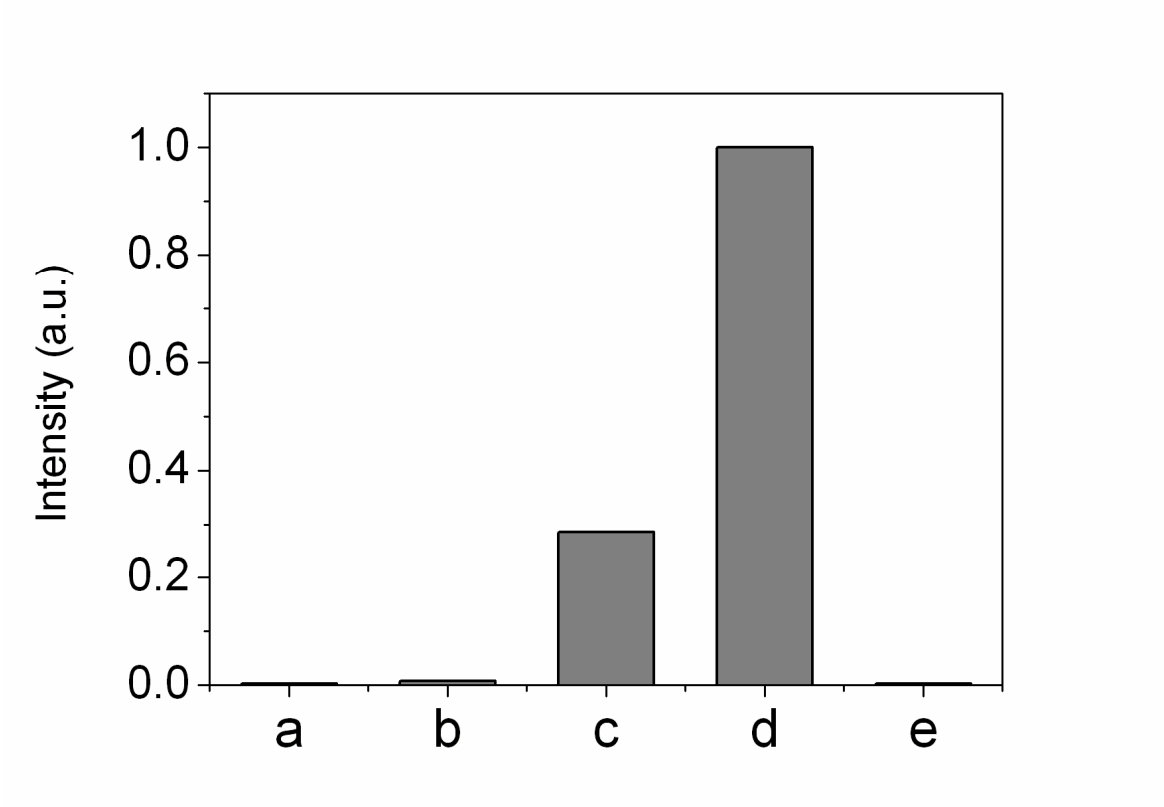

Figure 4.4 Fluorescence intensity observed from porous Si films oxidized to different degrees. An aliquot of 0.8 μL of 1 mg/mL fluorescein in ethanol was added onto each of the porous Si films and dried at room temperature under ambient atmosphere. Fluorescence from the samples was then measured: (a) freshly etched porous Si; (b) porous Si oxidized at 300 ºC for 1 hour; (c) porous Si oxidized at 500 ºC for 1 hour; (d) porous Si oxidized at 950 ºC for 1.5 hours; (e) polished quartz slide control.

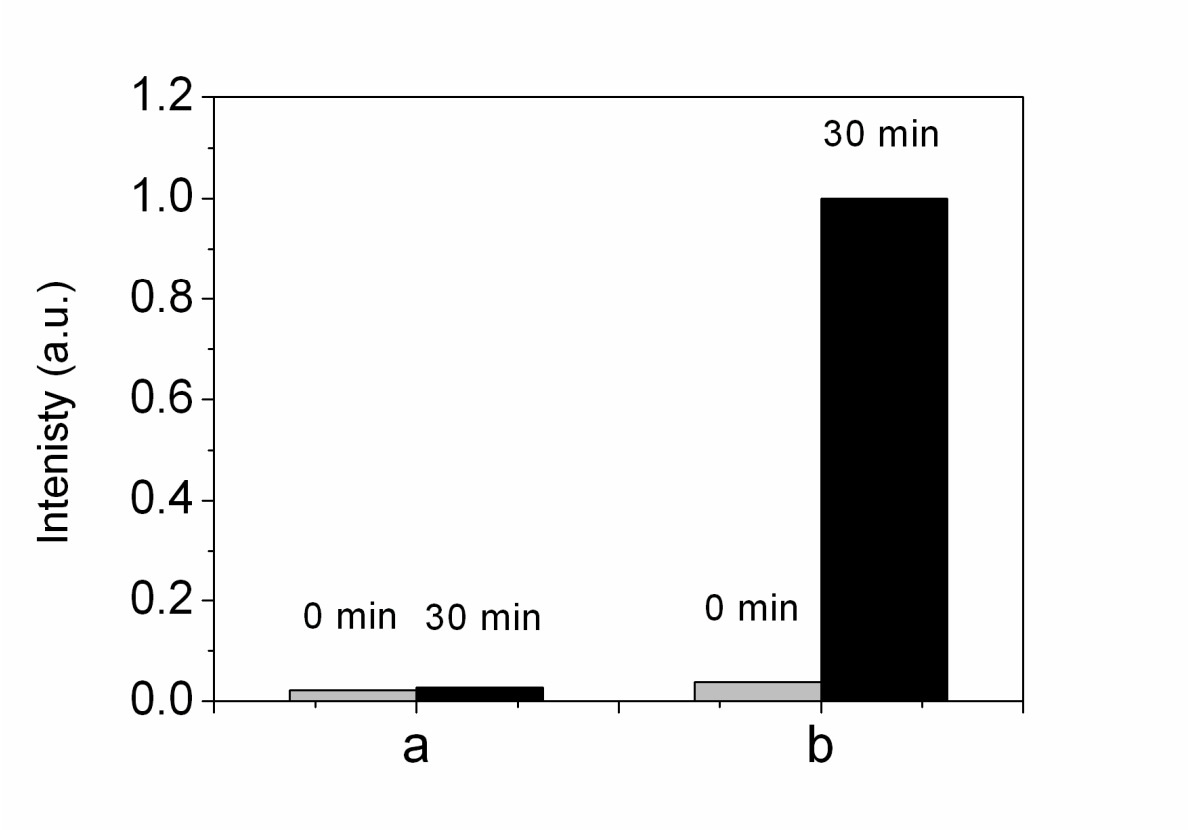

Figure 4.5 Comparison of fluorescence intensity from fluorescein released into water from (a) freshly etched and (b) partially oxidized porous Si films. A 7 μL aliquot of deionized water was deposited onto each of the fluorescein-loaded samples. The fluorescence intensity in the water droplets was measured after 0 and 30 minutes. The partially oxidized sample displays strong fluorescence after 30 minutes, whereas the freshly etched sample displays little change.

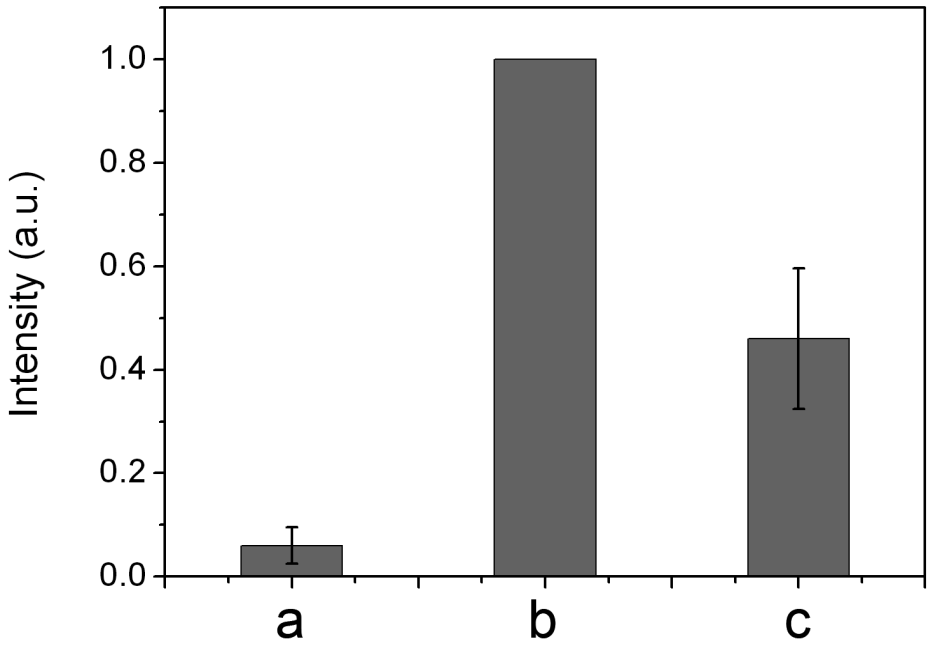

Figure 4.6 Protease-triggered increase in fluorescence intensity from a dye-impregnated, zein-coated porous Si substrate. Relative fluorescence intensity of (a) 7 μL H_2O blank control, (b) 7 μL 0.5 mg/mL Pronase E, and (c) 7 μL 0.5 mg/mL heat-denatured Pronase E solution. All measurements performed after 30 min room-temperature incubation on the sensor. A unit of pronase E is defined by hydrolysis of casein to produce a color equivalent to 1.0 mmole (181 μg) of tyrosine per min at pH 7.5 at 37 ℃ (color by Folin-C iocalteu reagent).

Chapter four, in part, is a reprint (with co-author permission) of the material as it appears in the following publication: Gu, L., Orosco, M.M., Sailor, M.J., Detection of protease activity by FRET using porous silicon as an energy acceptor. Phys. Stat. Sol. A, 2009, in press. The author of this dissertation is the co-author of this manuscript.

Appendix A. On-Chip, Label-Free Sensor for Detection of Bacterial Protease Activity

A.1 Abstract

In this work, protease activity in a marine Flavobacteria sp. BBFL7 was measured by changes in local refractive index of the porous silicon layer. Porous silicon samples were oxidized for stability in high salt and pH conditions. The first method employs the use of large nanometer sized pores prepared from electrochemical etch of polished silicon wafers. The large dimensions of the pores (>100nm) allow large protein (in the present case, α casein) to adsorb to the inner pore walls. Removal of α-casein is caused by protease activity that changes the local index of refraction (n) from protein (n~1.40) to seawater (n=1.34) resulting in a blue shift. The other approach follows the method described in Chapter 2 in which protein substrate is excluded from the porous silicon matrix. When active proteases are present in solution, the protein substrate is cleaved into small peptide fragments that can then infiltrate the small pores. This will result in a red shift due to index changes from seawater (n=1.34) to peptide fragments (n~1.40). The data shows some promising results but the utility of this method for measuring protease activity is limited when compared to standard proteases detection assays for cells.

A.2 Introduction

There is a need for rapid detection of protease activity in whole bacterial cells. Some bacterial cells use proteases for virulence factors[4], gene activitation[20], and protein catabolism[85]. Most methods for the detection of

protease activity involve fluorogenic substrate that fluoresce when cleaved[6]. The issue with using this kind of substrate is the engineered peptide bond does not represent the real kinetics of its natural substrate especially for protein substrates. Also, peptide substrates can be costly, as analysis requires sensitive fluorometers.

The drawbacks of fluorescent peptides lead to developing an on-chip protease assay to detect protease activity in marine isolate BBFL7. This isolates was isolated from waters nearby Scripps Institution of Oceanography, La Jolla, California, USA. It exhibits high ecto-protease activity and has proteolytic enzyme activity making it a good candidate for a proof of concept for development of a method for protease activity. Protease activity plays an important role in the ocean's cycle of various elements (i.e. carbon, nitrogen, silicon) and has been an indicator of gene activation in biofilms[89]. Building an on-chip, label-free sensor for detection of protease activity in marine bacteria can include patterned arrays with various substrates for high throughput screening.

In the present work, two methods for the detection of protease activity are employed. The first method uses large pores (>100nm) electrochemically prepared by etching polished silicon wafers at a high current density (close to the electropolishing regime) and then oxidized to impart stability of the porous structure (see Figure A.1). The large pores are necessary for proteins to be able to diffuse readily and adsorb into the inner pore walls. As protein enters and adsorbs to the pore walls, the local index of refraction (n) changes from seawater (n=1.34) to protein substrate (n~1.40) causing a red shift (increase) in the

effective optical thickness (2nL). This shift can be measured as a function of time. Prior to adding protein substrate, porous silicon was loaded with seawater to change the index of refraction of porous silica. Now, when the protein solution is added, the index changes are only produced by the protein itself and not by the seawater. Protein substrate was cycled through the porous film with a flow cell and the relative change in 2nL was allowed to equilibrate (until there is a baseline for 2nL). Excess protein that is not adsorbed was removed by a rinse cycle and as a consequence, some of the adsorbed protein is removed as well. In this case, it is important to measure the protein diffusion out of the pores (characterized by the change in 2nL/time). If protein is removed (i.e. diffusion or removal by proteases), the 2nL value will decrease as a result of the porous layer shifting to a lower index. This rate can be measured in real-time and would provide label-free detection of bacterial proteases.

The second method is similar to the method described in Chapter 2 except a protein layer is not used on the surface of porous silicon (Figure A.2). Marine bacteria BBFL7 was directly incubated with protein substrate in solution and allowed to digest the substrate into small peptide fragments. This solution was added to the porous silica that was etched with small pores (to exclude whole protein substrate) and oxidized to impart stability. The peptides produced from the digestion can freely diffuse into the small porous layer. This cause a change in local refractive index as peptides (n~1.40) displaces seawater (n=1.34) and an increase (red shift) in 2nL. This measurement just shows the extent of protease activity in a given concentration of BBF7 in a label-free manner. A caveat is that

any peptides released from the metabolic pools of bacteria would cause an over estimation of the protease activity.

A.3 Experimental

A.3.1 Sample Preparation

Porous Si samples were prepared by anodic electrochemical etch of highly B-doped (p^{++}-type), (100)-oriented silicon wafers with resistivity of ~ 0.8 mΩ-cm (Siltronix), in a 3:1 (v/v), 49% aqueous HF/ethanol solution. A Teflon etching cell that exposed 1.2 cm^2 of the silicon wafer was employed. For porous silicon with large pores, the exposed polished surface was etched at a current density of 707 mA/cm^2 for 10 s. Making porous silicon with small pores involved etching at a current density of 44 mA/cm^2 for 170 s. Samples were then thermally oxidized at 800 ℃ for 1.5 h. Each sample s was mounted in a flow cell chamber and was exposed to a 1 cm-diameter optical window through which the reflectivity spectrum of the porous silicon film could be monitored.

A.3.2 Data Acquisition and Analysis

Interferometric reflectance spectra were collected by using an Ocean Optics S-2000 CCD spectrometer fitted with a microscope objective lens coupled to a bifurcated fiber optic cable. A tungsten light source was focused onto the center of the porous Si sample surface with a spot size approximately 1.5 mm in diameter. Both the illumination of the surface and the detection of the reflected light were performed along an axis coincident with the surface normal.

Reflectivity spectra were recorded in the wavelength range 400-1000 nm, with a spectral acquisition time of 10 ms. Typically 100 spectral scans (2 s total integration time) were averaged for Fourier transform processing. Details of the Fourier transform and spectral data fitting routines are published elsewhere[26].

A.3.3 Measuring Protease Activity

An overnight culture of BBFL7 was grown in DIFCO media and centrifuged at 15000g in an Eppendorff centrifuge and washed 3x with a 0.2μm filtered autoclaved seawater. The washed pellet was resuspended in 0.2μm filtered autoclaved seawater to various optical densities. The optical density was measure to calculate the concentration of BBFL7. Measurements were taken in an airtight flow cell chamber connected to a peristaltic pump which pumps in one direction. For porous silica with large pores, a solution of α-casein (1mg/ml) mixed in seawater was flowed at a rate of 500μL/minute through the porous silica layer and the 2nL was allowed to equilibrate. Excess substrate was removed by subsequent rinsing with seawater. After a stable baseline had been achieved with seawater, a specific concentration of BBFL7 was then cycled through the protein loaded porous silica layer (total volume cycled=3.5ml). The value of a 2nL was monitored over time. The slopes (2nL/sec) are a measure of protease activity and are compared to the rate at which the protein is diffusing out of the pores. For porous silica with small pores, a solution of α-casein was directly mixed with BBFL7 at a specific concentration and incubated for 1 day at room temperature. After a stable baseline had been achieved with seawater, the

mixture of bacteria/substrate was cycled through the flow cell (cycled rate= 500μL/min, total volume =3.5mL) and the change in 2nL was monitored.

A.4 Results and Discussion

A.4.1 Porous Silicon with Large Pore Dimensions

This method uses porous silica with large pores to detect protease activity in BBFL7 (see Figure A.1). Because seawater has high pH (~8.1) and salts, the surface of the porous film was thermally treated to create a stable SiO_2 surface. This type of surface resists corrosion from solutions on the timescale of the experiment (Figure A.3). One factor that must be considered is that bacteria cells have an index of refraction and this could interfere with the change in 2nL measurement. As an example, the cell's index might be close to that of the protein since the cells themselves have various proteins, sugars, and lipids. If BBFL7 was able to enter the pores, the local refractive index of the pores will increase and this could be construed as a false positive. Figure A.3 shows that there is no change on 2nL when incubated with BBFL7 alone in seawater suggesting that the bacteria don't enter the pores (bacteria size ~1μm, see Figure A.4). The loading of substrate α-casein causes a change in local refractive index of the porous layer as the substrate adsorbs to the inner pore walls and displaces seawater. For α-casein (1mg/ml), this shift is typically 80-110nm (Figure A.5). The slope of the seawater rinse is characterized by the change in 2nL over a given amount of time (30 minutes in this case). This slope represents the amount of substrate that is able to diffuse out of porous layer. It is assumed

that if proteases were available they would be able to cleave the substrate to peptide fragments. These fragments are less likely to adsorb to the inner pore walls because there is less chemical interaction causing a decrease in the 2nL value. BBFL7 (OD=0.180) was then incubated with the α-casein loaded porous silicon sensor and the change in 2nL over time was measured. The ratio of these slopes (slope of BBFL7/slope of seawater) represents the protease activity of BBFL7. If the ratio is greater than 1, then this would suggest that there is protease activity. This ratio actually turns out to be lower than 1(0.824). There are a number of reasons why a higher ratio was not seen (corresponding to high protease activity). One reason could be that bacteria are excluded from the pores and most of the proteases are located on the cell surface. This could be an issue if the proteases cannot reach the substrate deep within the pores. Another reason for a low ratio could be that in fact the BBFL7 suspension had low protease activity. Achieving a high ratio strongly depends on the assumption that products will be removed from the pores. If they remain there, the 2nL value will not shift very much. Another possibility is that the hydrolysis and uptake of hydrolysis products are tightly coupled processes. There is also the possibility that the cells are attached to the surface and keeping the substrate/products inside the pores.

An experiment was done with heat-killed BBFL7 to show that there should be little protease activity characterized by a small change in 2nL/time. This ratio is close to rate of diffusion of substrate (1.34) but larger than live BBFL7 (0.824). The heat treatment could affect the shape of the cell and its ability to attach to

the surface. This would favor the idea that BBFL7 cells are keeping the substrate/products inside the pores. To test that these sensors can detect protease activity, Pronase E was cycled through and the change in 2nL was measured over time (Figure A.6). Almost immediately, there was a large change in 2nL for Pronase E (1mg/ml, ratio=27). To show that only active protease can remove the protein substrate, heat-treated Pronase E (1mg/ml) was flowed over these sensors. No significant change in 2nL was observed suggesting that only active protease can remove the protein layer. The large change in 2nL can be attributed to the enzyme being able to freely diffuse in and out of the pores and its high protease activity (a combination of 10 proteases). Although the idea of having an on-chip, label free, real time protease sensor for cells could be possible, the methods lacks, at the present time, sensitivity when compared to synthetic peptide substrates. It is also possible that the method is suitable only for bacteria that release proteases into the environment

A.4.2 Porous Silicon with Small Pore Dimensions

The issues with the method described above lead to a new approach similar to that described in Chapter 2. Rather than porous silica housing the substrate, it excludes it with small pores (see Figure A.2). Natural protein substrate is incubated with BBFL7 in solution for 1 day. After a baseline with seawater, the mixture was cycled through and the change in 2nL was measured. Figure A.7 shows the changes attributed to loading of peptides fragments generated by BBFL7 when incubated with substrate. As a control, α-casein

(1mg/ml) was cycled through and change in 2nL was measured. This change is less when compared to BBFL7 plus substrate solution. The change in 2nL from protein substrate could be attributed to α-casein adsorbing to the surface and changing the local refractive index of the porous silicon layer (a combination of higher n and increased thickness of the porous film). There is no 2nL shift for BBFL7 alone showing that the index changes come from the protein substrates and products generated. This work shows promising results but only shows the extent of protease activity in these cells. The drawbacks are that this assay does not work in real-time and the kinetics of the enzymes cannot be measured. The time it takes for the digestion is significantly higher when compared to typical protease assays. Time of incubation with bacteria and substrate was also varied (1 and 12 hours) however, this timescale is below the detection limit in this method that cannot be seen. It is possible that BBFL7 initially have high protease activity and they uptake the peptides generated. It would appear then at some point BBFL7 is unable to uptake the peptides generated and the products accumulate in solution (noticed after 16 hours).

A.5 Conclusions

This work was a large effort to detect protease activity in marine bacteria BBFL7 without the use of synthetic peptide substrates. Porous silica was considered a good candidate because the nanostructure could provide interfermetric measurements and this could possibly be integrated into microarray technologies. These optical transducers respond to the presence of bacterial proteases but that response is not amplified (which is the trade-off for

most label-free biosensors). The main goal of this work was to have an on-chip, label free protease sensor that can interface with bacteria. If fully realized, this method could be used to study cycling of organic compounds and the behavior of bacterial communities in biofilms.

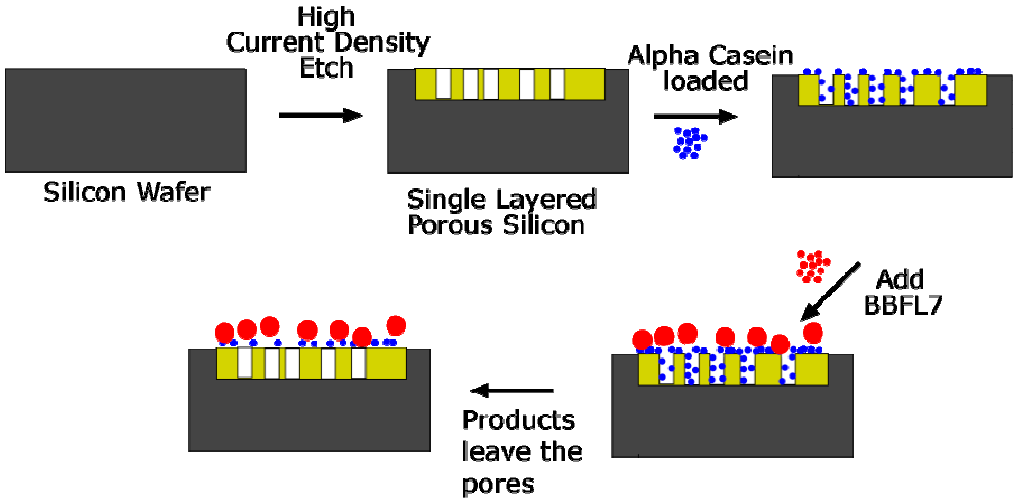

Figure A.1 Protease biosensor using protein coated porous silica. Porous silica with larger pores (>100nm) was coated with α-casein protein substrate. In this schematic, the protein is digested by proteases produced by marine Flavobacteria BBFL7. Digestion of protein substrate by proteases generates peptide fragments that can be uptaken by BBFL7 or become free in solution. If there is significant cleave of substrate, then larger changes in 2nL will be observed.

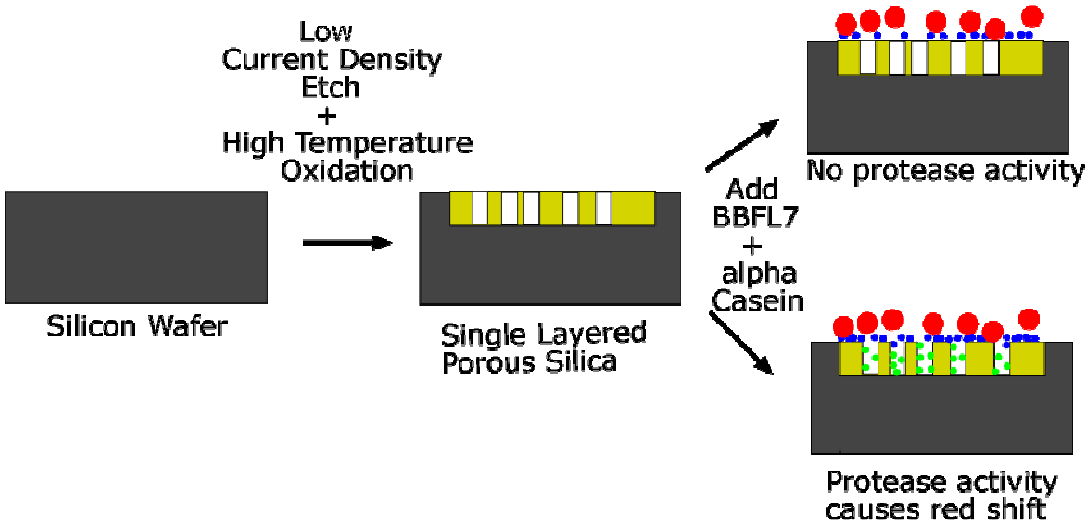

Figure A.2 Protease biosensor using porous silica with small pores Porous silica with small pores (<10 nm) was coated with α-casein protein substrate. In this schematic, the protein is digested by proteases produced by BBFL7 and then introduced to the porous silica film. If the proteases are about to cleave the protein substrate sufficiently, small peptides will be generated and these peptides can enter the small pores.

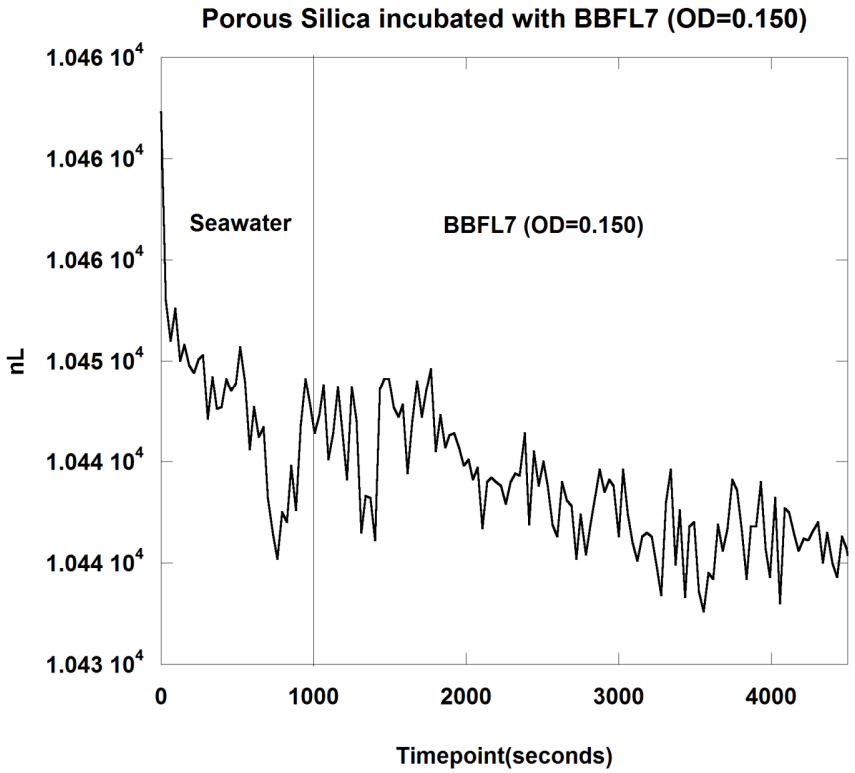

Figure A.3 2nL changes due to BBFL7. After baseline with seawater, BBFL7 of a given concentration was incubated with a porous silica film. The presence of BBFL7 does little changes to the 2nL value.

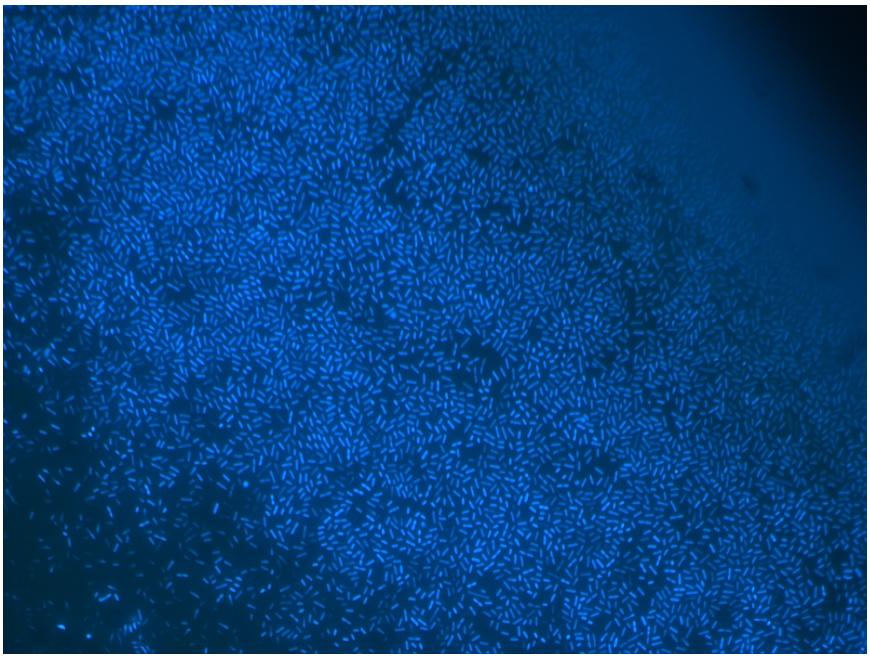

Figure A.4 BBFL7 lawn on top of a protein coated porous silica film. This image was obtained on an Oplympus 1X-51 epifluorescence microscope at 200X final magnification. Prior to imaging, BBFL7 were stained with DAPI for visualization of the nucleus and excited with a UV light source. The width of the image is 80μm.

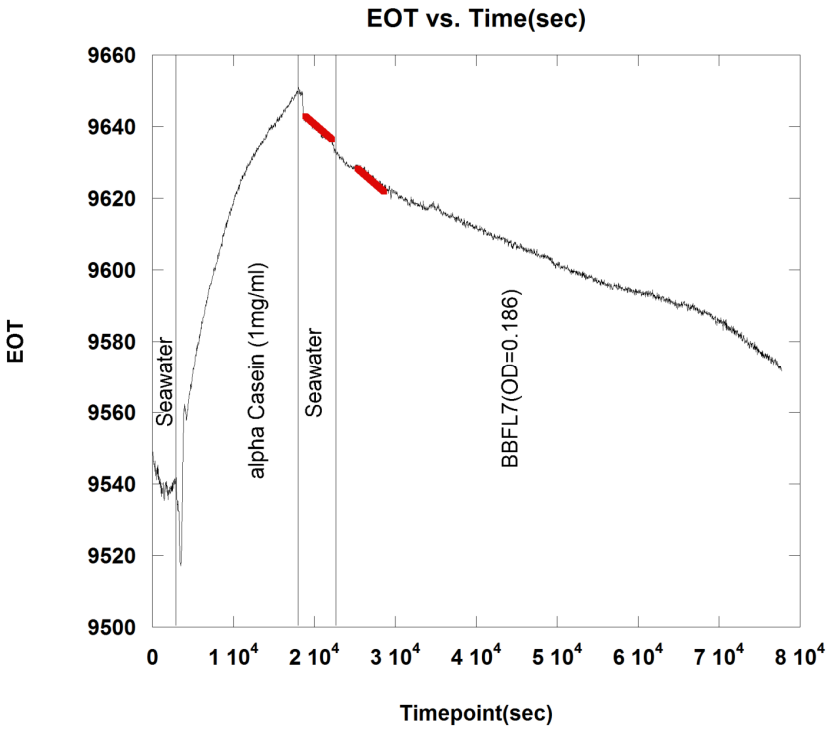

Figure A.5 Porous silica sensor incubated with BBFL7. Prior to adding BBFL7, the porous silica sensor was incubated with α-casein (1mg/ml). After rinsing excess substrate with seawater, BBFL7 was cycled through the film and 2nL changes were measured over time. The red traces indicate where the slope was taken for each given solution.

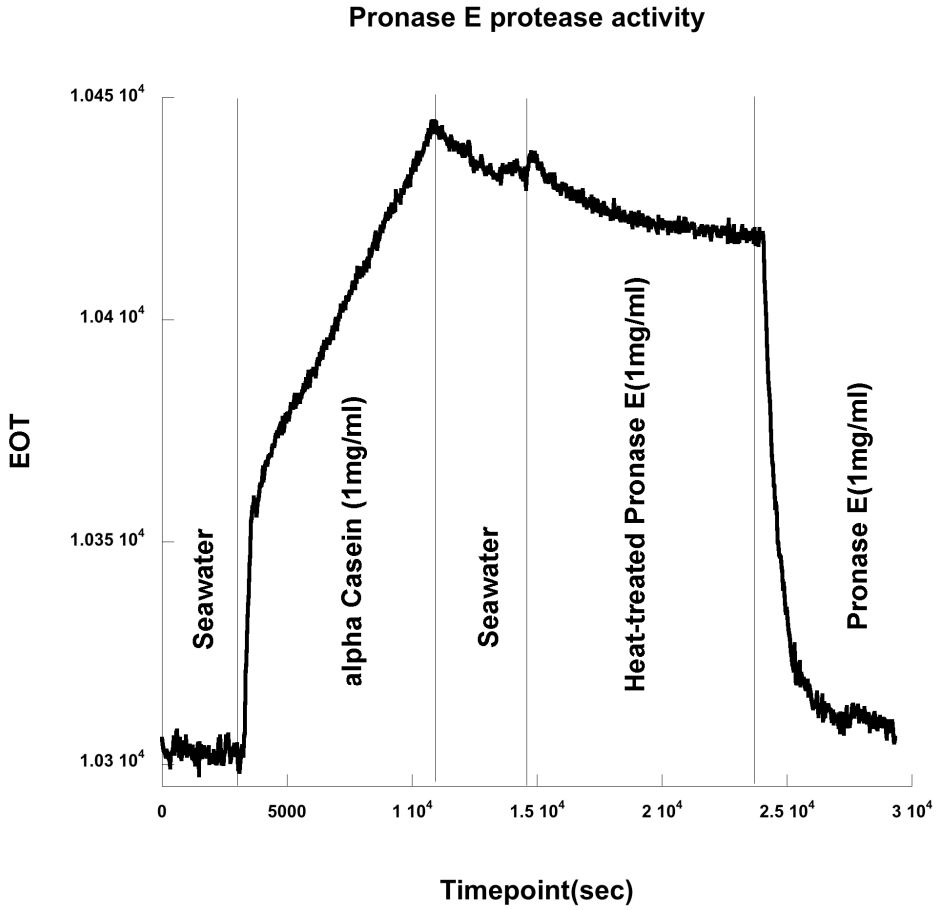

Figure A.6 Protease sensor incubated with Pronase E. After loading with substrate, a solution of inactivated Pronase E (1mg/ml) was cycle through and the change in 2nL was measured. After rinsing, a solution of active Pronase E was cycled which caused a large decrease in 2nL. A unit of pronase E is defined by hydrolysis of casein to produce a color equivalent to 1.0 mmole (181 µg) of tyrosine per min at pH 7.5 at 37 ℃ (color by Folin-C iocalteu reagent).

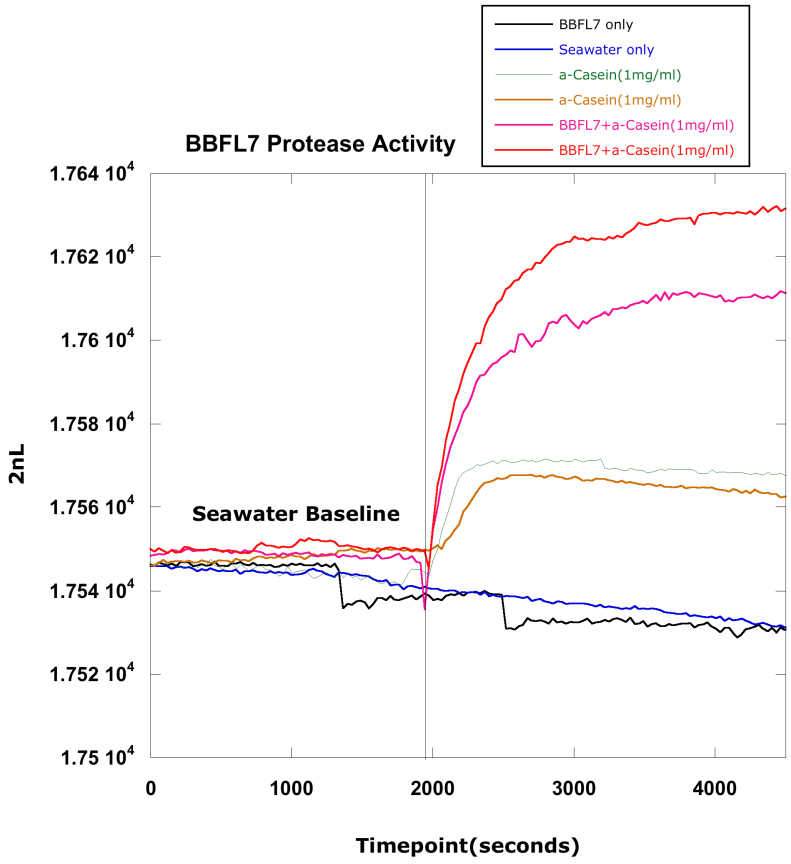

Figure A.7 BBFL7 protease activity measurement using porous silica with small pores. Prior to optical measurements, BBFL7 was incubated with substrate and allowed to digest into small peptides fragments. These products can enter the small pores and a measurable change in 2nL is observed.

Appendix B. Effect of Porosity and Thickness on Nanostructure-Initiator Mass Spectrometry.

B.1 Abstract

A challenge to label-free detection of protease activity is achieving high sensitivity. Matrix-Assisted Laser Desorption/ Ionization (MALDI) is a useful mass spectrometry technique used for measuring masses for charged molecules. This method can be directly used to study enzymatic cleavage of a peptide or protein substrate although this method limits the sensitivity of detection of masses <500Da because the organic matrix mass is within than range. Desorption/ionization on Silicon (DIOS) has advanced mass spectrometry because of its ability to detect small masses without the use of an organic matrix. Nanostructure-Initiator Mass Spectroscopy (NIMS) provides detection of a wide range of masses and still affords high sensitivity with the use of an initiator. Analyte materials adsorb onto the surface and are released by laser irradiation for mass analysis. This general method can produce high signal-to-noise ratios and low background noise allowing for sensitive measurements. NIMS mainly has been use detect masses of small molecules by coupling laser desorption to nanostructed membranes such as porous silicon. This approach allows for desorption/ionization without the use of an organic matrix. In this study, the porosity and thickness of porous silicon samples were investigated as a function of desorption/ionization of analyte. Fine tuning such factors can give greater sensitivity of analyte and could be used to detect specific masses of enzymatic digests.

B.2 Introduction

Typical desorption/ionization is matrix assisted by co-crystallization of the molecule of interest with an organic molecule[74]. The energy generated from the laser is absorbed by the organic molecule and the charge is transferred to the molecule of interest. This process protects the molecule from being directly damaged by the laser and also facilitates desorption/ionization of the molecule. Ions observed after this process consist of a neutral molecule [M] and an added or removed ion. Together, they form a quasimolecular ion, for example [M+H]+ in the case of an added proton, [M+Na]+ in the case of an added sodium ion, or [M-H]- in the case of a removed proton. MALDI is capable of creating singly-charged ions, but multiply charged ions ([M+nH]n+) can also be created, as a function of the matrix, the laser intensity and/or the voltage used. Determination of the masses of each molecule is based on the mass to charge ratio characterized by Time of Flight (TOF) spectrometry. Ions are accelerated by an electric field of a known strength and results in having the same kinetic energy as any other ion with the same charge. The time that it subsequently takes for the ions to reach a detector at a known distance is measured. This time will depend on the mass-to-charge ratio of the ion (heavier ions are accelerated to slower velocities). From this time and the known experimental parameters one can determine the mass-to-charge ratio of the ion (directly proportional to m/z). The main disadvantage to MALDI-MS is that background ions from the organic matrix itself can flood the detector making smaller masses harder to detect. Also, the molecules of interest

must be able to co-crystallize with the matrix itself in order to get desorption/ionization.

A relatively new approach uses porous silicon to generate desorption/ionization[75-77]. Porous silicon is used because of its high surface area and its ability to absorb strongly the UV laser energy. Hydride terminated silicon can further be functionalized to facilitate desorption/ionization of a variety of molecules. First demonstrated by Siuzdak et. al, porous silicon could be could coupled with TOF spectrometry to detect masses of small molecules[75]. This technique was useful in finding masses of small molecules but limited because larger masses (>3000Da) could not be detected. This was due to the fact that porous silicon cannot absorb enough laser energy to desorb larger masses. Recently, Siuzdak et. al published a new approach to get better desorption/ionization with a wide mass range[78]. Nanostructure-initiator mass spectrometry (NIMS) is a new surface-based mass spectrometry technique that uses a nanostructure surface (i.e. porous silicon) to trap initiator compounds. Upon laser induced surface heating, the fluorinated siloxane initiator is released. The molecule(s) of interest are subsequently absorbed on the initiator surface then desorbed when the initiator is vaporized by laser induced irradiation. These initiators are typically do not ionize on their own and are transparent to the UV laser. This technique does not require the analyte to be co-crystallized with the initiator allowing for a wide range on analyte to be detected and improves signal-to-noise(S/N) ratios with minimal background ion interference. Ion-NIMS is similar to laser-NIMS except it uses nanoparticles trapped in the porous silicon

matrix and desorption/ionization occurs by a thermal driven process[79]. NIMS thus allows for a versatile platform for sensitive detection of analyte that can be easily translated into high-throughput mass analysis.

One topic with NIMS that has not been fully investigated is the effect of nanostructure on the desorption/ionization of the analyte. In one study, the authors varied the current etch time to change the thickness of the film while keeping the current constant (See reference 79). They state that the thickness is changing but there is no mention of the porosity changing. Although the thickness is changing as a function of time, the porosity will change as well. To address the issue of which factor has a greater influence on NIMS, a nano-engineered porous silicon gradient was used for desorption/ionization of Angiotensin II (1046.6 *m/z*, Asp-Arg-Val-Tyr-Ile-His-Pro-Phe).This porous silicon gradient varies in porosity and thickness along the x-direction and is electrochemically machined by asymmetrically etching of bulk silicon[80]. The potential at the silicon electrode-solution interface varies as a function of distance from Pt counter electrode due to solution resistance, leading to a decrease in current density as the distance from the counter electrode increases. Porosity and thickness are affected by a number of factors such as HF concentration, dopant type and density in the silicon substrate, and current density used in the electrochemical etch. The asymmetric arrangement of the electrode results in a distinct variation in pore morphology and thickness. In this work, the ion signals produced by desorption/ionization of analyte is directly compared to porosity and thickness of the film along the x-direction. Separate samples with fixed thickness

and various porosities (and vice versa) were also analyzed to determine if the porosity or the thickness (or both) have an effect the desorption/ionization.

B.3 Experimental

B.3.1 Sample Preparation

Prior to etching, silicon wafers with resistivity of >1 mΩ-cm (Siltronix), <100)>oriented, highly B-doped (p^{++}-type) were cleaned using a mixture of sulfuric acid and hydrogen peroxide (2:1) and allowed to sit for 1 hour. Samples were subsequently rinsed with nano-pure water (x3), methanol (x3), and dried with a stream of nitrogen. These samples were then electrochemical etched in a 1.5:1 (v/v), 49% aqueous HF/ethanol solution. A Teflon etching cell that exposed 1.2 cm^2 of the silicon wafer was employed. The Pt counter electrode was placed 1.5mm above the silicon wafer as described in Figure B.1. The exposed polished surface was then asymmetrically etched at a current density of 22mA/cm^2 for 1 minute, 30seconds for samples with same porosity and varying thickness. Samples were then rinsed with methanol (x3) and dried with nitrogen after it is taken out of the etch cell to remove any HF residue. For samples with a fix thickness, a mesh Pt electrode was used to provide an even etch throughout the silicon wafer The dried samples were then incubated with initiator Bis(tridecafluoro-1,1,2,2-tetrahydrooctyl) tetramethyldisiloxane(Bis-26) for 30 minutes and excess was removed via a cycle of heating and drying by a stream of nitrogen.

B.3.2. Desorption/Ionization of Analyte

600μL of 1pmol/μL of analyte was applied to the prepared samples described above and incubated for 5 minutes. The excess solution of analyte was removed by pipetting the solution up into the pipet tip (z-touch method)[79]. This amount of solution was used to ensure that the whole porous film is covered with analyte. Samples were then placed in a modified AnchorChip 600 aluminum MALDI-target plate (Bruker Daltonics) which were used to house the porous silicon samples. These porous silicon samples were fixed to the target plate using clear scotch tape around the edges. The target plate was engineered to have a recess (0.5mm) so that the laser was able to focus for better for ion extraction efficiency (See reference 79). Mass profiling was performed on a Bruker Daltonics Autoflex II MALDI-TOF mass spectrometer operated by Flex Control software. External mass calibration was performed to within 10 ppm mass accuracy using Burker Daltonics Peptide Calibration Standard mixture. Positive ion reflection mode mass spectra were acquired in the mass range of 200-1400 m/z (100 averages per spectra). This system is equipped with a charge-coupled device camera and a camera for visualization of the porous silicon sample. The edge of the porous silicon sample closest to where the Pt electrode was visually distorted using 80% laser power(160μJ) using a pulsed nitrogen laser operating at 337nm with a trigger frequency of 16.7Hz. From that position, spectra were taken every 0.7 mm along the porous gradient until the other edge of film. Each recorded mass spectrum resulted from 100 averaged

laser shots along the x-direction. The laser attenuation was 60% offset /40% range with 30% laser power (160μJ), 100ns laser pulse extraction, and an extraction voltage of 20kV. The raw data were visualized following spectral smoothing and baseline subtraction in FlexAnalysis software (Burker Daltonics).

B.4. Results and Discussion

B.4.1. Characterization of NIMS surfaces

After electrochemically etching these surfaces, the porosity and thickness were measured optically by Spectroscopic Liquid Infiltration Method (SLIM). This optical measurement involves acquisition of the white light reflectivity spectrum, which consists of a series of peaks corresponding to constructive Fabry-Perot interference in the porous silicon film. Fourier transforms of the spectrum yields the quantity 2nL also referred as effective optical thickness (EOT). The relationship between 2nL and the Fourier transform is determined by the following relationship:

$$m\lambda=2nL \qquad \text{Eq. B.1}$$

where λ is the wavelength of maximum constructive interference for spectral fringe of order m, n the index of refraction of the porous layer and its contents, and L is the thickness of the porous layer. Fourier transformation of the reflectivity spectrum results in a peak whose position along the x-axis is equal to the quantity (2nL). Differences in the refractive index of the porous silicon layer when it is infiltrated with a solvent or with air allows the determination of thickness and porosity[26]. SLIM determines thickness and porosity of a

porous optical film by least-squares fitting of the EOT (2nL) data to a Bruggeman effective medium model[81-83]. In this work, samples were prepared at the same resistivity. Depending on the sample, the electrolyte composition, etch time, and electrode configuration varied. These parameters have a great influence on the film thickness and porosity.

The ability of NIMS to effectively desorb or ionize an analyte depends on the nanostructure used. In the case of porous silicon, porosity and thickness play a tremendous role in the desorption/ionization process. But which factor has more of an influence? To investigate this, samples were prepared with either varying the thickness of the film with fix range of porosity or vice versa. A porous silicon gradient with varying thickness and porosity fixed was made by an asymmetric etch were the electrode was placed 1.5mm above the silicon wafer next to the o-ring (Figure B.1). When the sample was etched at a low current (in this case 22mA/cm^2), the porosity didn't vary much but the thickness gradually changed over a given distance (x) (Figure B.2 and B.3). It is difficult to achieve a varying porosity and fixed thickness with an asymmetric electrode configuration, thus samples that had be prepared with individually with a normal electrode configuration where a mesh ring electrode is placed 1cm above the silicon wafer. In order to maintain the same thickness, etching silicon at a specific current density and a specific time was used (Table B.1).

B.4.2 Desorption/Ionization with Varying Porosity and Thickness

To show the affect of thickness on desorption/ionization of peptide Angiotensin II, a porous silicon gradient was made with varying thickness and a fixed range of porosity. The main peak measured in the analysis was the mass peak at 1046.6 *m/*z ([M+H]+). A fixed concentration was used to limit the amount of factors that can affect desportion/ionization process. However, the natural progression of the work would be to use a range of different concentrations and amounts of peptide. After incubation of Angiotensin II on the porous silicon surface, the sample was put into a TOF-MS for detection of the peptide mass at 1046.6 *m/z*. The signal to noise ratio and signal intensity were measured as a function of thickness and porosity along the x-axis of the gradient film starting at the position of the electrode (Figures B.2 and B.3). Each measurement was taken every 0.7mm until the edge of the chip was reached (total of 15 measurements, diameter of porous silicon=1.0 cm). Figure B.2 is plot of signal to noise ratio compared with the thickness and porosity. By making a limited range in the porosity, the signal to noise ratios remains about the same values as the porosity. When comparing the thickness of the film to the signal to noise ratio, the change in signal to noise of Angiotensin II does not follow the same trend as the thickness (Figure B.2b). This experiment favors the case of the thickness having a minor role in desorption/ionization of the analyte (this is, however, in contrast to reference 79). This also appears to be the case for raw signal intensities (Figure

B.3). Given this information, the porosity could be tuned to achieve the greatest desorption/ionization when the porous silicon sample has a fixed thickness.

To show the affect of porosity on desorption/ionization of peptide Angiotensin II, various samples with different porosity and fixed thickness were made. A porous silicon gradient could not be used in this case because the thickness varies along the x-axis. Table B.1 shows the extent to which the porosity affects the desorption/ionization of Angiotensin II. As the porosity increase, the signal area will decrease as well. When comparing the signal intensities, there appears to be a threshold in achieving maximum signal intensity. The highest porosity in Table B.1 does not give the highest signal. One argument for the signal intensities observed is the affect that porosity has on surface area. If the surface area is related to porosity, then after a specific porosity the surface area would decrease because there is less silicon (which is characterized by larger pores).In the simplest case, more small pores in a given area will have greater surface area than larger pores in that same area. Thickness of the film would have less of an effect on surface area because the changes in thickness observed translate into small changes in surface area. This work suggests that the porosity has a major role in the desorption/ionization of the analyte as it can directly influence the surface area. Further characterization of the surface area is need and could be easily performed using BET nitrogen adsorption.

When comparing the use of NIMS to DIOS, peptides greater than >3000Da can be detected with great sensitivity with a wider range of mass

because the use of an initiator allows for greater desorption/ionization of analyte. Although DIOS is still able to generate in intact gas phase, it is highly dependent on the type of modification of porous silicon used. Porous silicon for NIMS is solely used to absorb energy from the laser to vaporize the initiator for desorption/ionization of analyte. Although many factors such as concentration of analyte, type of initiator, type of silicon, and modifications to porous silicon have been investigated by other groups[78-79], the porosity and thickness factors have not been fully investigated. This work gives insight into fine tuning such factors for improving the mass signal.

B.4.3. Desorption/Ionization with a Gradient Porous Silicon Film

A porous silicon gradient was electrochemically etched with varying porosity and thickness. The intensity of the Angiotensin II peak (1046.6*m/z*) starts to decrease as a function of x along the gradient (Figure B.4). This effect is most likely due to both the porosity and thickness changes (with the thickness playing a minor role) along the gradient (Figure B.5). When looking at each factor separately, the thickness is constantly decreasing along the x-axis. This is also the case for the porosity (to some extent). When comparing the intensity values, they match the porosity profile more than the thickness (Figure B.5). As position changes along the porous silicon gradient, the porosity is changing as well. Given that the porosity plays a major role in the signal intensity, the effect it can have on the desorption/ionization of Angiotensin II is very significant. Figure B.4 shows that at lower porosity, the signal becomes more suppressed than at

higher porosity. This information could be used to create nanostructures that can allow for maximum signal intensity with the least amount of signal suppression.

These NIMS films can also be used to detect peptides generated from proteases. A trypsin digest of bovine serum albumin (Bruker Daltonics) was digested for 24 hours to generate sufficient cleavage of protein substrate (Figure B.6). 50pmol of the digest were added directly to the NIMS surface and incubated for 5 minutes before removing the excess mixture. These samples were allowed to dry and then put into a TOF-MS. The peptide sequence coverage for the cleavage of BSA by trypsin was about 29% according to Mascot database search. This sequence coverage is directly comparable to other NIMS surfaces performed by the Siuzdak group[79]. Although this data is part of the initial steps, it suggests that this type of NIMS gradient could detect masses of peptide cleavage products. Investigation of the mass signatures of digests at various points along the gradient could also be investigated be were not performed in this thesis work. The next step that would be taken in this research would be to investigate the affect of concentration of analyte. In this case, individual porous silicon samples would have to be prepared separately because the porosity and thickness will vary on the film. The concentration of digest that was used gives reproducible signals that can be used to identify mass signatures. It would be interesting to see if concentration can affect the mass signature of a protein/peptide digest. Going a step further in this research, the porous silicon gradient could theoretically be used as filters to separate peptides based on size. Along the gradient, the porosity and thickness change as well as pore size. The

possibility of using on-chip porous silicon filter that can be coupled to NIMS to achieve great sensitivity and specificity would advance mass spectrometry and separation of molecules of interest. The next steps in this thesis would be to look at the effect that concentration has on mass signal.

B.5 Conclusions

The desorption/ionization of Angiotensin II was investigated by treating porosity and thickness as independent variables. Porosity seems to have a great effect on efficiency of extraction of analyte with thickness having a minor role. One can envision having a gradient of porosity (varying pore size) that can act as size exclusion matrixes that filter out larger polypeptides from smaller one. This system could potentially be coupled to NIMS to detect a range peptide mass in patient's samples. In particular, digestion of peptide substrates with enzymes would be of great use in characterization of the enzyme's specific mode of cleavage. The next steps in this thesis work would be to reproduce the work with the BSA digest and see if the mass signatures change along the gradient. A study where the concentration of analyte is a variable is also necessary to see if the mass signature is varies as well. Characterization of the pore size and shape would be necessary if these gradients were to be used as filters for peptides and be able to couple them to NIMS. Ultimately, this system will be compared to current methods of detection of peptide masses (i.e. DIOS, MADLI).

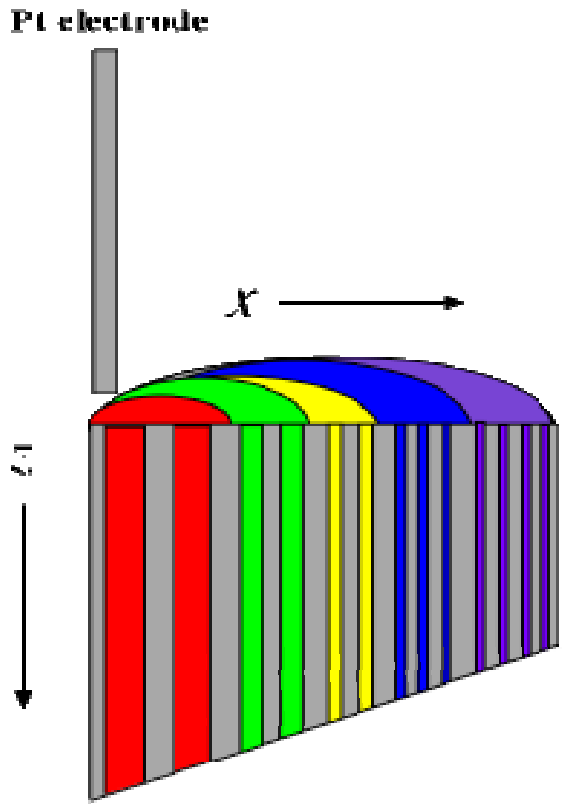

Figure B.1 Schematic of an asymmetric electrochemical etch. A Pt electrode is place above the surface of a polished silicon wafer and a current is applied. The current density changes as a function of x that creates a gradient of porosity and thickness (porous silicon cross section).

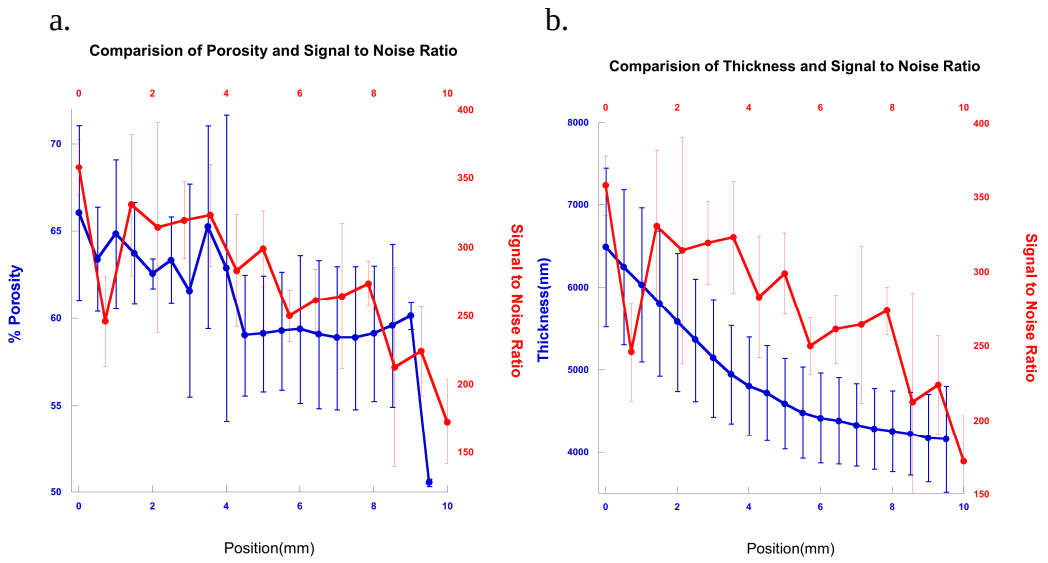

Figure B.2 Signal to noise ratios of fixed porosity with varying thickness of porous silicon samples. a. The porosity of porous silicon follows the trend of the signal to noise ratio. In this case, the higher the porosity, the greater the signal to noise ratio.b. The signal to noise ratio does not follow the same trend gradual change in thickness along the porous silicon gradient. This would suggest that the thickness play a minor role in the signal to noise. Each measurement was made in triplicate with the error representing 1+/- s.d. from the mean.

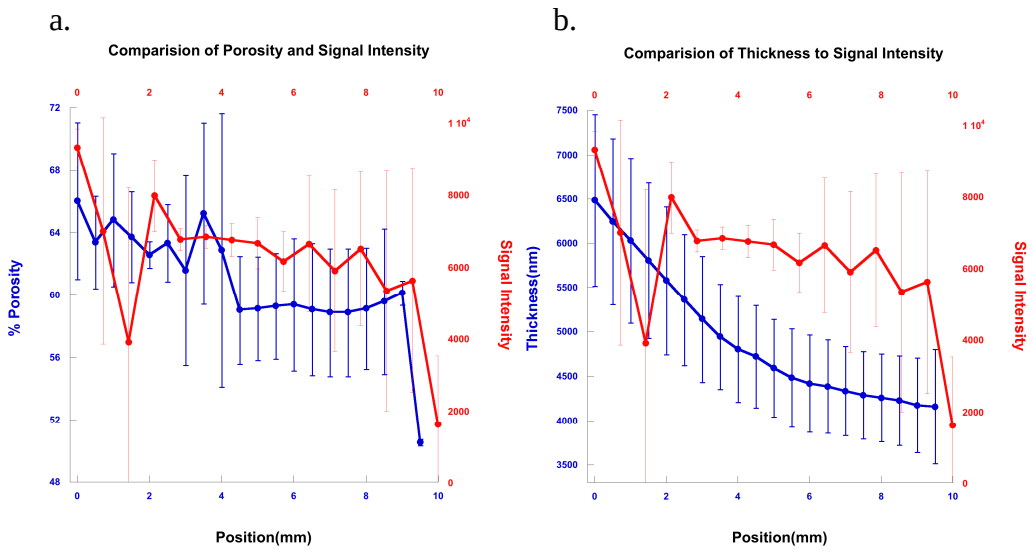

Figure B.3 Signal intensity of fixed porosity with varying thickness of porous silicon samples. a. The porosity of porous silicon follows the trend of the signal intensity. In this case, the higher the porosity, the greater the signal intensity. b. The signal intensity does not follow the same trend gradual change in thickness along the porous silicon gradient. This would suggest that the thickness play a minor role in the signal intensity. Each measurement was made in triplicate with the error representing 1+/- s.d. from the mean.

Table B.1 Varying the porosity with a fixed thickness. Porosity,thickness, signal intensity and area measured in triplicate and the error represent 1+/- s.d. from the mean.

	531mA/cm2 for 20sec	221mA/cm2 for 41sec	62mA/cm2 for 118sec
Porosity	78 +/- 1	63 +/- 2	52 +/- 3
Signal Intensity	7802+/- 659	10481+/- 521	5423+/- 342
Area	10811 +/- 316	13891+/- 100	15966 +/- 222
Thickness (nm)	4426 +/- 52	4363 +/- 25	4343 +/- 50

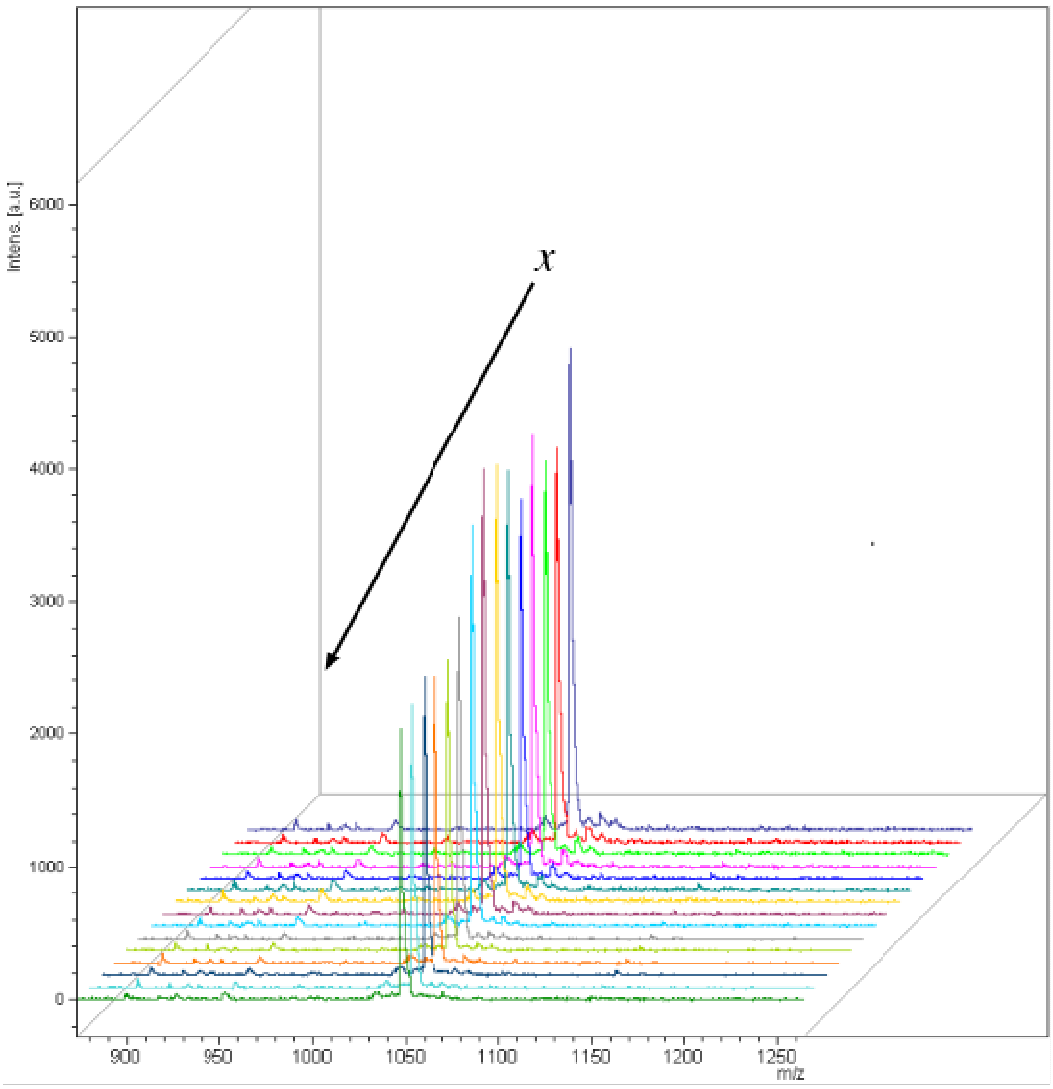

Figure B.4 Angiotensin II signal as a function of gradient position. The blue trace(far back spectrum) is the Angiotensin II mass peak (1046.6 *m/z*, [M+H]+) at the Pt electrode. Moving further away from the electrode in the x direction shows a decrease in signal intensity. The etch conditions for this gradient was 108mA/cm^2 for 1 minute 30 seconds.

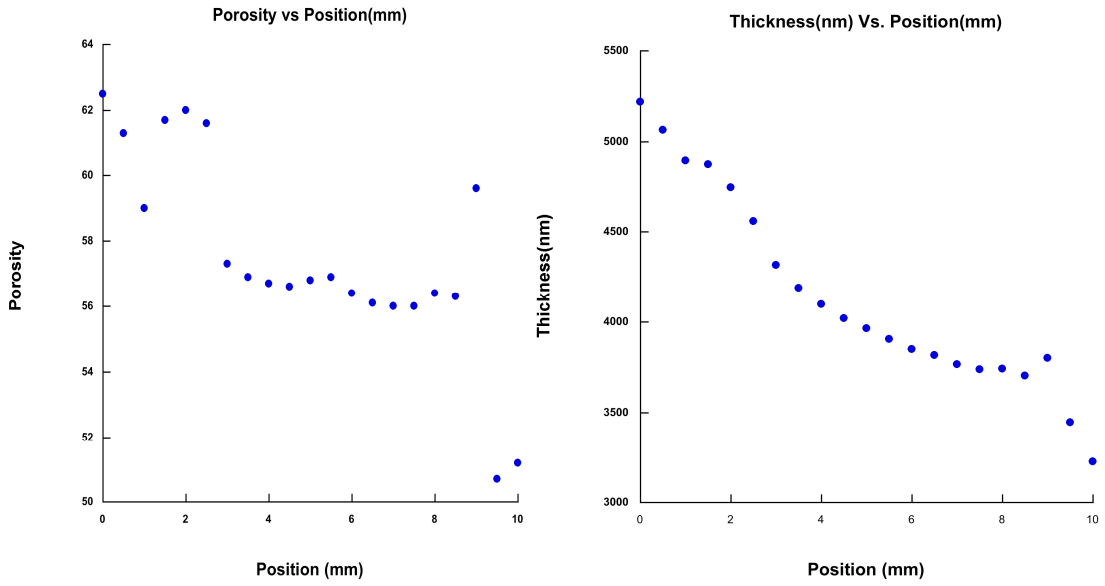

Figure B.5 Porosity and thickness measurements for Figure B.4.

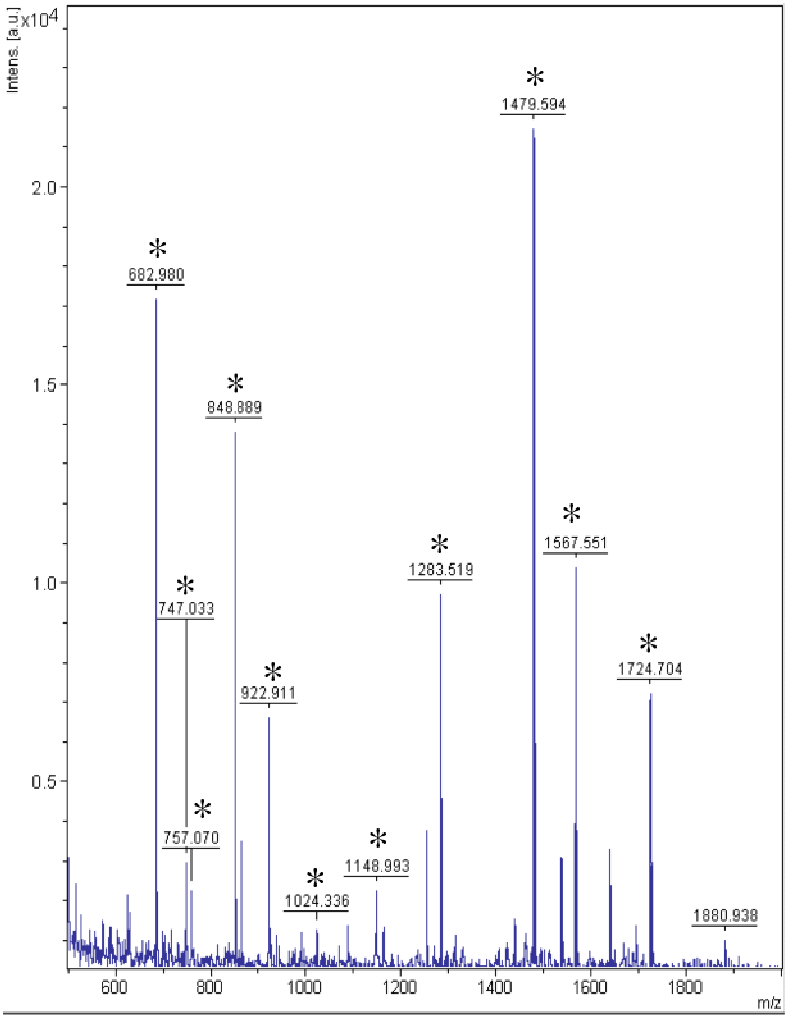

Figure B.6 BSA digest on a NIMS gradient surface. Process spectra with baseline correction, noise filtering and monoisotopic peak list filtering using FlexAnalysis software (Bruker Daltonics). The BSA digest spectra (range of 500-2000*m/z*) were calibrated with an external peptide standard. The spectral mass peak lists were found using Mascot peptide mass fingerprint with the following parameters: SwissProtein database, mammalian taxonomy, missed cleavage of 1 and ±100 p.p.m. peptide tolerance ([M+H]+). The (*) represent the relevant mass peaks ([M+H]+) of the digest in the spectrum. The spectrum represents a BSA digest at the Pt electrode x position along the porous silicon gradient. The sequence % is about 29% that is comparable to other NIMS surfaces for a BSA digest with trypsin (see reference 79).

References

1. Puente, X.S., Sanchez, L.M., Overall, C.M. & Lopez-Otin, C. Human and mouse proteases: a comparative genomic approach. *Nat Rev Genet* **4**, 544-558 (2003).

2. Lopez-Otin, C. & Overall, C.M. Protease degradomics: A new challenge for proteomics. *Nat Rev Mol Cell Biol* **3**, 509-519 (2002).

3. Coussens, L.M., Fingleton, B. & Matrisian, L.M. Matrix Metalloproteinase Inhibitors and Cancer--Trials and Tribulations. *Science* **295**, 2387-2392 (2002).

4. Klimpel, K.R., Molloy, S.S., Thomas, G. & Leppla, S.H. Anthrax toxin protective antigen is activated by a cell surface protease with the sequence specificity and catalytic properties of furin. *Proceedings of the National Academy of Sciences of the United States of America* **89**, 10277-10281 (1992).

5. Valeur, B. Molecular Fluoresecnce: Principles and Applications. (Wiley-VCH, 2002).

6. Bond, R.B.a.J.S. Proteolytic Enzymes Edn. Second Edition. (Oxford University Press, 2001).

7. Jones, B.L., Fontanini, D., Jarvinen, M. & Pekkarinen, A. Simplified Endoproteinase Assays Using Gelatin or Azogelatin. *Analytical Biochemistry* **263**, 214-220 (1998).

8. Singleton, V.L., Orthofer, R., Lamuela-RaventÛs, R.M. & Lester, P. in Methods in Enzymology, Vol. Volume 299 152-178 (Academic Press, 1999).

9. Burokerkilgore, M. & Wang, K.K.W. A Coomassie Brilliant Blue G-250-Based Colorimetric Assay for Measuring Activity of Calpain and Other Proteases. *Analytical Biochemistry* **208**, 387-392 (1993).

10. Esler, W.P. & Wolfe, M.S. A portrait of Alzheimer secretases--new features and familiar faces. *Science* **293**, 1449-1454 (2001).

11. Twining, S.S. Fluorescein isothiocyanate-labeled casein assay for proteolytic enzymes. *Analytical Biochemistry* **143**, 30-34 (1984).

12. Jones, L.J. et al. Quenched BODIPY Dye-Labeled Casein Substrates for the Assay of Protease Activity by Direct Fluorescence Measurement. *Analytical Biochemistry* **251**, 144-152 (1997).

13. Lee, H.-J., LaRue, J.N. & Wilson, I.B. A simple spectrophotometric assay for amino acyl arylamidases (naphthylamidases, aminopeptidases). *Analytical Biochemistry* **41**, 397-401 (1971).

14. Barrett, A.J. A new assay for cathepsin B1 and other thiol proteinases. *Analytical Biochemistry* **47**, 280-293 (1972).

15. Powers, J.C., Kam, C.-M. & Alan, J.B. in Methods in Enzymology, Vol. Volume 248 3-18 (Academic Press, 1995).

16. Auld, D.S., Latt, S.A. & Vallee, B.L. Approach to inhibition kinetics. Measurement of enzyme-substrate complexes by electronic energy transfer. *Biochemistry* **11**, 4994-4999 (1972).

17. Zimmerman, M., Yurewicz, E. & Patel, G. A new fluorogenic substrate for chymotrypsin. *Analytical Biochemistry* **70**, 258-262 (1976).

18. Medintz, I.L. et al. Proteolytic activity monitored by fluorescence resonance energy transfer through quantum-dot-peptide conjugates. *Nat Mater* **5**, 581-589 (2006).

19. Green, J.D. Detection of femtomole quantities of proteases by high-performance liquid chromatography. *Analytical Biochemistry* **152**, 83-88 (1986).

20. Harcum, S.W. & Bentley, W.E. Detection, quantification, and characterization of proteases in recombinant Escherichia coli. *Biotechnology Techniques* **7**, 441-447 (1993).

21. Barber, M., Bordoli, R.S., Sedgwick, R.D. & Tyler, A.N. Fast atom bombardment of solids as an ion source in mass spectrometry. *Nature* **293**, 270-275 (1981).

22. J.C. Pehrson, A.W., J. Markwell, G. Sarath and S.D. Schwartzbach Use of GFP as a Reporter for the Facile Analysis of Sequence-Specific Proteases. *BioTechniques* **27**, 28-32 (1999).

23. Uhlir, A. Electrolytic Shaping of Germanium and Silicon. *Bell System Technology Journal* **35**, 333-347 (1956).

24. Canham, L.T. Silicon quantum wire array fabrication by electrochemical and chemical dissolution of wafers. *Applied Physics Letters* **57**, 1046-1048 (1990).

25. Buriak, J.M. Organometallic Chemistry on Silicon and Germanium Surfaces. *Chem. Rev.* **102**, 1271-1308 (2002).

26. Pacholski, C., Sartor, M., Sailor, M.J., Cunin, F. & Miskelly, G.M. Biosensing using porous silicon double-layer interferometers: reflective interferometric Fourier transform spectroscopy. *J. Am. Chem. Soc.* **127**, 11636-11645 (2005).

27. Schwartz, M.P., Alvarez, S.D. & Sailor, M.J. Porous SiO2 Interferometric Biosensor for Quantitative Determination of Protein Interactions: Binding of Protein A to Immunoglobulins Derived from Different Species. *Anal. Chem.* **79**, 327-334 (2007).

28. Pavesi, L. & Dubos, P. Random porous silicon multilayers: application to distributed Bragg reflectors and interferential Fabry - Pérot filters. *Semiconductor Science and Technology* **12**, 570-575 (1997).

29. Hecht, E. Optics, Edn. 3rd ed. (Addison-Wesley: Reading, Ma, 1998).

30. Allcock, P. & Snow, P.A. Time-resolved sensing of organic vapors in low modulating porous silicon dielectric mirrors. *Journal of Applied Physics* **90**, 5052-5057 (2001).

31. Gao, J., Gao, T., Li, Y.Y. & Sailor, M.J. Vapor Sensors Based on Optical Interferometry from Oxidized Microporous Silicon Films. *Langmuir* **18**, 2229-2233 (2002).

32. Janshoff, A. et al. Macroporous p-Type Silicon Fabry-Perot Layers. Fabrication, Characterization, and Applications in Biosensing. *J. Am. Chem. Soc.* **120**, 12108-12116 (1998).

33. Lin, V.S.Y., Motesharei, K., Dancil, K.-P.S., Sailor, M.J. & Ghadiri, M.R. A Porous Silicon-Based Optical Interferometric Biosensor. *Science* **278**, 840-843 (1997).

34. Dancil, K.P.S., Greiner, D.P. & Sailor, M.J. A Porous Silicon Optical Biosensor: Detection of Reversible Binding of IgG to a Protein A-Modified Surface. *J. Am. Chem. Soc.* **121**, 7925-7930 (1999).

35. Pacholski, C., Yu, C., Miskelly, G.M., Godin, D. & Sailor, M.J. Reflective Interferometric Fourier Transform Spectroscopy: A Self-Compensating Label-Free Immunosensor Using Double-Layers of Porous SiO2. *J. Am. Chem. Soc.* **128**, 4250-4252 (2006).

36. Wiesner, R. & Troll, W. A new assay for proteases using fluorescent labeling of proteins. *Anal. biochem.* **121**, 290-294 (1982).

37. Folin, O., Ciocalteu, V. On tryrosine and tryptophane determinations in proteins. *J. Biol. Chem.* **73**, 627-650 (1927).

38. Lin, V.S.-Y., Motesharei, K., Dancil, K.S., Sailor, M.J. & Ghadiri, M.R. A Porous Silicon-Based Optical Interferometric Biosensor. *Science* **278**, 840-843 (1997).

39. Chan, S., Fauchet, P.M., Li, Y., Rothberg, L.J. & Miller, B.L. Porous silicon microcavities for biosensing applications. *Phys. Status Solidi A* **182**, 541-546 (2000).

40. Chan, S., Horner, S.R., Miller, B.L. & Fauchet, P.M. Identification of gram negative bacteria using nanoscale silicon microcavities. *J. Am. Chem. Soc.* **123**, 11797-11798 (2001).

41. Meade, S.O., Yoon, M.S., Ahn, K.H. & Sailor, M.J. Porous silicon photonic crystals as encoded microcarriers. *Adv. Mater.* **16**, 1811-1814 (2004).

42. Cunin, F. et al. Biomolecular screening with encoded porous silicon photonic crystals. *Nature Mater.* **1**, 39-41 (2002).

43. Schmedake, T.A., Cunin, F., Link, J.R. & Sailor, M.J. Standoff detection of chemicals using porous silicon "Smart Dust" particles. *Adv. Mater.* **14**, 1270-1272 (2002).

44. Berger, M.G. et al. Dielectric filters made of porous silicon: advanced performance by oxidation and new layer structures. *Thin Sol. Films* **297**, 237-240 (1997).

45. Gurtner, C., Wun, A.W. & Sailor, M.J. Surface modification of porous silicon by electrochemical reduction of organo halides. *Angew. Chem. Int. Ed.* **38**, 1966-1968 (1999).

46. Wang, Q., Wang, J., Geil, P.H. & Padua, G.W. Zein absorption by hydrophilic and hydrophobic surfaces investigated by surface plasmon resonance. *Biomacromolecules* **5**, 1356-1361 (2004).

47. Sailor, M.J. & Link, J.R. "Smart dust": nanostructured devices in a grain of sand. *Chemical Communications*, 1375-1383 (2005).

48. Bovard, B.G. Rugate filter theory: an overview. *Appl. Optics* **32**, 5427-5442 (1993).

49. Chatgilialoglu, C. Organosilanes as radical-based reducing agents in synthesis. *Accounts of Chemical Research* **25**, 188-194 (1992).

50. Lees, I.N. et al. Chemical Stability of Porous Silicon Surfaces Electrochemically Modified with Functional Alkyl Species. *Langmuir* **19**, 9812-9817 (2003).

51. Zangooie, S., Jansson, R. & Arwin, H. Ellipsometric characterization of anisotropic porous silicon Fabry--P[e-acute]rot filters and investigation of temperature effects on capillary condensation efficiency. *Journal of Applied Physics* **86**, 850-858 (1999).

52. Vassar, R. et al. Beta-secretase cleavage of Alzheimer's amyloid precursor protein by the transmembrane aspartic protease BACE. *Science* **286**, 735-741 (1999).

53. Jones, L.J. et al. Quenched BODIPY dye-labeled casein substrates for the assay of protease activity by direct fluorescence measurement. *Anal. Biochem.* **251**, 144-152 (1997).

54. Zhang, J., Campbell, R.E., Ting, A.Y. & Tsien, R.Y. Creating new fluorescent probes for cell biology. *Nat Rev Mol Cell Biol* **3**, 906-918 (2002).

55. Schwartz, M.P., Alvarez, S.D. & Sailor, M.J. A Porous SiO2 Interferometric Biosensor for Quantitative Determination of Protein Interactions: Binding of Protein A to Immunoglobulins Derived from Different Species. *Anal. Chem.* **79**, 327-334 (2007).

56. Park, J.S. et al. Enhancement of sensitivity in interferometric biosensing by using a new biolinker and prebinding antibody. *J. Microbiol. Biotechnol.* **16**, 1968-1976 (2006).

57. Tinsley-Bown, A. et al. Immunoassays in a porous silicon interferometric biosensor combined with sensitive signal processing. *Phys. Status Solidi A-Appl. Mat.* **202**, 1347-1356 (2005).

58. Dancil, K.-P.S., Greiner, D.P. & Sailor, M.J. A porous silicon optical biosensor: detection of reversible binding of IgG to a protein A-modified surface. *J. Am. Chem. Soc.* **121**, 7925-7930 (1999).

59. Pacholski, C., Yu, C., Miskelly, G.M., Godin, D. & Sailor, M.J. Reflective Interferometric Fourier Transform Spectroscopy: A Self-Compensating Label-Free Immunosensor Using Double-layers of Porous SiO2. *J. Am. Chem. Soc.* **128**, 4250-4252 (2006).

60. Kilian, K.A., Böcking, T., Gaus, K., Gal, M. & Gooding, J.J. Peptide-Modified Optical Filters for Detecting Protease Activity. *ACS Nano* **1**, 355-361 (2007).

61. Orosco, M.M., Pacholski, C., Miskelly, G.M. & Sailor, M.J. Protein-coated porous silicon photonic crystals for amplified optical detection of protease activity. *Adv. Mater.* **18**, 1393-1396 (2006).

62. Zhang, X.G. Morphology and Formation Mechanisms of Porous Silicon. *J. Electrochem. Soc.* **151**, C69-C80 (2004).

63. Leong, W.Y., Loni, A. & Canham, L.T. Electrically enhanced erosion of porous Si material in electrolyte by pH modulation and its application in chronotherapy. *Phys. Status Solidi A-Appl. Mat.* **204**, 1486-1490 (2007).

64. Thomas, J.C., Pacholski, C. & Sailor, M.J. Delivery of Nanogram Payloads Using Magnetic Porous Silicon Microcarriers. *Lab Chip* **6**, 782 - 787 (2006).

65. Striemer, C.C., Gaborski, T.R., McGrath, J.L. & Fauchet, P.M. Charge- and size-based separation of macromolecules using ultrathin silicon membranes. *Nature* **445**, 749-753 (2007).

66. Collins, B.E., Dancil, K.-P., Abbi, G. & Sailor, M.J. Determining protein size using an electrochemically machined pore gradient in silicon. *Adv. Funct. Mater.* **12**, 187-191 (2002).

67. Schwartz, M.P., Derfus, A.M., Alvarez, S.D., Bhatia, S.N. & Sailor, M.J. The smart petri dish: A nanostructured photonic crystal for real-time monitoring of living cells. *Langmuir* **22**, 7084-7090 (2006).

68. Fruton, J.S. Active site of pepsin. *Acc. Chem. Res.* **7**, 241-246 (1974).

69. Inouye, K. & Fruton, J.S. Inhibition of pepsin action. *Biochemistry* **7**, 1611-1615 (1968).

70. Malamud, D. & Drysdale, J.W. Isoelectric points of proteins: A table. *Anal. Biochem.* **86**, 620-647 (1978).

71. Fujinaga, M., Chernaia, M.M., Tarasova, N.I., Mosimann, S.C. & James, M.N. Crystal structure of human pepsin and its complex with pepstatin. *Protein science : a publication of the Protein Society* **4**, 960-972 (1995).

72. Sachdev, G.P. & Fruton, J.S. Kinetics of Action of Pepsin on Fluorescent Peptide Substrates. *Proc. Nat. Acad. Sci.* **72**, 3424-3427 (1975).

73. Cancilla, M.T., Leavell, M.D., Chow, J. & Leary, J.A. Mass spectrometry and immobilized enzymes for the screening of inhibitor libraries. *Proc. Nat. Acad. Sci.* **97**, 12008-12013 (2000).

74. Karas, M. & Hillenkamp, F. Laser desorption ionization of proteins with molecular masses exceeding 10,000 daltons. *Analytical Chemistry* **60**, 2299-2301 (1988).

75. Wei, J., Buriak, J.M. & Siuzdak, G. Desorption-ionization mass spectrometry on porous silicon. *Nature* **399**, 243-246 (1999).

76. Nayak, R., Liu, J., Sen, A.K. & Knapp, D.R. Dual Desorption Electrospray Ionization−Laser Desorption Ionization Mass Spectrometry on a Common Nanoporous Alumina Platform for Enhanced Shotgun Proteomic Analysis. *Analytical Chemistry* **80**, 8840-8844 (2008).

77. Rebecca A. Kruse, S.S.R.E.V.R.P.W.B.J.V.S. Direct assay of Aplysia tissues and cells with laser desorption/ionization mass spectrometry on porous silicon. *Journal of Mass Spectrometry* **36**, 1317-1322 (2001).

78. Northen, T.R. et al. Clathrate nanostructures for mass spectrometry. *Nature* **449**, 1033-1036 (2007).

79. Woo, H.-K., Northen, T.R., Yanes, O. & Siuzdak, G. Nanostructure-initiator mass spectrometry: a protocol for preparing and applying NIMS surfaces for high-sensitivity mass analysis. *Nat. Protocols* **3**, 1341-1349 (2008).

80. B.E. Collins, K.P.S.D.G.A.M.J.S. Determining Protein Size Using an Electrochemically Machined Pore Gradient in Silicon. *Advanced Functional Materials* **12**, 187-191 (2002).

81. Anglin, E.J., Schwartz, M.P., Ng, V.P., Perelman, L.A. & Sailor, M.J. Engineering the chemistry and nanostructure of porous silicon Fabry-Pérot films for loading and release of a steroid. *Langmuir* **20**, 11264-11269 (2004).

82. E. Segal, L.A.P.F.C.F.D.R.J.M.D.Y.Y.L.M.J.S. Confinement of Thermoresponsive Hydrogels in Nanostructured Porous Silicon Dioxide Templates. *Advanced Functional Materials* **17**, 1153-1162 (2007).

83. Jianmin Wu, M.J.S. Chitosan Hydrogel-Capped Porous SiO as a pH Responsive Nano-Valve for Triggered Release of Insulin. *Advanced Functional Materials* **9999**, NA (2009).

84. Manuel Orosco, C.P.G.M.M.M.J.S. Protein-Coated Porous-Silicon Photonic Crystals for Amplified Optical Detection of Protease Activity. *Advanced Materials* **18**, 1393-1396 (2006).

85. Bidle, K.D. & Azam, F. Accelerated dissolution of diatom silica by marine bacterial assemblages. *Nature (London)* **397**, 508-512 (1999).

86. Wang, Q., Wang, J.-F., Geil, P.H. & Padua, G.W. Zein Adsorption to Hydrophilic and Hydrophobic Surfaces Investigated by Surface Plasmon Resonance. *Biomacromolecules* **5**, 1356-1361 (2004).

87. Michael J. Sailor, K.L.K. Porous silicon - what is responsible for the visible luminescence? *Advanced Materials* **4**, 432-434 (1992).

88. M. P. Stewart, J.M.B. Chemical and Biological Applications of Porous Silicon Technology. *Advanced Materials* **12**, 859-869 (2000).

89. Folkesson, A., Haagensen, J.A.J., Zampaloni, C., Sternberg, C. & Molin, S.r. Biofilm Induced Tolerance towards Antimicrobial Peptides. *PLoS ONE* **3**, e1891 (2008).